**UNIVERSIDADE ESTADUAL DE CAMPINAS**

UNICAMP

**INSTITUTO DE QUÍMICA**
**DEPARTAMENTO DE FÍSICO-QUÍMICA**

# Propriedades de soluções de copolímeros estatísticos em comparação com copolímeros em bloco: diagramas de fase binários e interação com surfatantes

**Tese de Doutorado**

**Autora: Anna Barbara Niemiec**

**Orientador: Prof. Dr. Watson Loh**

**Agosto 2008**

# FICHA CATALOGRÁFICA ELABORADA PELA BIBLIOTECA DO INSTITUTO DE QUÍMICA DA UNICAMP

N555p
Niemiec, Anna Barbara.
Propriedades de soluções de copolímeros estatísticos em comparação com copolímeros em bloco: diagramas de fase binários e interação com surfatantes / Anna Bárbara Niemiec. – Campinas, SP: [s.n], 2008.

Orientador: Watson Loh.

Tese - Universidade Estadual de Campinas, Instituto de Química.

1. Copolímeros bloco. 2. Copolímeros estatísticos. 3. Surfatantes. 4. Calorimetria. I. Loh, Watson. II. Universidade Estadual de Campinas. Instituto de Química. III. Título.

**Título em inglês:** Properties of solutions of random copolymers in comparison to block copolymers: bynary phase diagrams and interactions with surfactants

**Palavras-chaves em inglês:** Block copolymers, Random copolymers, Surfactants, Calorimetry

**Área de concentração:** Físico-Química

**Titulação:** Doutor em Ciências

**Banca examinadora:** Prof. Dr. Watson Loh (orientador), Prof. Dr. Luis Henrique Mendes da Silva (DQ-UFV), Prof. Dr. Pedro de Alcântara Pessoa Filho (DEQ-Poli-USP-SP), Prof. Dr. Fred Yukio Fujiwara (IQ-UNICAMP), Prof. Dr. Edvaldo Sabadini (IQ-UNICAMP)

**Data de defesa:** 19/08/2008

Dedico esta tese aos meus pais Krystyna e Czeslaw (*in memorian)* e a minha irmã Izabela pelo incentivo apoio e cooperação.

E principalmente ao meu marido Rodrigo pelo mútuo aprendizado de vida durante nossa convivência tanto nos momentos de tristezas e também de alegrias.

*"Insanity: doing the same thing over and over again and expecting different results"*

**Albert Einstein**

# AGRADECIMENTOS

Ao Prof. Watson Loh pelas orientações durante este tempo de colaboração, tão importantes para a minha formação cientifica e preparação profissional.

Às Professoras Gerd Olofsson e Karin Shillén da Universidade de Lund pelo acompanhamento ao longo de todos estes anos e pelas dicas valiosas, especialmente na área de calorimetria e espalhamento de luz durante desenvolvimento deste estudo.

Aos meus todos colegas do laboratório I-114 pela ajuda em dia – dia e na adaptação em novo ambiente especialmente durante do meu primeiro ano da estádia no Brasil.

Aos meus amigos Carla e Fabio, Ana Claudia e Renato, Anna e Marcelo, Marysia e Wojtek, Patrícia e Tomek pelos bons momentos durante nossos encontros.

Ao CNPq e FAPESP pelo suporte financeiro (processo 141565/2002-0)

---

# Curriculum Vitae

**Nome:** Anna Barabara Niemiec
**Data de nascimento:** 06.05.1978, Polônia

**Mestre em Química**

**Período: de outubro de 1997 a julho de 2002.**
**Departamento de Tecnologia de Polímeros – Universidade de Cracóvia**

**Dissertação de Mestrado:** *"Influence of non-ionic surfactants on the aggregation of P123 studied by differential scanning calorimetry, isothermal titration calorimetry, light scattering and analytical ultracentrifugation"*

## Lista de Publicações

Esta tese contempla descrição sobre interações entre copolímeros blocos vs. estatísticos com surfatantes iônicos e não iônicos como também estudo sobre diagramas binários destes polímeros, resumida na forma de dois artigos e um manuscrito listados abaixo.

## Artigo I

A Calorimetry and Light Scattering Study of the Formation and Shape Transition of Mixed Micelles of $EO_{20}PO_{68}PO_{20}$ Triblock Copolymer (P123) and Nonionic Surfactant ($C_{12}EO_6$)

Löf, David; Niemiec, Anna; Schillén, Karin; Loh, Watson; Olofsson, Gerd

*J. Phys. Chem. B* **2007**, 111, 5911-5920,

---

## Artigo II

Interaction of ethylene oxide – propylene oxide copolymers with ionic surfactants studied by calorimetry: random vs. block copolymers

Niemiec, Anna and Loh, Watson

*J. Phys. Chem. B,* **2008**, 112, 727

## Manuscrito I

Binary phase diagrams of block vs. random copolymers in water and organic solvents

Niemiec, Anna and Loh, Watson

Para ser submetido ao *J. Braz. Chem. Soc.*

O artigo número IV, resultado de participação em colaboração com o grupo de pesquisa do Prof. Eloi Feitosa, UNESP, não foi apresentado neste testo, porque não contém assuntos diretamente correlacionados com esta tese.

## Artigo III

Cationic liposomes in mixed didodecyldimethylammonium bromide and dioctadecyldimethylammonium bromide aqueous dispersions studied by differential scanning calorimetry, nile red fluorescence, and turbidity

Feitosa, Eloi; Alves, Fernanda Rosa; Niemiec, Anna; Oliveira, M. Elisabete; Castanheira, Elisabete M. S.; Baptista, Adelina L. F.

*Langmuir*, **2006**, 22, 3579

## Apresentações em congressos:

1. Apresentação de poster no “ICSS Congress”, Foz de Iguaçú, setembro de 2003
2. Apresentação de poster no “27° Encontro da Sociedade Brasileira de Química”, Salvador, maio de 2004.
3. Apresentação de poster no” SIS Symposium”, Fortaleza, junho de 2004.
4. Apresentação oral do trabalho: “Investigations on interaction of random versus block copolymers with ionic surfactants aqueous solutions studied by calorimetry” no CLAFQO8, Florianópolis, junho de 2005.
5. Apresentação de pôster no Congresso de Calorimetria, Águas de São Pedro, abril de 2006.

## Prêmios:

**Ganhadora do prêmio The William F. Giauque Memorial Award** durante 61st Calorimetry Conference, Boulder- EUA, agosto de 2006.

**Apresentação oral do trabalho:** „Random vs. block copolymers of Polyethylene Oxide and Polypropylene Oxide in Aqueous Solutions: Interaction with Ionic Surfactants”

# PROPERTIES OF SOLUTIONS OF RANDOM COPOLYMERS IN COMPARISON TO BLOCK COPOLYMERS: PHASE SEPARATION BINARY LIQUID SYSTEM FORMATION AND INTERACTION WITH SURFACTANTS

The subject of the thesis, as suggested by the title, draws on the formation of binary systems of copolymers in different solvents, as well as interaction of block and random copolymers of poly (ethylene oxide) and poly (propylene oxide) with various types of ionic surfactants: cationic, anionic and non-ionic. These studies are divided in three stages and each of it was concluded with publication or manuscript. In the first article it is included all investigation on interaction between block copolymer P123 and noni-onic surfactant $C_{12}EO_6$ monitored by calorimetry and light scattering. By applying these techniques a new phenomenon was observed in the P123-$C_{12}EO_6$ system, namely a well-defined sphere-to-rod transition of the mixed micelles and interesting application of calorimetric techniques has been identified due to its high sensitivity to this kind of intermolecular events detection. These studies were performed in collaboration with our partners from Lund University, Sweden, who conducted light scattering measurements. On the other hand, measurements on calorimetry have been done within our research group. Moreover, in the second paper interactions between random vs. block copolymers with ionic surfactants (cationic and anionic) has been discussed. These studies revealed an interaction similar to that observed with other hydrophilic homopolymers. Effects of temperature and of the nature of the ionic surfactants on their interaction with these copolymers were found to agree with the previously reported trends. As a complementary part of this article some additional results on interaction between random copolymer and non-ionic surfactants have been included in this thesis. Once again it was confirmed what is reported in the literature that non-ionic surfactants generally do not interact associatively with non-ionic polymers and interaction between P123 and $C_{12}EO_6$ is special to this system. As the last, it was included in this work the manuscript, which contains the comparative studies of biphasic systems constructed from block vs. random copolymers. It was verified in this studies that random copolymers present different phase behaviour than block copolymers. Lack of auto-association of these copolymers promotes their cloud points to be lower then cloud points of block copolymers. Due to this property these copolymers has enormous application in academic area in biochemistry or biotechnology for purification of biological materials as well as in other areas: for pollutants analysis, organic materials or metals.

# PROPRIEDADES DE SOLUÇÕES DE COPOLÍMEROS ESTATÍSTICOS EM COMPARAÇÃO COM EM BLOCO: SEPARAÇÃO DE FASES, FORMAÇÃO DE SISTEMAS LÍQUIDOS BIFÁSICOS E INTERAÇÃO COM SURFATANTES

O tema desta tese como sugerido pelo titulo aborda assuntos correlacionados com formação de sistemas binários de copolímeros em diferentes solventes como também com a interação entre copolímeros bloco e estatísticos de oxido de poli etileno e oxido de poli propileno com vários tipos de surfatantes iônicos: catiônicos, aniônicos e não iônicos. Os estudos deste trabalho foram divididos em três etapas, que foram concluídas com duas publicações e um manuscrito. Em primeiro artigo incluiu se todas as investigações correspondentes aos estudos de interação entre copolímeros em bloco P123 e surfatante não iônico $C_{12}EO_6$ monitorada por calorimetria e espalhamento de luz. Através deste estudo o novo fenômeno para sistema de P123 - $C_{12}EO_6$ foi observado, chamado de transição esferas-bastonetes e identificou-se alta aplicação de técnicas calorimétricas para monitoramento deste tipo de eventos intermoleculares. Este estudo foi executado em colaboração com o grupo de pesquisa da Universidade Lund na Suécia, que conduziu todos os experimentos que envolvem o espalhamento de luz. Por outro lado os experimentos na parte de calorimetria foram feitos dentro do nosso grupo. O segundo artigo descreve sistemas de copolímeros em bloco vs. estatísticos na interação com surfatantes iônicos: aniônicos, catiônicos. Estes estudos revelaram que copolímeros estatísticos interagem com copolímeros aniônicos da maneira parecida com que homopolímeros hidrofílicos. Efeito de temperatura foi investigado também através das técnicas calorimétricas e tendências previamente relatadas foram confirmadas. Como parte complementar a este artigo foram incluídos nesta tese alguns resultados calorimétricos da interação entre copolímeros estatísticos na região do ponto de turvação deles e surfatantes não iônicos, confirmando mais uma vez o que é conhecido da literatura que os surfatantes não-iônicos geralmente não interagem associativamente com polímeros não-iônicos e esta interação é especial para sistema P123 - $C_{12}EO_6$. Por último inclui se neste trabalho o manuscrito que contem um estudo comparativo de sistemas bifásicos de copolímeros em bloco vs. estatísticos. Verificou se neste estudo que os copolímeros estatísticos apresentam diferente comportamento na separação de fases, do que copolímeros em bloco. Devido a falta de auto - agregação destes copolímeros os pontos de turvação deles são menos elevados em comparação com copolímeros em bloco o que devido a esta propriedade tem enorme aplicação na área acadêmica em bioquímica e biotecnologia para purificação de materiais biológicos como também em outras áreas: analise de poluentes, compostos orgânicos,metais.

# ÍNDICE

CAPÍTULO I – INTRODUÇÃO.....................................................................1

1.1 – Sistemas Poliméricos.................................................................2

1.2 – Sistemas de surfatantes iônicos e não iônicos.............................. 4

1.3 – Copolímeros bloco vs. estatísticos................................................5

1.3.1 – Comportamentos LCST e UCST.....................................5

1.3.2 - Interações entre copolímeros bloco vs. estatísticos com surfatantes.........................................8

1.3.2.1 Copolímeros e surfatantes aniônicos…………….......8

1.3.2.2 Copolímeros e surfatantes catiônicos…………....13

1.3.2.3 Copolímeros e surfatantes não – iônicos..............15

1.3.2.4 Copolímeros estatísticos e surfatantes não iônicos........................................................19

Bibliografia.........................................................................................21

CAPÍTULO II - OBJETIVOS.....................................................23

CAPÍTULO III - PARTE EXPERIMENTAL

3.1 - Reagentes........................................................................................24

3.2 - Metodologia....................................................................................27

3.3 - Equipamentos

3.3.1 – VP-ITC - Titulação Calorimétrica Isotérmica.................27

3.3.2 - VP-DSC - Calorimetria Diferencial de Varredura............30
3.4 – Análise de Dados
3.4.1 – VP-ITC......................................................................30
3.4.2 – VP-DSC....................................................................33
3.5 - Técnicas Experimentais Complementares……………..……......34
Bibliografia...................................................................................35

**CAPÍTULO IV – ARTIGO I –** A Calorimetic and Light Scattering Study of the formation and shapeTransition of Mixed Micelles of $EO_{20}PO_{68}EO_{20}$ Triblock Copolymers (P123) and Nonionic Surfactants ($C_{12}EO_6$)

Abstract.......................................................................................38
Introduction..................................................................................39

Experimental

Materials......................................................................................41
Isothermal Titration Calorimetry...............................................42
Dinamic and Static Light Scattering…………………..................42
DLS Data Analysis.....................................................................43

Results

DSC Measurements...................................................................45
Phase Map..................................................................................50
ITC Measurements.....................................................................51
Dinamic and Static Light Scattering..........................................56
Time-resolved DLS and SLS.....................................................61

Discussion……………………………………………………..………63
Acknowledgements……………………………………………..……..68
References.........................................................................................69

**CAPÍTULO V – ARTIGO II** – Interaction of propylene oxide-ethylene oxide-propylene oxide copolymers with ionic surfactants studied by calorimetry: random *versus* block copolymers

Abstract…………………………………………………………......75
Introduction.......................................................................................76

Experimental

Materials...........................................................................................79
Isothermal Titration Calorimetry...............................................82
Differential Scanning Calorimetry…………………......................82
Nuclear Magnetic Resonance.........................................................................83
Gel Permeation chromatography……………………...……..83
Cloud Point Measurements………………………………………..84

Results

Interaction between SDS and random copolymers……….....…84
Random copolymers versus block copolymers...........................91
Effects of temperature and surfactant structure on the interaction……………………………………………………96
Discussion.........................................................................................99

Conclusions........................................................................................106
Acknowledgements………………………….....………………107
References...........................................................................................107

## **CAPÍTULO VI – ARTIGO III** – Binary phase diagrams of block vs. random ethylene oxide propylene copolymers in water and organic solvents

Abstract…………………………………………………...…112
Introduction........................................................................................113

Experimental

Materials...............................................................................................118
Phase Binary Diagrams Determination
by Visual Analysis Method…...............................................................119

Results

Binary phase diagrams of block vs.
random copolymers in water…………………………..……….120
Binary phase diagrams of block vs.
random copolymers organic solvents……………………...……….123
Discussion...........................................................................................130
Conclusions........................................................................................134
Acknowledgements…………………………………………...…134
References...........................................................................................134

**CAPÍTULO VII - CONCLUSÃO**...............................................137

# CAPÍTULO I - INTRODUÇÃO

Este estudo sobre sistemas de misturas entre copolímeros e surfatantes, foi escolhido devido à importância considerável destes sistemas, tanto em pesquisa cientifica como em aplicações industriais. Na literatura existem vários trabalhos que caracterizam separadamente estes copolímeros, mas não se encontra nenhum estudo comparativo falando das diferenças e similaridades de alguns destes copolímeros. Através desta perspectiva, nosso interesse neste trabalho foi comparar propriedades de soluções de copolímeros em bloco *versus* estatísticos, usando técnicas mencionadas acima. Como resultado deste estudo foram publicados dois artigos apresentados ao longo do texto (vide capitulo IV e V) e a terceira parte do trabalho está descrita na forma de um manuscrito (capitulo V) também incluído nesta tese.

Neste estudo, usaram-se como ferramentas principais as seguintes técnicas calorimétricas:

- Calorimetria Isotérmica de Titulação (ITC);
- Calorimetria Diferencial de Varredura de Alta Sensibilidade (HS-DSC);

para a determinação de vários parâmetros termodinâmicos importantes, permitindo, desta maneira, a caracterização da interação entre copolímeros e surfatantes.

Também neste trabalho foram utilizados como técnicas/métodos complementares:

- Medidas de Espalhamento de luz (DLS/SLS)
- Cromatografia por Permeação em Gel (GPC)
- Ressonância Magnética Nuclear (RMN)

- Métodos de Análise Visual;

para a determinação de estrutura, tamanho e composição de complexos formados entre copolímeros e surfatantes, como também para o mapeamento de diagramas de fases binários de copolímeros bloco *versus* estatísticos. Estes estudos permitiram observar a influência da temperatura, composição, massa molar e balanço hidrofóbico / hidrofílico dos copolímeros para suas possíveis separação de fases. Estas técnicas de avaliação são descritas detalhadamente na parte experimental deste trabalho.

## 1.1 Sistemas poliméricos.

Copolímeros são derivados de mais de uma espécie de monômeros permitindo desta forma uma combinação de propriedades de diferentes polímeros. Dependendo do procedimento de polimerização, eles podem apresentar vários tipos de arranjos moleculares como, por exemplo, copolímero em bloco, estatístico, grafitizado ou na forma de estrela.

Os copolímeros consistem de unidades de monômeros (iônicas ou não-iônicas) de diferentes composições químicas, por exemplo, A e B. Quando as unidades de monômeros de cada tipo estão organizadas em seqüências, separadas em blocos, como AAAA ou BBBB, estes blocos fazem ligações entre si, e o polímero recebe o nome de copolímero-bloco[1,2]. Os copolímeros triblocos não-iônicos são amplamente discutidos na literatura. Os mais estudados consistem de partes hidrofílicas – blocos de poli (óxido de etileno), PEO - e partes hidrofóbicas – blocos de poli (óxido de propileno), PPO (por causa da presença do grupo de metila) - também abreviados por PEO-PPO-PEO (ou $EO_n$-$PO_m$-$EO_n$).

A principal diferença entre copolímeros em bloco e estatísticos é a distribuição destes grupos na cadeia polimérica. No caso de copolímeros - bloco quando são hidrofílicos / hidrofóbicos são tensoativos e formam micelas em soluções aquosas, dependendo dos comprimentos relativos dos blocos, da concentração e da temperatura.

Por outro lado os copolímeros estatísticos não contêm uma seqüência agrupada das unidades de monômeros na cadeia polimérica, sendo conhecidos também como copolímeros aleatórios, e a sua estrutura determina provavelmente a não ocorrência de auto-agregação. É possível assumir que apesar da grande maioria dos copolímeros estatísticos serem preparados por polimerização simultânea de óxido de etileno e óxido de propileno, não é possível excluir o fato que algumas partes da cadeia polimérica sejam ricas em óxido de propileno, permitindo a formação de domínios hidrofóbicos. Mesmo assim, os resultados obtidos por medidas de espalhamento de luz e relatados na literatura[3] confirmaram a ausência de agregados intermoleculares para vários copolímeros estatísticos EO/PO em solução aquosa, e a existência de moléculas não agregadas em solução aquosa.Os resultados obtidos por calorimetria e descritos nesta tese também confirmaram esta hipótese. A alta sensibilidade dos calorímetros utilizados, permitiu uma grande aplicação na determinação deste tipo de interações intermoleculares, além de outros efeitos que poderão ser monitorados utilizando esta técnica.

Neste estudo os copolímeros foram organizados em agrupamentos que permitiram a comparação direta em termos de quantidade de grupos EO e massa molar do copolímero. Por exemplo, o copolímero bloco de massa molar 1900 g/mol e 50 % m/m de grupos EO foi comparado com copolímero estatístico de massa molar semelhante (1700 g/mol) com a mesma quantidade de grupos EO. Além disso, foram estudados, para melhor compreensão da interação entre copolímero bloco *versus* estatístico com surfatantes, sistemas de homopolímeros de PPO e PEO e suas misturas físicas.

## 1.2 Sistemas de surfatantes iônicos e não iônicos

Surfatantes conhecidos também pelo nome de tensoativos, são substâncias que apresentam adsorção em superfícies ou interfaces. Tensoativos, em conjunto com polímeros têm enorme aplicação para garantir a estabilidade de dispersões ou emulsões, modificações de reologia e outras características específicas de uma formulação. Numa certa concentração crítica de unímeros de surfatantes eles tendem a se agrupar, formando agregados chamados de micelas. Esta concentração pode ser chamada também de concentração micelar critica, geralmente abreviada como *cmc*. Dependendo de sua estrutura química, os surfatantes são divididos em classes: aniônicas, catiônicas, não-iônicas e zwiteriônicas[4].

Vários surfatantes iônicos e não iônicos foram utilizados neste estudo. Estruturas apresentadas em primeiro lugar são de surfatantes iônicos: catiônicos e aniônicos. A principal diferença entre eles seria: comprimento da cadeia carbônica, tamanho de grupo polar, carga e tipo de contra íon. Durante este estudo foram utilizados: CTAB (brometo de cetiltrimetilamônio), um surfatante catiônico constituído de dezesseis átomos de carbonos na cadeia alquílica. O restante dos surfatantes aplicados neste trabalho, como DAC (cloreto de dodecil amônio) e SDS (dodecilsulfato de sódio) apresentam doze átomos de carbonos na cadeia carbônica. Os dois surfatantes CTAB e DTAB têm exatamente o mesmo grupo polar (trimetil amônio), em contrapartida, o DAC tem um grupo polar menor constituído somente por um grupo amônio e SDS como um surfatante aniônico contém grupos aniônicos de sulfato. Os surfatantes não iônicos utilizados neste estudo, hexaetileno glicol mono-n-dodecil éter - $C_{12}EO_6$, e octaetileno glicol mono-n- dodecil éter - $C_{12}EO_8$ também contém doze átomos de carbonos na cadeia carbônica, que estão interligados com mais seis ou oito grupos de oxido de etileno. As interações entre copolímeros estatísticos ou copolímeros bloco com surfatantes iônicos e não iônicos foram monitoradas por medidas de calorimetria e espalhamento de luz.

## 1.3 Copolímeros bloco vs. estatísticos

### 1.3.1 Comportamentos LCST e UCST

Através deste trabalho, desenvolvido em nosso grupo de pesquisa, foi possível verificar que os copolímeros EO/PO apresentam um comportamento oposto de miscibilidade com a variação de temperatura LCST (*lower critical solution temperature*) em água e UCST (*upper critical solution temperature*) em solventes orgânicos. O sistema que separa em fases com o abaixamento da temperatura apresenta uma temperatura crítica que é denominada UCST e o sistema que demonstra o comportamento oposto com aumento da temperatura possui uma temperatura crítica denominada LCST, conforme apresentado na **Figura 1 a, b.**

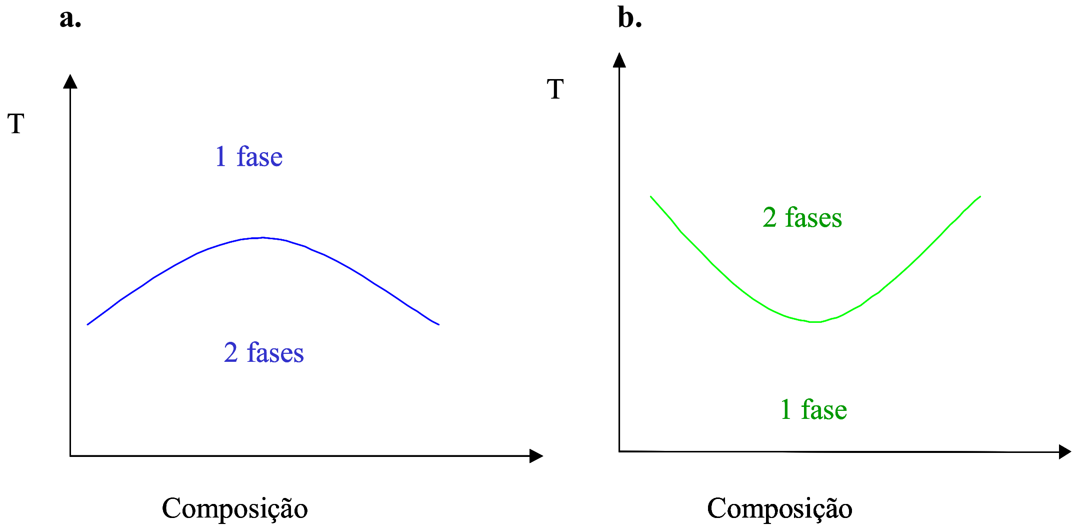

**Figura 1.** Comportamento **a.** UCST **b.** LCST de sistemas binários em função da temperatura e composição para copolímero em bloco e / ou copolímero estatístico em água.

Este comportamento é característico também no caso de soluções contendo o polímero PEO. Saeki[5] e colaboradores obtiveram previamente diagramas de fases de PEO, de diferentes massas molares em água e acetato de t - butila. Na literatura existem vários modelos que explicam a separação de fases do tipo LCST que apresenta PEO em água. Alguns destes modelos propõem que o PEO é altamente solúvel em água, devido à capacidade de realizar ligações de hidrogênio. A separação de fases em temperaturas maiores ocorre porque parte destas ligações seriam desfeitas[6]. Outros justificam esta alta solubilidade correlacionando a alta capacidade de acomodação da estrutura do PEO na estrutura hexagonal da água ou por causa da diminuição da liberdade conformacional do polímero, devido à negativa entropia de mistura entre o polímero e água[7,8]. Estudos para sistemas semelhantes foram realizados e relatados por Ananthapadmanabhan e Goddard[9] e também pelo grupo de Tjerneld[10].

Para os sistemas estudados em nosso grupo de pesquisa foi possível observar que, em água, copolímeros bloco com similar massa molar e porcentagem de EO de copolímeros estatísticos, apresentaram maiores temperaturas de turvação Tc (menor região de duas fases) devido à sua auto-associação em água. Estes copolímeros conseguem esconder as suas partes menos hidrofílicas (unidades PO) e expor as unidades mais hidrofílicas (unidades EO), formando micelas ou mesofases (estruturas organizadas de diferentes geometrias como, por exemplo, estrutura hexagonal, lamelar etc), em temperaturas superiores quando ocorre um aumento da desidratação da cadeia polimérica, conforme apresentado na Figura 2.

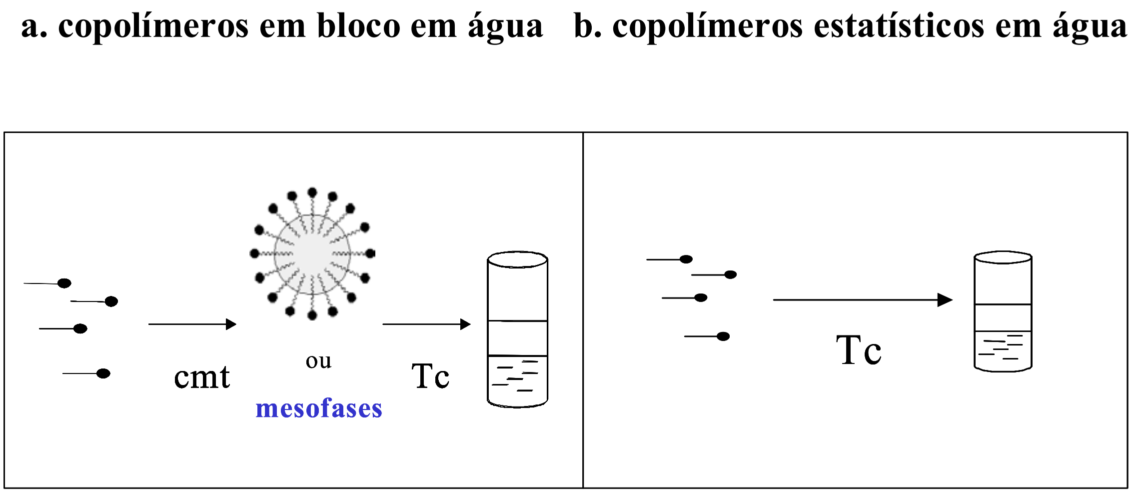

**a. copolímeros em bloco em água** **b. copolímeros estatísticos em água**

**Figura 2:** Comportamento de soluções aquosas de copolímeros em bloco **a.** *versus* copolímeros estatísticos **b.** de similar massa molar e porcentagem de grupos EO em função de temperatura e composição.

Devido, provavelmente, ao rompimento das ligações de hidrogênio entre a água e as unidades EO, ocorre primeiramente a formação de agregados (na temperatura crítica de micelização, *cmt*) o que pode ser seguido por um crescimento dos mesmos até que ocorra finalmente (na temperatura de turvação, Tc) a separação em fases. Em contrapartida, a situação para polímeros em solventes orgânicos é mais complexa, onde algumas hipóteses podem ser aplicadas. A região de duas fases no caso de solventes orgânicos é menor em comparação com soluções aquosas. Existe a possibilidade de formação de vários tipos de agregados, como por exemplo, micelas reversas ou micelas esféricas em solvente seletivo ao bloco do meio da cadeia polimérica ou podem se formar redes micelares[11]. A falta de dados relacionados aos equilíbrios de fase nestes sistemas binários (polímeros aleatórios vs. bloco com água/solvente orgânico) incentivou o estudo relacionado a este tema e esta relatado com mais detalhes no manuscrito.

### 1.3.2 Interações entre copolímeros bloco *versus* estatísticos com surfatantes

#### 1.3.2.1 Polímeros e surfatantes aniônicos

Polímeros em geral têm a habilidade de induzir a agregação de surfatante e as técnicas calorimétricas são muito sensíveis para a detecção deste tipo de eventos intermoleculares. A interação entre polímero e surfatante depende de vários parâmetros como, por exemplo: temperatura, porcentagem de grupos EO e estrutura do polímero e surfatante.

Como um exemplo, o monitoramento da interação entre o polímero PEO 3500 e surfatante SDS, está apresentado na Figura 3.

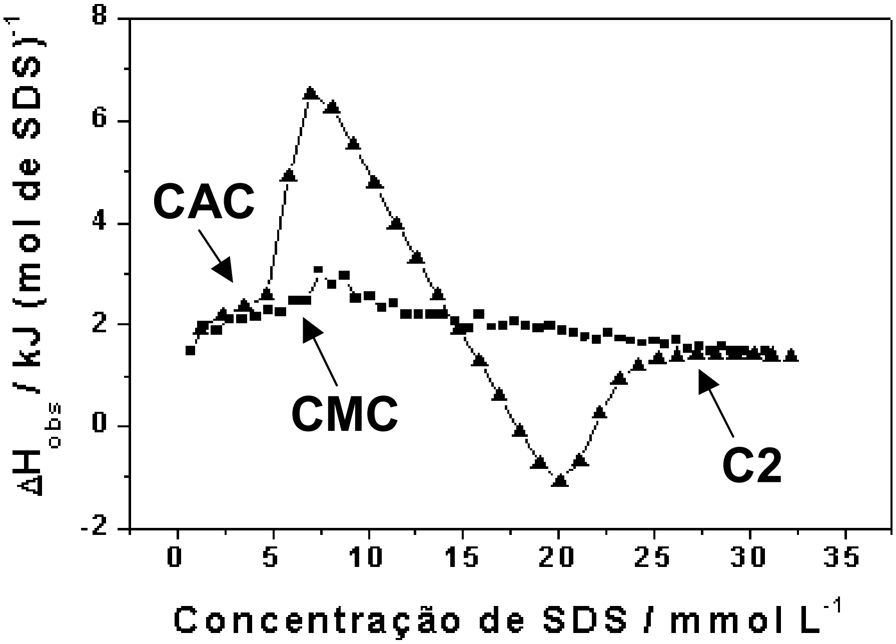

**Figura 3:** Resultado de uma medida feita por ITC para a adição de ■ 10 m/m % SDS para ▲ 0,1 m/m % PEO 3500 em água à 25°C[19].

A alta sensibilidade das técnicas calorimétricas permite o acompanhamento da evolução do processo de agregação quando a temperatura ou a composição da solução é variada. As técnicas calorimétricas fornecem também a possibilidade de monitoramento da intensidade de interação por meio do parâmetro denominado *cac* (concentração de agregação crítica), que corresponde à concentração de surfatante na qual o complexo polímero-surfatante começa a ser formado cooperativamente conforme indicado na Figura 3, como também informação sobre mudanças na hidratação do polímero, número de moléculas de surfatante ligadas por cadeia de polímero etc. É muito comum encontrar na literatura estudos sobre misturas de copolímeros e surfatantes. Especialmente os copolímeros em bloco da família de EO-PO-EO que apresentam comportamento de surfatantes devido à auto-agregação deles em soluções aquosas conforme foi extensivamente investigada[11,12,13].No caso destes copolímeros foi comprovado que a agregação pode ser promovida por mudanças de temperatura (associada com a temperatura critica de micelização - *cmt*) como também pelas variações na concentração da solução aquosa do copolímero (definida como concentração crítica micelar – *cmc*). Esta agregação é um processo endotérmico dirigido pelo ganho de entropia associado com liberação de moléculas de água após da micelização do copolímero, permitindo desta forma afastamento da água dos grupos hidrofóbicos PO, que agora estarão escondidos na parte interior da micela. Estes copolímeros tendem também a formar outros tipos de agregados, que apresentam diferentes geometrias, incluindo mesofases[13] ou vesículas[14]. Adição de surfatante afeta significativamente os agregados destes copolímeros. Com adição de surfatante iônico, como SDS os dois tipos de estruturas mesofases e / ou micelas de copolímeros se rompem, o que resulta na formação de agregados mistos solúveis em água que podem coexistir em solução junto com outras populações de agregados[26, 15].

Na literatura existem estudos com sistema de PEO na forma de estrela, com sistema de copolímero inverso PO-EO-PO[16] ou com PEO *end-capped*[17] formados por grupos hidrofóbicos interagindo com surfatantes que confirmou a importância da influencia da geometria do polímero na associação. Estes estudos preliminares motivaram as investigações comparando o comportamento destes sistemas de copolímeros em bloco versus estatísticos na interação com surfatantes iônicos.

Para o sistema de surfatante iônico (SDS) interagindo com o copolímero estatístico, mediu-se durante todo este estudo, por meio de calorimetria a variação de entalpia, à temperatura constante. O polímero interage com micelas de SDS e, para o surfatante poder esconder as suas partes mais hidrofóbicas (grupos alquila), ocorre a interação com grupos hidrofílicos EO, precedida pela desidratação do PEO. Adição de maior quantidade de surfatante causa, provavelmente, à reidratação de polímero, quando as partes mais hidrofílicas do polímero (grupos EO no caso) estejam mais expostas para o contato com a água. Por fim, a saturação de polímero pelas moléculas de surfatante ocorre, denominada como $C_2$ (concentração de saturação) e não observa se mais a interação, o que geralmente é visualizado por duas curvas que começam se sobrepor como apresentado na Figura 3.

No caso de copolímero bloco e surfatante SDS, este experimento de calorimetria pode ser feito abaixo da *cmt* do polímero, quando as macromoléculas existem em solução na forma não agregada, denominada unímero. A desidratação do polímero ocorre devido à competição entre as moléculas de água e as de surfatante.O surfatante acaba interagindo com o polímero. Como as cadeias dos grupos EO são, neste caso, suficientemente pequenas (massa molar até 1500 g/mol) não há formação de agregados, o que já foi relatado anterioramente para outros sistemas,[19] e somente grupos PO participam nesta interação com o surfatante[18]. A *cac*, neste caso, é de 0,9 mmol/L e este valor é parecido com aquele para um homopolímero de PPO interagindo com SDS, e também com a *cac* da mistura física entre homopolímero PEO e PPO.

Outro conjunto de resultados, para um outro copolímero bloco e SDS *versus* mistura física de homopolímeros e SDS, mostraram uma alteração na curva calorimétrica. Os resultados apresentaram que além da primeira região endotérmica correspondente à interação entre grupos PPO e SDS aparece também a segunda região endotérmica devido à interação entre SDS e PEO. Isto acontece somente para copolímeros bloco ou misturas físicas de PEO e PPO contendo PEO de M >1500g/mol. Novamente, os dados relatados na literatura para PEO pequenos interagindo com SDS demonstram falta de interação entre estes polímeros e este surfatante[19].

Ao fazer uma comparação direta da interação entre SDS e copolímero bloco *versus* estatístico, observa-se que esta interação para SDS e copolímero bloco é mais intensa do que a interação do copolímero estatístico e o mesmo surfatante (por exemplo, entre $EO_{34}$-$PO_{25}$ e SDS), o que reflete nos valores de *cac* que para copolímeros bloco serem menores do que para copolímeros estatísticos. Isto significa que copolímeros bloco interagem com surfatantes iônicos de modo diferente do que os copolímeros estatístico, devido, provavelmente, à diferente distribuição de grupos PO na cadeia polimérica.

A partir das curvas de titulação dos copolímeros estatísticos com SDS, os valores para *cac* podem ser calculados e comparados com os valores dos *cac* para interação com homopolímeros de PPO e PEO. Para o PPO, o efeito de sua massa molar é observado e a *cac*. diminui com o aumento da massa molar do polímero. Os polímeros PEO com massa molar maior do que 1500 g/mol apresentaram valores constantes para a *cac*, ao redor de 4,2 mmol/L[20]. A partir da comparação destes valores de *cac* é possível indicar que a *cac* está diminuindo com o aumento do número de grupos EO da cadeia polimérica. Isto significa que a hidrofobicidade da cadeia polimérica está influenciando a interação entre polímeros e surfatantes e por causa disso existe uma considerável interferência na *cac* para interações de vários polímeros com SDS; PEO[18,19,21,22]; PNIPAM[23]; PPO [21,24]; copolímeros bloco EO/PO e copolímeros aleatórios EO/PO. A interação torna-se mais intensa com o aumento da porcentagem de unidades PO no caso de copolímeros bloco ou estatísticos.

Conforme já descrito anteriormente, os polímeros estatísticos apresentaram uma forte dependência da temperatura para o seu comportamento em solução, estando de acordo com seu baixo LCST. Este tipo de comportamento está de acordo com os estudos relatados para PNIPAM e SDS, sugerindo mecanismo semelhante de interação[23] Por outro lado, para sistema de PEO e SDS relatado na literatura [19] não se observou mudança no modo de interação entre polímero e surfatante com variação de temperatura.

#### 1.3.2.2 Copolímeros e surfatantes catiônicos

A interação dos surfatantes catiônicos (DTAB, CTAB) com os copolímeros estatísticos também foi estudada usando calorimetria e neste caso, nenhum sinal de interação com surfatantes catiônicos, mesmo em altas temperaturas, foi observado. É conhecido que surfatantes catiônicos não interagem tão fortemente (ou não interagem por completo) com polímeros não-iônicos, em comparação aos surfatantes aniônicos. Ao elevar a temperatura para 60°C, 66°C (isto é na região próximo ou acima do ponto de turvação de polímero) observa-se mudança na forma da curva. Entre 60-66°C pode ser observado um processo exotérmico, devido a reidratação do polímero, causada pela presença do surfatante, que desagrega o polímero o que também reflete no aumento de temperatura de turvação do polímero nesta concentração de surfatante. O processo de reidratação é seguido por um processo de desidratação do polímero, novamente semelhante à interação com os copolímeros - bloco.

Ao utilizarmos diferentes surfatantes iônicos, foram observadas contribuições distintas devido às diferentes estruturas químicas de surfatantes. No caso da DAC, DTAB, CTAB, observa-se a influência dos volumes dos grupos polares (DAC *versus* DTAB) e da hidrofobicidade de cadeia de hidrocarboneto do surfatante (CTAB *versus* DTAB). Somente os copolímeros estatísticos com baixas temperaturas de turvação [$T_c$] apresentaram interação com os surfatantes CTAB, DTAB ou DAC perto do $T_c$ ou acima de $T_c$. Valores de *cac* representam a intensidade de interação destes surfatantes com o copolímero estatístico. Para caracterizar esta intensidade de interação entre copolímeros estatísticos e surfatantes iônicos, utilizou-se o parâmetro termodinâmico $\Delta G_{p,s}$. A equação que calcula a variação da energia livre é [23]:

$$\Delta G_{p,s} = \Delta G_{agg} - \Delta G_{mic} = RT \ln\left(\frac{cac}{cmc}\right) \qquad \text{eq. 1}$$

onde, $\Delta G_{p,s}$ é um parâmetro referente à diferença entre energia livre do monômero de surfatante presente na micela livre e energia livre do monômero dentro do agregado.

Portanto quando mais negativo o valor desta energia $\Delta G_{p,s}$ mais favorável é a transferência do surfatante para o agregado, ou seja, a interação entre o polímero e surfatante é mais intensa. A variação da energia livre de Gibbs, $\Delta G_{p,s}$ foi estimada para vários surfatantes e um escolhido copolímero estatístico $EO_{34}PO_{25}$ na temperatura de turvação, 58°C. Os valores de $\Delta G$ (-5,0; -3,9; -2,7; -1,2 kJ/mol) respectivamente, para interação surfatantes -

copolímero estatístico determinaram a seqüência de intensidade de interação entre surfatante e copolímero: **SDS>CTAB>DAC>DTAB**

### 1.3.2.3 Copolímeros e surfatantes não – iônicos

Por último estudou-se a interação entre copolímero bloco e surfatante não-iônico $C_{12}EO_6$ em colaboração com grupo da Universidade Lund, Suécia. A interação entre surfatantes iônicos e polímeros não-iônicos foi extensivamente estudada e relatada na literatura [25,26], mas somente alguns estudos foram realizados a respeito da interação entre polímeros não-iônicos e surfatantes não-iônicos. Técnicas calorimétricas demonstraram, neste caso, sua importância, produzindo surpreendentes resultados que confirmaram a afinidade entre estas duas espécies químicas. Para estudos preliminares, foi escolhido um polímero bloco de nome comercial P123 ($EO_{20}$-$PO_{68}$-$EO_{20}$) e surfatante $C_{12}EO_6$ , monodecil éter de hexa(óxido de etileno). Os estudos foram realizados utilizando as técnicas de ITC e HSDSC e como resultado obtiveram se várias curvas apresentadas no artigo publicado. As medidas de titulação calorimétrica foram realizadas em condições isotérmicas, à 40°C, onde o copolímero P123 apresentava sua forma micelar esférica (para concentrações ao redor de 1% m/m, confirmada por experimentos de HSDSC**.** Uma solução concentrada contendo micelas de $C_{12}EO_6$ foi titulada em pequenas porções dentro de uma solução de micelas de $EO_{20}$-$PO_{68}$-$EO_{20}$. O sinal apresentado pelo calorímetro mostrou a interação observada para a variação de entalpia por mol de surfatante. Adições de surfatante em concentração baixa produzem alterações na entalpia de interação, devido à quebra das micelas de surfatante e a formação de novos agregados junto com o polímero. A formação de complexo misto foi confirmada também pelos diagramas de fases determinados por Löf e colaboradores[27], confirmando a existência de todas as soluções em uma única fase (em todas as temperaturas estudadas) e ocorrência de separação de fases associativa. Além disso, na curva de titulação, para uma razão molar específica, a diminuição de seus valores de ΔH observada ocorre na região de mínimo. A mudança da concentração de polímero de 0,1-1,0% m/m titulado por $C_{12}EO_{6}$, não muda a posição do mínimo, quando comparando as curvas em termos de razões molares, que confirma o mesmo comportamento sempre na mesma razão molar entre copolímero e surfatante. A origem desta região menos endotérmica é atribuída á interação entre polímero e surfatante causando a transição da forma das micelas de P123, de esféricas para cilindros. Olhando os resultados provenientes do calorímetro de titulação observa se que na região de razão molar 2,1-2,2 esta transição apresentou um processo rápido endotérmico e em seguida um processo exotérmico lento (conforme apresentado no zoom) que durou entre 15 - 20 min. (Figura 4).

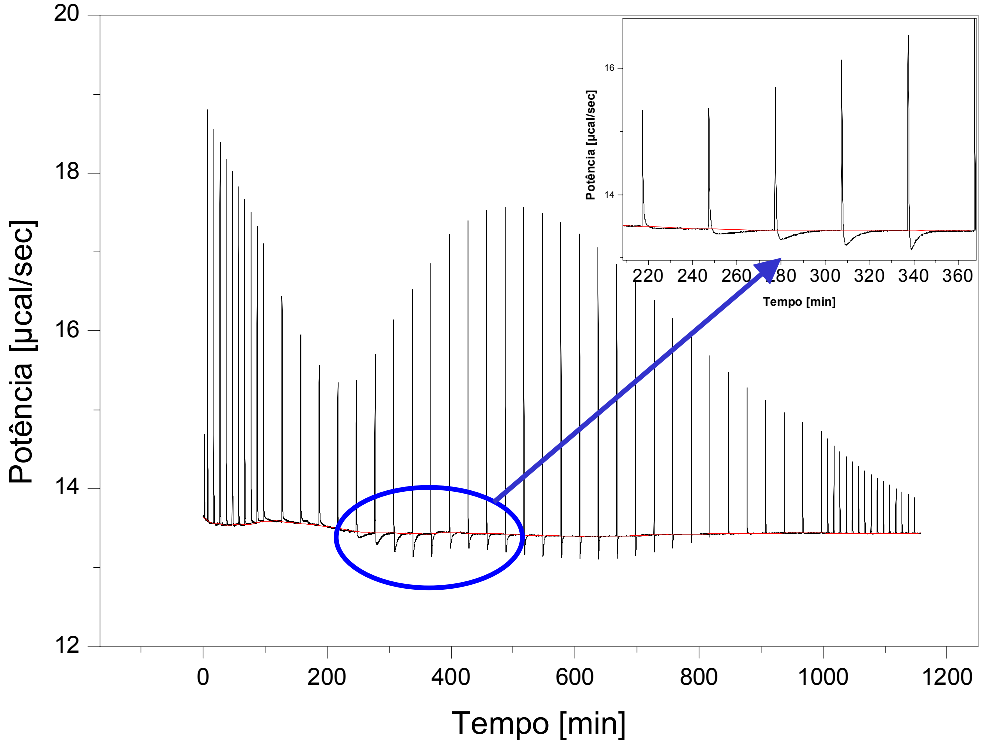

**Figura 4:** Resultado proveniente do calorímetro ITC para sistema de $EO_{20}$-$PO_{68}$-$EO_{20}$ (P123) e $C_{12}EO_6$.

Estes processos correspondem perfeitamente à razão molar na qual processos lentos também foram observadas com experimentos de espalhamento de luz, à 40°C. Estas observações estão de acordo com os resultados obtidos por DSC, conforme apresentado na Figura 5.

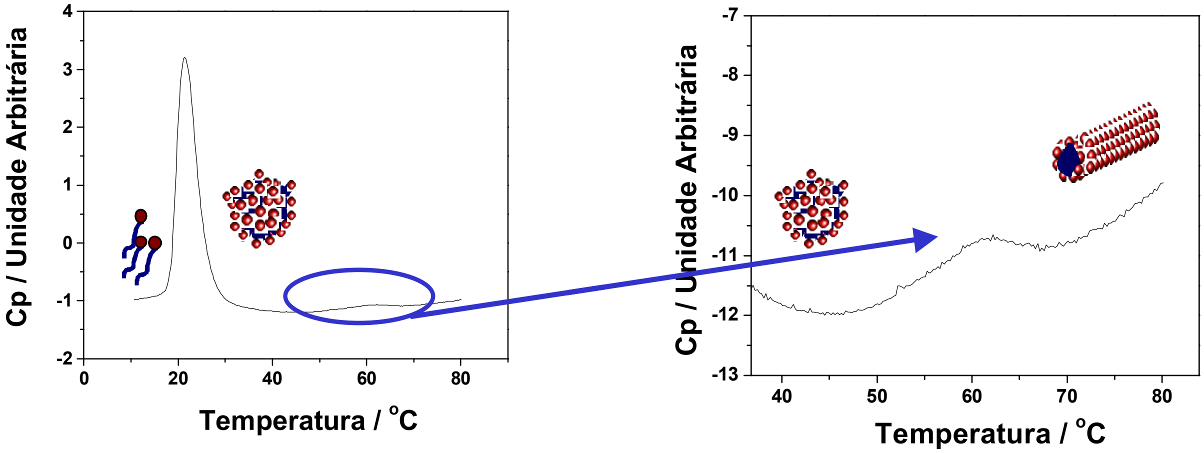

**a.** agregação de copolímero

**b.** transição esfera-cilindro

**Figura 5:** Curva de DSC para copolímero – bloco P123.

Análises mais detalhadas foram realizadas com relação às curvas de DSC (capacidade calorífica aparente *versus* temperatura) e confirmou-se o que foi visto por ITC. Para P123, em água, a curva maior (na região de temperaturas menores cerca de 20ºC) é devido à agregação em micelas e um pico muito menor é evidente em altas temperaturas com T(onset) = 48-50°C (a temperatura na qual se iniciou a transição de processo de agregação de copolímero) e T(max) = 61°C (à temperatura máxima da transição de polímero da forma de unímeros para agregados) . A origem deste pico é a transição da forma das micelas de P123, de esféricas para cilindros. O processo de micelização e de transição da forma micelar esférica para cilindro apresenta uma dependência com aumento da concentração de surfatante. A temperatura de formação de micelas (*cmt*) diminui com aumento da concentração de surfatante e a temperatura de transição da forma da micela também muda conforme aumentando a concentração do surfatante. Para a razão molar igual a 2,1-2,2, estes valores de temperatura estão em acordo com os resultados obtidos por ITC.

### 1.3.2.4 Copolímeros estatísticos e surfatantes não ionicos

Conforme mencionado na seção acima, normalmente não se espera uma interação entre polímero não-iônico e surfatante não-iônico e devido a isto, existem poucos estudos sobre este tipo de sistemas na literatura. Verificou-se que para copolímeros-bloco em condições específicas, esta interação pode ocorrer e surgiu a dúvida se o mesmo efeito poderia se repetir para copolímeros estatísticos caso a interação entre o polímero e surfatante fosse medida na região próxima ou acima de turvação do polímero, isto é, na região de formação de agregados. Para o copolímero estatístico escolhido ($EO_{34}$-$PO_{25}$), esta temperatura de agregação é de 58°C. As Figuras 6 a, b obtidas após o experimento estão apresentadas abaixo, para o polímero $EO_{34}$-$PO_{25}$ e surfatantes não iônicos $C_{12}EO_6$ e $C_{12}EO_8$, confirmando a não detecção de interação.

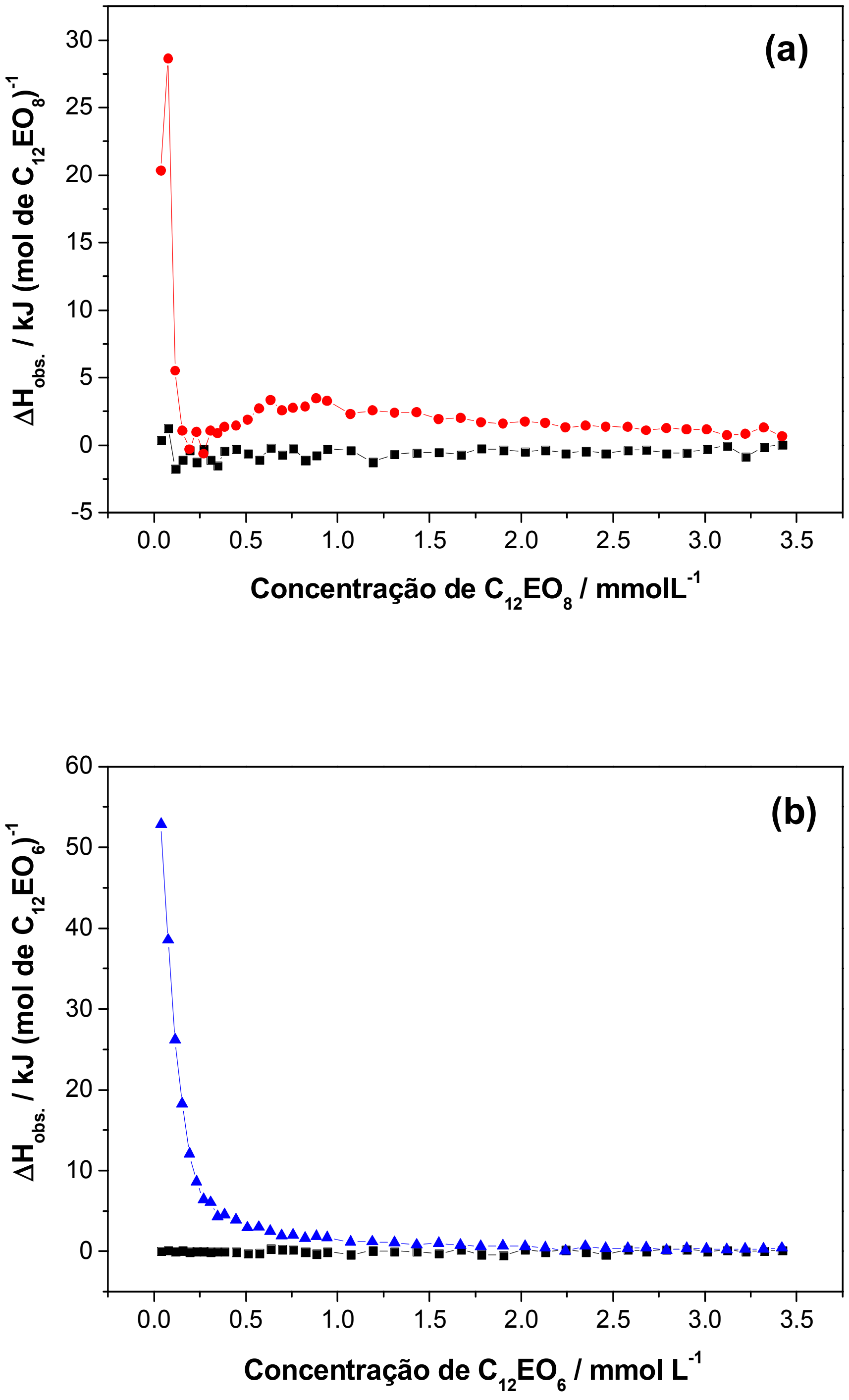

**Figura 6:** Curvas de ITC : ■ solução aquosa de 0.1 m/m % polímero $EO_{34}$-$PO_{25}$ titulada com **(a)** ● 1.0m/m% $C_{12}EO_8$ e **(b)** ▲ 1.0 m/m % $C_{12}EO_6$, à 58°C.

# BIBLIOGRAFIA

[1] Schillén K.; Solution Properties of Block Copolymers Studied Using Light Scattering, Universidade Uppsala 1994, Tese de doutorado.

[2] Riess, G.; Hurtez,G.; Bahadur, P. In *Encyclopedia of Polymer Science & Engineering*, 2nd ed., Vol.2;John Wiley & Sons: New York, 1985, p 324

[3] Nilsson A., Neves-Petersen MT., Johansson HO., Jansson J., Schillen K., Tjerneld F., Petersen SB; *Biochim. Biophys. Acta- Proteins and Proteomics,* **2003**, 1646, 57

[4] Jönsson, B.; Lindman, B.; Holmberg, K.; Kronberg, B.; *"Surfactants and Polymers in Aqueous Solution"*, John Wiley & Sons: New York 1999, p 2

[5] Saeki S., Kuwahara N., Nakata M., Kaneko., M; *Polymer*, **1976**, 17, 685

[6] Goldstein, R.E.; *J. Chem. Phys*, **1984**, 80, 5340

[7] Blandemer M. J., Fox M.F., Powell E., Stafford J.W., *Makromol. Chem,* **1969**, 124, 222

[8] Kjellander R., Florin E., *J. Chem. Soc. Faraday Trans. I,* **1981**, 77, 2053

[9] Ananthapadmanabhan K.P ., Goddard E.D; *Colloids Surf.*, **1987**, 25, 393

[10] Cunha M.T., Tjerneld F.,Cabral J.M.S., Aires-Barros M.R.; *J. Chromat. B,* **1998**, 53, 60

[11] Loh, W.; Block copolymer micelles. In: Arthur Hubbard. (Ed.). Encyclopedia of Colloid and Surface Science. New York: Marcel Dekker, 2002, p 802

[12] Mortensen, K. *J. Phys. Cond. Matt.* **1996**, 8, 103

[13] Alexandridis, P.; Hatton, T. A.; *Colloids Surf. A,* **1995,** 96, 1 .

[14] Bryskhe, K.; Jansson, J.; Topgaard, D.; Schillen, K.; Olsson, U. *J. Phys. Chem. B* **2004**, 108, 9710

[15] Jansson, J; Schillen, K; Olofsson, G; da Silva, RC; Loh, W. *J. Phys. Chem. B* **2004**, 108, 82

[16] Dai, S.; Tam, K.C.; Li, L. *Macromolecules* **2001**, 34, 7049

[17] Dai, S.; Tam, K.C.; Li, L. *Macromolecules* **2001**, 34, 4673

[18] Dai, S.; Tam, K.C. *Colloids and Surf. A,* **2006**, 289, 200

[19] da Silva, RC; Loh, W; Olofsson, G *Thermochim. Acta* **2004,** 417, 295

[20] Wang G, Ethyl(hydroxylethyl) cellulose and Some Model Uncharged Polymers: A Calorimetric Study of Their Interaction with Surfactants in Aqueous Solution, Universidade Lund 1997, Tese de doutorado.

[21] Wang G., Olofsson G., *J. Phys. Chem. B*, **1998**, 102, 9276
[22] Dai, S.; Tam, K.C. *J. Phys. Chem. B,* **2001**, 105, 10763
[23] Loh, W.; Teixeira, L.A.C.; Lee, L.T. *J. Phys. Chem. B,* **2004**,108,3196
[24] Dai, S.; Tam, K.C. *Langmuir* **2004**, 20, 2177
[25] Li Y., Xu R., Couderc S., Bloor D, M., Wyn-Jones E., Holtzwarth J.F. *Langumir* **2001**, 17,183
[26] da Silva RC, Olofsson G, Schillen K, Loh W; *J. Phys. Chem. B ,* 2002, ***106***, 1239.
[27] Jansson J, The Interaction Between Triblock Copolymers and Surfactants in Dilute Aqueous Solution*,* Universidade Lund 2004, Tese de doutorado

# CAPÍTULO II - OBJETIVOS

O objetivo deste projeto de doutorado foi comparar as propriedades físico – químicas de soluções de copolímeros estatísticos e copolímeros bloco, através de medidas de seus diagramas de fase binários com água e solventes orgânicos e estudo de diferenças na sua interação com surfatantes iônicos e não iônicos, monitorado por medidas calorimétricas e de espalhamento de luz.

# CAPÍTULO III - PARTE EXPERIMENTAL

## 3. 1. Reagentes

Os polímeros utilizados neste projeto estão listados na Tabela 1.

**Tabela 1:** Características físico-químicos dos copolímeros em bloco e estatístico.

| **Copolímero bloco** | **% m/m EO** | **M [g/mol]** | **Copolímero estatístico** | **% m/m EO** | **M [g/mol]** |
|---|---|---|---|---|---|
| $EO_{11}$-$PO_{16}$- $EO_{11}$ (L35) | 50 | 1900 | $EO_{19}$-$PO_{15}$ | 50 | 1700 |
| $EO_{13}$-$PO_{31}$-$EO_{13}$ (L64) | 50 | 2900 | $EO_{34}$-$PO_{25}$ | 50 | 2900 |
| $EO_{52}$-$PO_{35}$-$EO_{52}$ (F77) | 75 | 6600 | $EO_{106}$-$PO_{27}$ | 75 | 6200 |
| $EO_{114}$-$PO_{31}$-$EO_{114}$ (F88) | 85 | 11800 | $EO_{116}$-$PO_{48}$ | 65 | 7900 |
| $EO_{95}$-$PO_{62}$-$EO_{95}$ (F127) | 75 | 12000 | $EO_{204}$-$PO_{52}$ | 75 | 12000 |
| $EO_{16}$-$PO_{12}$-$EO_{16}$ (F38)<br>e<br>$EO_{11}$-$PO_{16}$-$EO_{11}$ (L35) | 85<br>50 | 4800<br>1900 | $EO_{43}$-$PO_{11}$ | 75 | 2500 |
| $EO_{20}$-$PO_{68}$-$EO_{20}$ (P123) | 31 | 5700 | - | - | - |

- Para comparação dos resultados, foram utilizados neste estudo também os homopolímeros PEO 600, 2000 e PPO 2000 que foram fornecidos pela Aldrich;
- Os copolímeros estatísticos foram obtidos da Laporte Performance Chemicals e Aldrich Chemical Company Inc ($EO_{204}$-$PO_{52}$ e $EO_{43}$-$PO_{11}$);
- Os copolímeros bloco foram doados, principalmente, pela ICI, exceto o $EO_{13}$-$PO_{31}$-$EO_{13}$ (L64) que foi fornecido pela BASF.

- A pureza dos surfatantes iônicos foi verificada através de medidas da *cmc* realizados pela técnica de titulação calorimétrica isotérmica. Os resultados obtidos estavam de acordo com dados da literatura[1,2], portanto utilizou-se estes surfatantes todos sem tratamento prévio:

- Aniônicos;

**SDS**

(dodecilsulfato de sódio, $M_w$=288,38 g/mol, 99% de pureza) da Aldrich Chemical Company Inc.

- Catiônico:

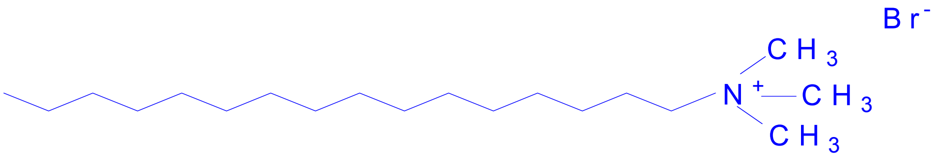

**CTAB**

(brometo de cetiltrimetilamonio, $M_w$=364,46 g/mol, 99% de pureza) da BDH Chemical Ltc. Poole, Ingalterra.

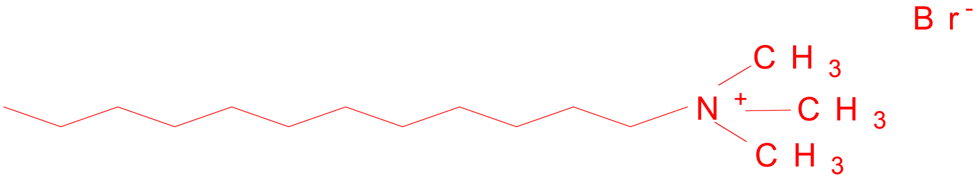

**DTAB**

(brometo de dodeciltrimetilamônio, $M_w$=308,35 g/mol, 99% de pureza) da Aldrich Chemical Company Inc.

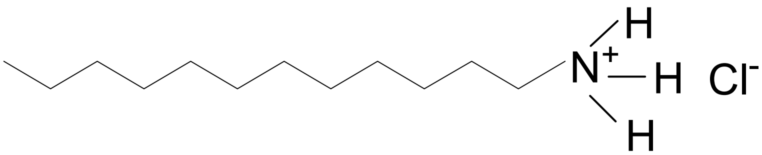

**DAC**

(cloreto de dodecil amônio, $M_w$=196,46 g/mol) foi sintetizado reagindo uma quantidade estequiométrica de HCl com dodecilamina (98 % de pureza, Sigma), e usando etanol como solvente. O produto foi recristalizado quatro vezes a partir de etanol e obtendo cristais brancos. Para verificação da pureza do produto foram feitas medidas calorimétricas com determinação do *cmc* e os resultados obtidos estavam em acordo com os valores reportados na literatura[1,2].

- surfatantes não-ionicos:

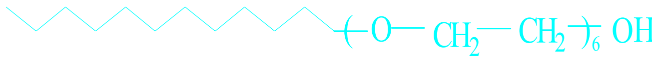

**$C_{12}EO_6$**

(hexaetileno glicol mono-n-dodecil éter, $M_w$=450,7 g/mol, pureza 99 %) da Nikko Chemicals Co.

**$C_{12}EO_8$**

(octaetileno glicol mono-n-dodecil éter, $M_w$=538,7 g/mol, pureza 99 %) da Nikko Chemicals Co.

Todas as soluções foram preparadas usando água purificada em sistema Milli Q.

# 3. 2. Metodologia

Para os experimentos calorimétricos foram utilizadas soluções de surfatante apresentando concentrações de 10 ou 1% em massa, e 1 ou 0,1% em massa para as soluções poliméricas. As medidas foram realizadas em diferentes temperaturas, usando os dois tipos de calorímetros descritos abaixo no 3.3:

## 3.3. Equipamentos

**3.3.1 VP-ITC** (Calorímetro Isotérmico de Titulação), MicroCal, Northampton, MA, USA (Figura 7). A cela calorimétrica apresenta um volume de 1,44 mL de solução polimérica (ou água). Contém, também, uma cela de referência, a qual é preenchida com água. Durante o experimento uma potência de aproximadamente 1 mW e aplicada na cela de referência, provocando ativação de um circuito que em resposta ajusta a diferença de temperatura entre as celas para zero. Os valores da entalpia de reação são obtidos por integração das deflexões ocorridas a partir da linha base (curva de fluxo de calor versus tempo)[3]. Sinais positivos de potencia resultam de fenômenos endotérmicos e sinais negativos resultam de fenômenos exotérmicos. Uma curva de potência em função de tempo de um experimento calorimétrico típico é mostrada na Figura 8.

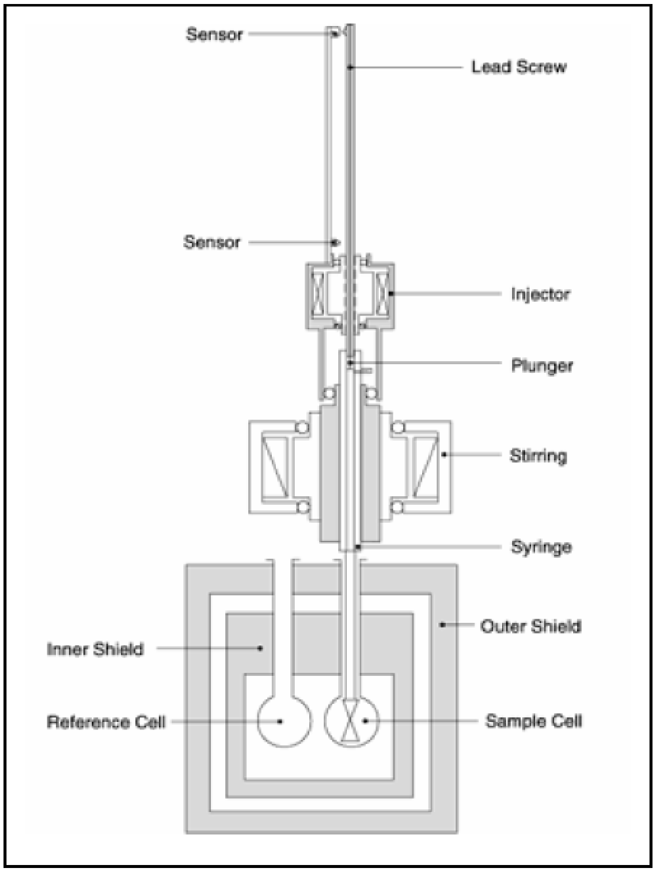

**Figura 7:** Desenho esquemático de um calorímetro isotémico de titulação (VP-ITC)

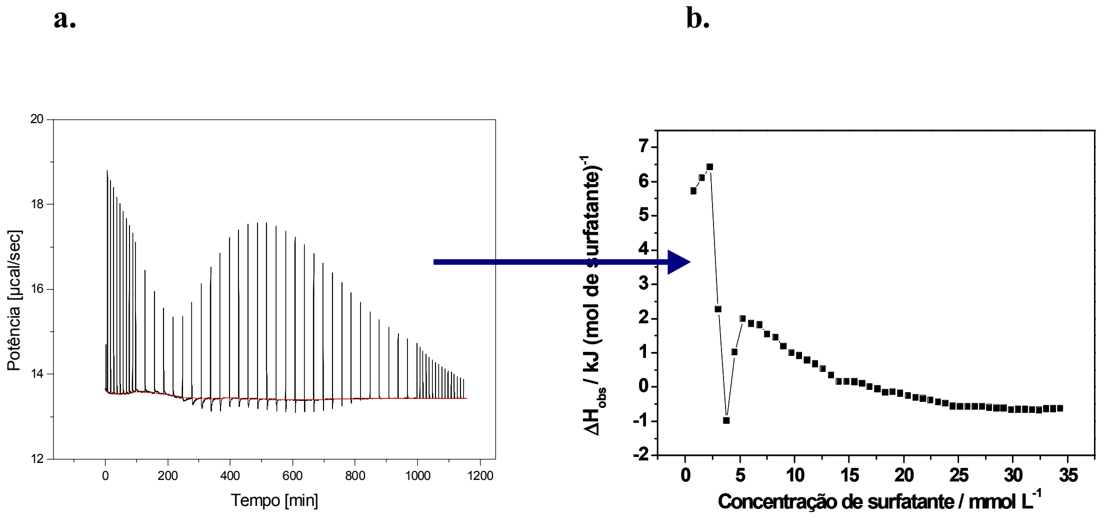

**Figura 8:** **a.** Resultado proveniente do calorímetro de titulação correspondente à variação de potência durante injeções consecutivas de solução de surfatante; **b.** Resultado de integração de cada pico resultante da titulação a partir da linha base correspondente a variação de entalpia (ΔH/µcal.s$^{-1}$) *versus* a concentração do titulante na cela reacional (mmol.L$^{-1}$)

As adições foram realizadas a partir de consecutivas injeções, utilizando uma seringa "gastight" controlada pelo instrumento. O intervalo entre as injeções foi de 600 – 1800 segundos.

Os volumes injetados variaram entre 3 e 15 µL. Mesmo com a adição da solução de surfatante, o volume da cela foi mantido constante pelo transbordamento da solução, que foi considerado durante os cálculos das concentrações reais de polímero e surfatante dentro da cela. A principal vantagem deste equipamento é a facilidade em mudar a temperatura da cela durante a realização de diferentes experimentos.

**3.3.2 VP-DSC** (calorímetro diferencial de varredura de alta sensibilidade), MicroCal, Northampton, MA (Figura 9). Este equipamento apresenta duas celas com volume de 0,542 mL, sendo uma para a referência e a outra para as amostras. As medidas foram realizadas com copolímeros bloco $EO_{95}$-$PO_{62}$-$EO_{95}$ e $EO_{114}$-$PO_{31}$-$EO_{114}$ em concentrações de 0,1 e 1% em massa, utilizando velocidade de varredura de 30°C/hora e uma faixa de temperatura entre 5-80°C.

Este método é bastante útil para a observação de todas as transições que possam aparecer no sistema (agregação, separação de fases, por exemplo).

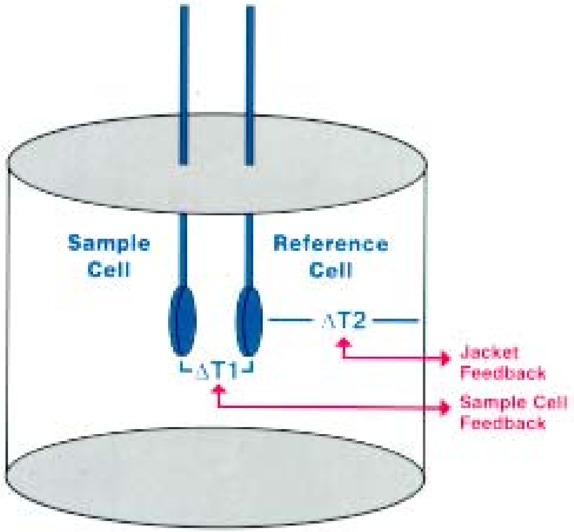

**Figura 9:** Desenho esquemático do calorímetro diferencial de varredura de alta sensibilidade (VP-DSC).

## 3.4. Análise de dados

**3.4.1 – VP-ITC:** Em experimentos de ITC, a variação da entalpia (ΔH) é medida diretamente, e associada ao processo que ocorre à temperatura constante. Através dos resultados obtidos foram construídos gráficos (Figura 10) que mostram a variação de entalpia observada para cada injeção ($\Delta H_{obs}$) em função da concentração de surfatante na cela.

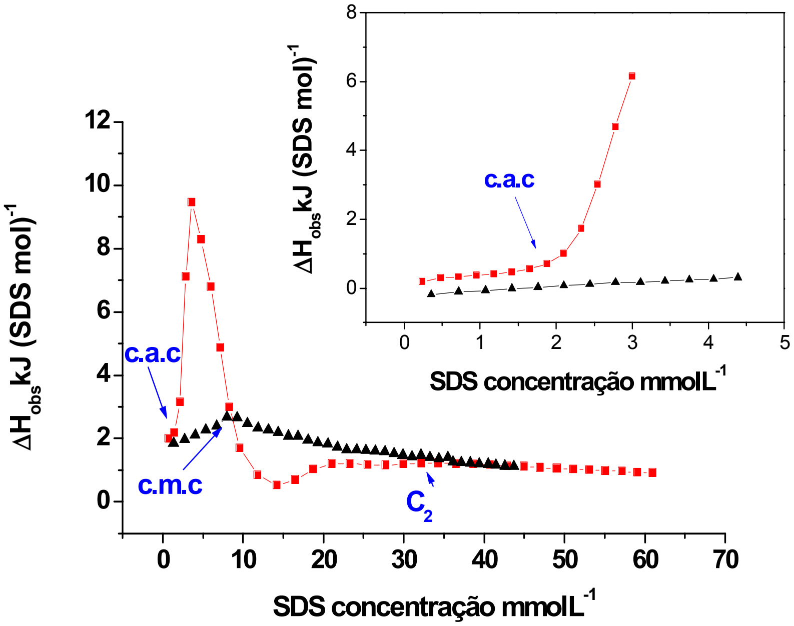

**Figura 10:** Curvas de ITC, adição de 5-15μL de SDS 10% em massa em ▲ água e ■ solução 0,1% em massa de $EO_{19}$ - $PO_{15}$ , $M_w$ = 1700g/mol, à 25°C.

É possível dividir um experimento calorimétrico de monitoramento da interação entre polímero e surfatante em etapas (Figura 11):

- curva preta corresponde à diluição do surfatante em água: a solução de surfatante que fica na seringa encontra-se na concentração acima de *cmc* (concentração micelar critica) e durante da diluição do surfatante estas micelas serão quebradas em monômeros, que estarão na concentração abaixo do *cmc* devido à diluição;
- diluição do polímero (não apresentada no gráfico): durante a titulação da solução de polímero com a solução de surfatante ocorrera a mudança na concentração da solução de polímero. A variação de entalpia não é significativa e apresenta uma ordem de grandeza similar ao ruído da energia liberada durante titulação da solução

de polímero com a solução de surfatante (~0,5μW), o que foi visto também previamente para sistema de PEO em água[4]. Por isto estes experimentos não foram realizados em todos estudos.

- curva vermelha apresenta a interação entre polímero e surfatante como esquematizado abaixo:

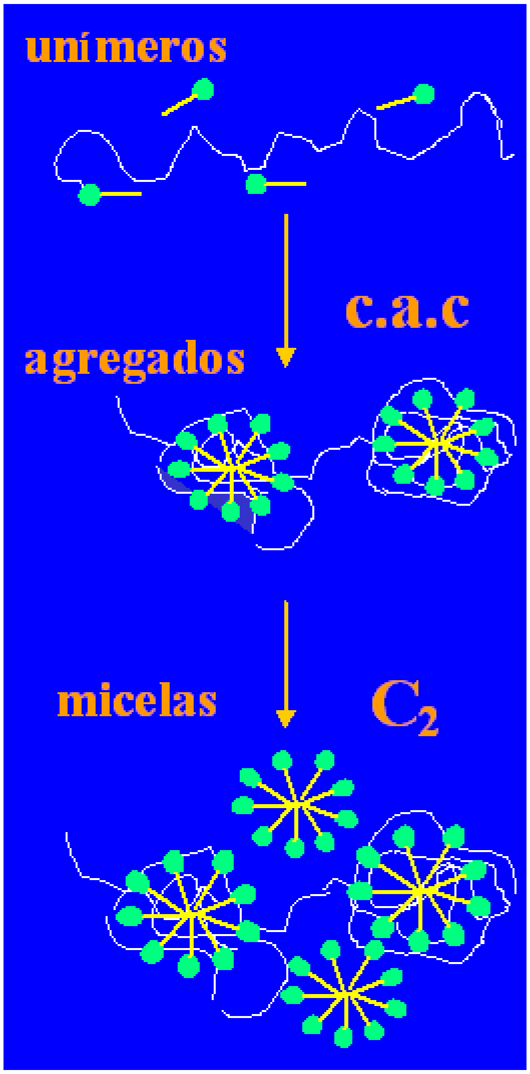

**Figura 11:** Desenho esquemático do sistema: Polímero + surfatante → complexo de polímero e surfatante + polímero livre e surfatante livre[5].

Esta etapa é a mais importante a ser analisada. Ela refere se à diluição do surfatante em água e à interação entre o polímero e o surfatante. A diluição do surfatante deve ser descontada da entalpia obtida para a interação entre o polímero e o surfatante.

Calorimetria, quando aplicada à investigação da interação de polímero-surfatante permite também a determinação dos importantes parâmetros que caracterizam esta interação[5,6,7,8,9], chamado *cac* (concentração de agregação critica), *cmc* (concentração micelar critica), ($C_2$) concentração de saturação, como exemplificado através da curva calorimétrica mostrada na Figura 10.

Para verificar o correto funcionamento do aparelho, uma calibração química foi realizada, que constitui na diluição de 10 µL de 10 % em massa de SDS (99% de pureza) em água. Foi obtido o resultado de 0,2 kJ/mol o qual se verificou estar em concordância aos valores da literatura[9].

**3.4.2 – VP-DSC:** Para determinar uma transição do sistema, é preciso estimar o $T_{onset}$ e a $T_m$ no sistema analisado. O primeiro pode ser definido como a temperatura na qual se inicia a transição de um processo (agregação de copolímeros, separação de fases) este ponto pode ser determinado pela interseção das tangentes da linha base inicial e da inflexão do pico. A segunda refere-se à temperatura máxima da transição de fases. A maneira pela qual são estimados o $T_{onset}$ e a Tm é apresentada na Figura 12:

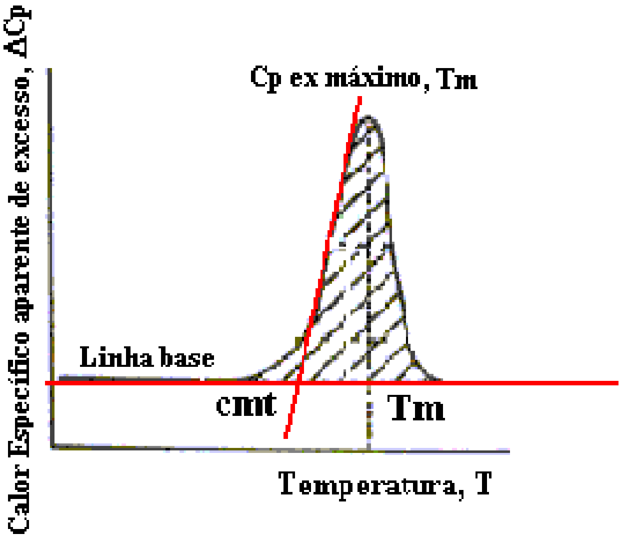

**Figura 12:** Figura esquemática da determinação da $T_{onset}$ (cmt) e da Tm através de uma curva de DSC.

Para medidas de DSC a variação de entalpia associada com cada transição foi calculada a partir da integração das curvas calorimétricas, utilizando um programa específico do equipamento (MicroCal Origin, v. 5.0).

## 3.5 Técnicas Experimentais Complementares

Durante este estudo foram aplicadas várias técnicas complementares para a caracterização dos copolímeros estudados. RMN (Ressonância Magnética Nuclear) foi utilizada para a identificação da razão entre grupos EO e PO na cadeia polimérica e GPC (Cromatografia por Permeação em Gel) foi aplicada para a determinação da massa molar e polidispersão do polímero. A utilização destas técnicas foi detalhadamente descrita no artigo 2. Além disso, para o monitoramento das dimensões da cadeia de polímero em solução e do complexo formado entre polímero e surfatante aplicou-se espalhamento de luz descrito com maiores detalhes na publicação 1. As medidas de espalhamento de luz foram feita em colaboração com os pesquisadores da Universidade de Lund, Suécia.

## BIBLIOGRAFIA

[1] Wang, G.; Olofsson, G. *J. Phys. Chem.*, **1995**, 99, 5588
[2] Loh, W.; Teixeira, L.A.C.; Lee, L.T. *J. Phys. Chem. B,* **2004**,108, 3196
[3] Marsh, K.N.; O' Hare, P.A.G., In Solution Calorimetry, Experimental Thermodynamics; vol.IV; Blackwell Publications: London, 1994, cap.12.
[4] da Silva, R.C, Aplicação de calorimetria ao estudo da interação entre polímeros não iônicos e surfatantes iônicos, Unicamp 2002, Tese de doutorado
[5] Wang G, Ethyl(hydroxylethyl) cellulose and Some Model Uncharged Polymers:A Calorimetric Study of Their Interaction with Surfactants in Aqueous Solution, Lund 1997, Tese de doutorado
[6] Olofsson, G.; Wang, G. *Pure&Appl.Chem.,* **1994**, 66, 527
[7] Tam, K.C.; Wyn-Jones, E. *Chem. Soc. Rev.,* **2006**, 35, 693
[8] Olofsson, G.; Wan, G. Polymer – Surfactant Systems, Kwak, J.C.T. eds, Marcel Decker, Nova York, 1998, cap. 8.
[9] da Silva, R.C.; Olofsson, G.; Schillén, K.; Loh, W. *J. Phys. Chem. B,* **2002**, 106, 1239
[10] Chowdhry, B. Z.; Cole, S. C. *Trends in Biotechnology,* **1989**, **7**, 1.

# CAPÍTULO IV – ARTIGO I

*J.Phys. Chem. B* **2007**, 111, 5911-5920,

# A Calorimetry and Light Scattering Study of the Formation and Shape Transition of Mixed Micelles of $EO_{20}PO_{68}EO_{20}$ Triblock Copolymer (P123) and Nonionic Surfactant ($C_{12}EO_6$)

*David Löf,† Anna Niemec,†† Karin Schillén,†* Watson Loh,††* Gerd Olofsson†*

† Physical Chemistry 1, Chemical Center, Lund University, P. O. Box 124,

SE-221 00 Lund, Sweden

†† Instituto de Quimica, Universidade Estadual de Campinas, C.P. 6154,

13084-970, Campinas, SP, Brazil

* Corresponding authors. E-mail addresses: Karin.Schillen@fkem1.lu.se,

wloh@iqm.unicamp.br

# ABSTRACT

The interaction between the nonionic surfactant $C_{12}EO_6$ and the poly(ethylene oxide)-poly(propylene oxide)-poly(ethylene oxide) triblock copolymer $EO_{20}PO_{68}EO_{20}$ (P123) has been investigated by means of isothermal titration and differential scanning calorimetry (DSC) as well as static and dynamic light scattering (SLS and DLS). P123 self-assembles in water into spherical micelles at ambient temperatures. At raised temperatures the DSC data revealed a sphere-to-rod transition of the P123 micelles around 60 °C. $C_{12}EO_6$ interacts strongly with P123 micelles in aqueous solution to give mixed micelles with a cmc well below the cmc for pure $C_{12}EO_6$. The presence of $C_{12}EO_6$ also lowers the critical micelle temperature of P123 so aggregation starts at significantly lower temperatures. A new phenomenon was observed in the P123-$C_{12}EO_6$ system, namely a well-defined sphere-to-rod transition of the mixed micelles. A visual phase study of mixtures containing 1.00 wt % P123 showed that in a narrow concentration range of $C_{12}EO_6$ both the sphere-to-rod transition and the liquid-liquid phase separation temperature are strongly depressed compared to the pure P123/water system. The hydrodynamic radius of spherical mixed micelles at $C_{12}EO_6$/P123 molar ratio 2.2 was estimated from DLS to be 9.1 nm, whereas it is 24.1 nm for the rod-like micelles. Furthermore, the hydrodynamic length of the rods at molar ratio 2.2 is in the range of 100 nm. The retarded kinetics of the shape transition was detected in titration calorimetric experiments at 40 °C and further studied by using time-resolved DLS and SLS. The rate of growth, which was slow (> 2000 s), was found to increase with the total concentration.

# INTRODUCTION

The triblock copolymers composed of poly(ethylene oxide) (PEO) and poly(propylene oxide) (PPO) are nonionic, water-soluble, low molar-mass polymers often abbreviated as PEO-PPO-PEO or $EO_nPO_mEO_n$.[1] These copolymers are produced in a broad range of compositions,[2] and they are widely used in industrial and scientific applications.[3-6] In dilute aqueous solutions, the PEO-PPO-PEO copolymers may self-assemble to form micelles, with a hydrophobic core containing PPO, which is protected from the surrounding water by a water-swollen PEO corona as established by light, X-ray (SAXS) and neutron (SANS) scattering investigations.[7-11] The thermodynamic characteristics of micelle formation derived from differential scanning calorimetry (DSC) and steady-state fluorescence spectrocopy experiments have been reported.[12,13] Three excellent reviews of the physical chemistry of PEO-PPO-PEO copolymers in water can be found in refs 14-16. In PEO-PPO-PEO-water systems, the micelles are spherical at ambient temperatures but they may change in shape at elevated temperatures, presenting a sphere-to-rod transition.[10,17-20] The change in shape is a combination of the conformational changes of PEO and a release of the imposed stretching of PPO blocks in the micellar core which is accompanied by the decrease of the cross-sectional radius of the micelles.[10,17,21] Salts like NaCl and KF lower the solubility of PEO in water and thus lower both the temperature for micelle formation and sphere-to-rod transition as well as the phase separation temperature.[22-24]

The formation of micelles of PEO-PPO-PEO copolymers is also promoted by hydrophobic substances, such as alcohols (pentanol or higher alcohols) benzene and tributylphosphate.[25-30] The authors of ref 28 conclude that the solubilization plays a role similar to that of a temperature increase, that is an increase of the hydrophobic character of the core and reduced hydration of the shell. Both effects promote the formation of micelles.

The interaction between PEO-PPO-PEO copolymers and nonionic $C_iEO_j$ surfactants and how that affects the copolymer self-assembly has been less investigated. The $C_{12}EO_6$ surfactant interacts synergistically with the copolymers F127 ($EO_{97}PO_{69}EO_{97}$) and L64 ($EO_{13}PO_{30}EO_{13}$) to form mixed micelles as shown in two recent studies.[31,32] A study of the ternary phase diagram of the copolymer P105 ($EO_{37}PO_{58}EO_{37}$) with $C_{12}EO_5$ in water showed that these two amphiphiles although of different sizes are miscible over large ranges of composition and temperature.[33]

We have performed in a separate study a static and dynamic light scattering (SLS and DLS) investigation of the self-assembly of the copolymer P123 ($EO_{20}PO_{68}EO_{20}$) and $C_{12}EO_6$ in dilute aqueous solution.[34] The physical properties of the P123-$C_{12}EO_6$ mixed micelles such as molar mass and hydrodynamic radius were determined for varying amounts of $C_{12}EO_6$ and at temperatures varying from 25 to 43 °C.[34] The measurements showed that at constant temperature, the size of the spherical mixed micelles decreases with increasing $C_{12}EO_6$ content up to a certain threshold, above which wormlike micelles form, similar to pure $C_{12}EO_6$ micelles, see for example refs 35 and 36 and references therein.

The purpose of this study was to further investigate the interparticle interaction and the mixed micellization process in the P123-$C_{12}EO_6$ system by using differential scanning and isothermal titration calorimetry, SLS and DLS. We have observed a shape transition of the P123-$C_{12}EO_6$ mixed micelles from spherical to rod-like. The retarded kinetics of this transition was studied by means of time-resolved SLS and DLS. It was also detected in titration calorimetric experiments. Such a shape transition has to our knowledge not been reported earlier. The sphere-to-rod transition temperature varied with the composition of the system and showed a minimum of about 40 °C for a $C_{12}EO_6$/P123 molar ratio of between 2 to 3. At the same composition the liquid-liquid phase separation temperature showed a pronounced minimum.

## EXPERIMENTAL

**Materials.** The PEO-PO-PEO triblock copolymer (denoted P123) has the average composition of $EO_{20}PO_{68}EO_{20}$ and a nominal molar mass of 5750 g mol$^{-1}$. The sample was a kind gift from BASF Corporation, Performance Chemicals, Mount Olive, New Jersey and used without further treatment. P123 is polydisperse both in molar mass and composition, which was previously found using gel permeation chromatography (GPC).[37] Hexa(ethylene glycol) monododecyl ether ($C_{12}EO_6$), was obtained from Nikko Chemicals Co., Tokyo, Japan, and used as received. The molar mass is 450.7 g mol$^{-1}$. Judging from the gas chromatogram provided by the manufacturer, the purity of the sample was better than 99 %. Water purified by a Milli-Q system (Millipore Corporation, Bedford, MA) was used in all solutions. The stock solutions of the P123 and $C_{12}EO_6$ were prepared by weight and left to equilibrate over night in a refrigerator at 4 °C. We estimate the relative uncertainty in the concentrations of solutions used in our study to be about 0.01.

Differential scanning calorimetry. Differential scanning calorimetry (DSC) measurements were made using Microcal MC-2 and Microcal VP-DSC high-sensitivity differential scanning calorimeters (Microcal Inc., Northampton, Ma, USA) in the temperature range 5 °C to usually 80 °C. The sample volume was 1.2 mL in the MC-2 instrument and 0.5 mL in the VP-DSC. The samples were kept at 5 °C for 20 min before the scan was started. The DSC thermograms record the differential power required to maintain the sample and the reference at the same temperature while scanning the temperature at a constant rate. Reference thermograms were recorded under the same conditions by filling both cells with water.

**Isothermal titration calorimetry**. The isothermal titration experiments were performed using a Microcal VP-ITC microcalorimeter. The experiments consisted of consecutive injections of concentrated surfactant solution into the calorimeter cell that initially contained 1.44 mL dilute P123 solution or water. The samples were added from a gastight syringe, the tip of which is modified to act as a stirrer. Injection volumes varied between 3 to 15 μL. The time between injections was usually 10 min but it was increased to 30 min in regions with slow equilibration. As the surfactant solution is added, the cell volume is kept constant by an overflow of solution, which is taken into account in the calculations of actual concentrations of polymer and surfactant in the cell. Measurements were made at 15 °C and 40 °C.

Phase studies. Samples of varying $C_{12}EO_6$/P123 molar ratios were prepared in closed glass vials that were kept in a thermostatic water bath. The temperature was increased in steps of 2 °C and the samples were inspected 12 and 24 hours after the temperature was changed.

**Dynamic and static light scattering**. The setup for the dynamic light scattering (DLS) and static light scattering (SLS) measurements employed an ALV/DLS/SLS-5000F, CGF-8F-based compact goniometer system from ALV-GmbH, Langen, Germany with vertical-vertical polarization geometry using Glan-Thomson polarizer and a Glan prism. The light source is a Nd:YAG solid-state Compass-DPSS laser (Coherent Inc., Santa Clara, California), which operates at 532 nm with a fixed output power of 400 mW that can be varied using an attenuator from Newport Inc. The cylindrical light scattering cell is immersed in a refractive-index-matching liquid (cisdecahydronaphthalene or decaline) kept in a cylindrical quartz container (VAT). The detection system includes a near-monomodal optical fiber and two matched photomultipliers in a pseudo-cross geometry. Two multiple t digital correlators with 320 spaced channels were utilized with an initial sampling time of 12.5 ns to construct the time correlation function (TCF) (pseudo-cross or auto) of the scattered intensity, $G^{(2)}(t)$. The static light scattering intensity was monitored and normalized to the incoming laser intensity. The temperature was varied and controlled to within ± 0.01 °C. A detailed description of the DLS/SLS equipment can be found in ref 37. Prior to the measurements, the solutions were equilibrated at room temperature for at least 20 min before filtered directly into the cylindrical light-scattering cell (both quartz and borosilicate cells were used) through a sterile, hydrophilic Minisart filter with a 0.2 $\mu$m pore diameter (Sartorius, Germany).

**DLS data analysis**. The analysis of the DLS data was directly performed on the normalized experimentally measured time correlation function of the scattering intensity, $g^{(2)}(t)$. The model used in the fitting procedures are expressed with respect to the normalized TCF of the electric field, $g^{(1)}(t)$, which is related to $g^{(2)}(t)$ by Siegert's relation:

$$g^{(2)}(t) - 1 = \beta \left| g^{(1)}(t) \right|^2 \quad (1)$$

where $t$ is the lag time and $\beta$ is the coherence factor (≤ 1) that takes deviations from the ideal correlation and the experimental geometry into account.

For a system that exhibits a multi-exponential decay with a distribution of relaxation times, $\tau$, $g^{(1)}(t)$ is described by a Laplace transform:

$$g^{(1)}(t) = \int_{-\infty}^{\infty} \tau A(\tau) \exp(-t/\tau) d \ln \tau \quad (2)$$

where $\tau = \Gamma^{-1}$, and $\Gamma$ is the relaxation or frequency rate.

The relaxation time distribution $A(\tau)$ can be obtained by performing an inverse Laplace transformation of the normalized intensity correlation function (with $g^{(1)}(t)$ expressed as in eq 2) using a non-linear constrained regularization method that minimizes the sum of the squared differences between the experimental and calculated $g^{(2)}(t)$.[38] The REPES algorithm incorporated into the GENDIST analysis package was used.[18] It iterates a penalizing parameter to the probability of rejecting the penalized solution selected by the user. In all analyses, the "probability-to-reject" term was set to 0.5. The relaxation time distributions presented are expressed in equal area representation as $\tau A(\tau)$ vs. $\log(\tau/\text{ms})$.[38]

The collective or mutual diffusion coefficient $D$ for particles undergoing translational motion, is related to the relaxation rate $\Gamma$, which is obtained in the output of the analysis:

$$D = \lim_{q \to 0} \frac{\Gamma}{q^2} \quad (3)$$

where $q$ is the magnitude of the scattering vector [$q = 4\pi n_0 \sin(\theta/2)/\lambda$, where $n_0$ is the refractive index of the solvent (here water), $\lambda$ is the incident wavelength and $\theta$ is the scattering angle]. In this study, $D$ is thus obtained from the slope of $\Gamma = f(q^2)$. The factor $(1-\phi)^2$, where $\phi$ is the volume fraction of the aggregate, has been omitted in the calculations of $D$ since it only becomes important in concentrated solutions.[39]

The apparent or effective hydrodynamic radius at a finite particle concentration can be calculated from $D$ using the Stokes-Einstein relation:

$$R_{H,app} = \frac{kT}{6\pi\eta_0 D} \quad (4)$$

where $k$ denotes Boltzmann's constant, $T$ is the absolute temperature and $\eta_0$ is the viscosity of water.

# RESULTS

## DSC measurements

DSC temperature scans were made on P123 solutions containing 1.00 wt % copolymer and varying amounts of $C_{12}EO_6$, from 5 °C up to usually 80 °C at a scan rate of 1 °C $min^{-1}$. Varying the scan rate between 0.5 to 1.5 °C $min^{-1}$ did not significantly change the recorded $C_p$ curves, even for a solution with a $C_{12}EO_6$/P123 molar ratio (MR) of about 2.2 (see below). The results of the DSC measurements are summarized in Figure 1, which shows typical DSC traces, and in Table 1, which gives characteristic temperature and enthalpy values for the observed transitions. Figure 1a shows DSC traces where apparent $C_p$ is plotted against temperature for samples containing $C_{12}EO_6$/P123 molar ratios up to 2.2. The concentration of P123 was constant at 1.00 wt % equal to 1.76 mmol $L^{-1}$.

**Table 1.** Summary of data for transitions observed in DSC curves of $C_{12}EO_6$ mixtures with P123

| Molar ratio | 1st peak $T_{onset}$ / °C | 1st peak $T_m$ / °C | 1st peak $\Delta H_{agg}$ / kJ $mol^{-1}$ | 2nd peak $T_m$(sphere-rod) / °C | $T_{ps}$ / °C |
|---|---|---|---|---|---|
| 0 | 17 | 21 | 460 ± 10 | 61 | 79 (> 70)* |
| 0.07 | 16 | 21 | 440 ± 15 | 61 | 77 |

| | | | | | |
|---|---|---|---|---|---|
| 0.7 | 14 | 21 | 440 ± 15 | 58 | ~75 (> 70) |
| 1.1 | 13 | 20 | 430 ± 15 | 58 | ~72 |
| 2.2 | 12 | 16 | 440 ± 15 | 41 | 56 (> 70) |
| 3.2 | 11 | 17 | 380 ± 25 | 43 | 57 |
| 6 | < 10 | 16 | 390 ± 15 | ~52 | 65 (66) |
| 11 | < 10 | 16 | 360 ± 35 | ~54 | 67 (68) |
| 46 | < 10 | ~12 | - | - | 54 (54) |

*Temperature values in parenthesis refer to data taken from the visual observations summarized in Figure 3.

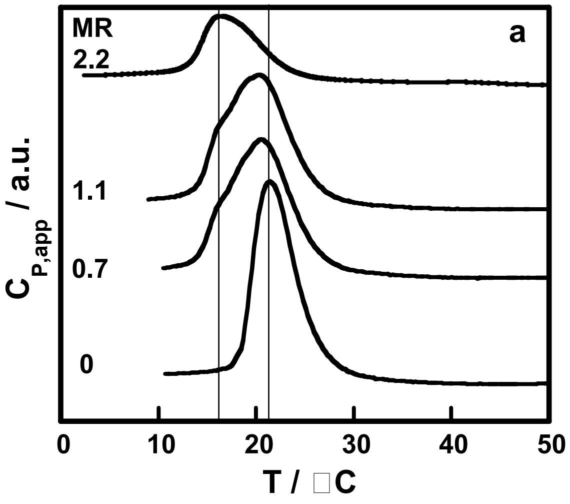

**Figure 1 (a).** DSC curves showing the main aggregation peak of 1.0 wt % P123 with varying amounts of $C_{12}EO_6$. **(a)** $C_{12}EO_6$/P123 molar ratios (MR) from 0 to 2.2. **(b)** MR from 2.2 to 46. The vertical lines at 16 °C and 21 °C indicate $T_m$.

The traces show one large peak characterized by a $T_{onset}$, defined as the temperature at the intersection of the extrapolated linear ascent of the peak with the extrapolated baseline and a $T_m$, which is the temperature of the peak maximum. The enthalpy of aggregation, $\Delta H_{agg}$ was calculated from the area under the peak and expressed in kJ per mole of P123. Values of $T_{onset}$, $T_m$ and $\Delta H_{agg}$ are given in columns 2 to 4 in Table 1. The uncertainty in $T_{onset}$ and $T_m$ is of about ± 1 °C for pure P123 solution while it is ± 2 °C for $T_{onset}$ for mixtures. The large peak in the curve for pure P123 represents the formation of block copolymer micelles with a CMT (critical micelle temperature) equal to $T_{onset}$. Values of $T_m$ are constant and the same from pure P123 to mixtures with MR up to 1.1. Also, values of $\Delta H_{agg}$ are not significantly changed for these mixtures. However, there is a significant decrease of $T_{onset}$ from 17 to 13 °C at MR equal to 1.1. This indicates that the presence of small amounts of $C_{12}EO_6$ induces aggregation of P123 and lowers its CMT. The slight shoulder observed in the peaks for MR = 0.7 and 1.1 are worth noticing. Solutions with MR = 2.2 show a significant decrease in $T_m$ to 16 °C, while $T_{onset}$ is unchanged nor is $\Delta H_{agg}$ significantly affected. The shoulder on the left-hand side of the peak has disappeared. It is possible that the process associated to the shoulder now has become dominant and is characterized by the new $T_m$. DSC traces for samples with MR between 2.2 and 11 are shown in Figure 1b, and their characteristic values listed in Table 1.

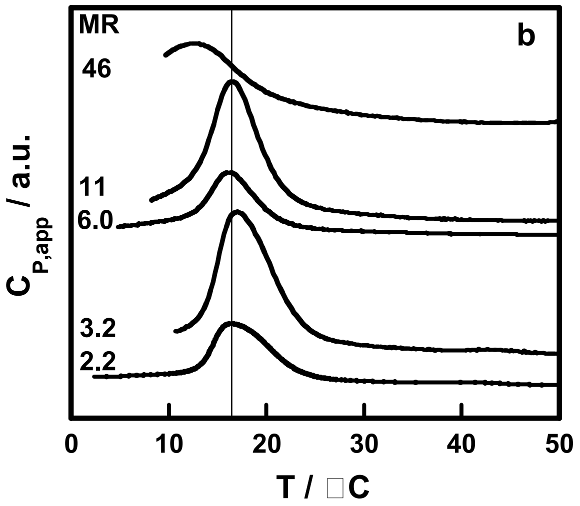

**Figure 1 (b)** DSC curves showing the main aggregation peak of 1.0 wt % P123 with varying amounts of $C_{12}EO_6$. **(a)** $C_{12}EO_6$/P123 molar ratios (MR) from 0 to 2.2. **(b)** MR from 2.2 to 46. The vertical lines at 16 °C and 21 °C indicate $T_m$.

In this composition range $T_m$ stays constant at about 16 °C while $T_{onset}$ decreases to below 10 °C. There also seem to be a significant decrease in $\Delta H_{agg}$. For samples of MR equal to 46 the aggregation peak is shifted to lower temperatures and only the top of the transition peak could be recorded.

At temperatures above the main aggregation peak the DSC curves show small broad peaks, which we ascribe to a sphere-to-rod transition of the aggregates. At higher temperatures there are steps in the apparent $C_p$, which indicate liquid-liquid phase separation. Enlargements of the DSC traces in the temperature region above the main transition peak are shown in Figure 2.

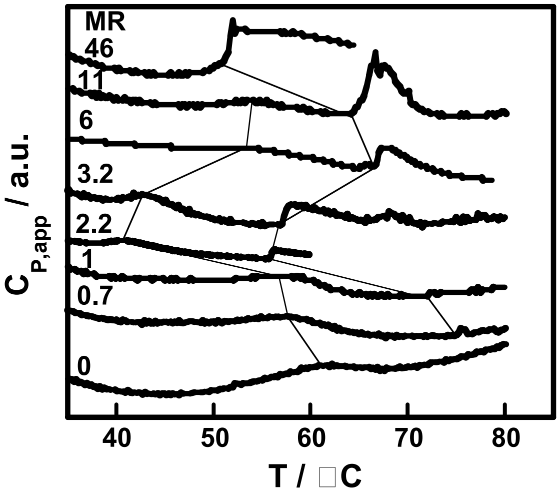

**Figure 2.** Enlargements of DSC curves above the aggregation peak for 1.0 wt % P123 and $C_{12}EO_6$/P123 molar ratios (MR) from 0 to 46. Values for the transition temperatures (sphere-to-rod and phase separation) are joined by lines as guides for the eye.

Values for temperatures of the maximum of the second peak, $T_m$(sphere-rod), and of phase separation, $T_{ps}$, are shown in columns 5 and 6 of Table 1. Solutions with molar ratios 2.2 and 3.2 give the narrowest and best-defined peaks with a width of 6 to 7 °C. At both higher and lower molar ratios the peaks had a width of about 15 °C. The area of the peaks corresponds to about 10 kJ mol$^{-1}$, which would represent the enthalpy change for the sphere-to-rod transition. In Figure 2, the values for the transition temperatures for mixtures with different compositions are joined by lines to help comparison with results of the phase studies (see below).

In DSC traces of pure $C_{12}EO_6$ solution a small, fairly broad, peak is seen, corresponding to enthalpy changes of about 1-2 kJ mol$^{-1}$. In 10 mmol L$^{-1}$ solutions, it is centered at 27 °C, and in 50 mmol L$^{-1}$ solutions at 21 °C. This peak most probably arises from the growth of $C_{12}EO_6$ micelles from spheres to elongated cylinders, as observed by Grell *et al.* in analogous $C_{14}EO_8$ and $C_{16}EO_8$ systems.[40,41] It has also been observed in 10 mmol $L^{-1}$ $C_{12}EO_6$ solutions[31] but the authors ascribed the peak to the formation of micelles of $C_{12}EO_6$, which is not correct as the concentration is well above the critical micelle concentration (cmc) of $6.5\cdot10^{-5}$ mol $L^{-1}$.[42]

### Phase map

The phase map in Figure 3, based on visual inspection of P123-$C_{12}EO_6$ mixtures as a function of temperature, indicates a transition detected from the appearance of the first signs of turbidity and liquid-liquid phase separation.

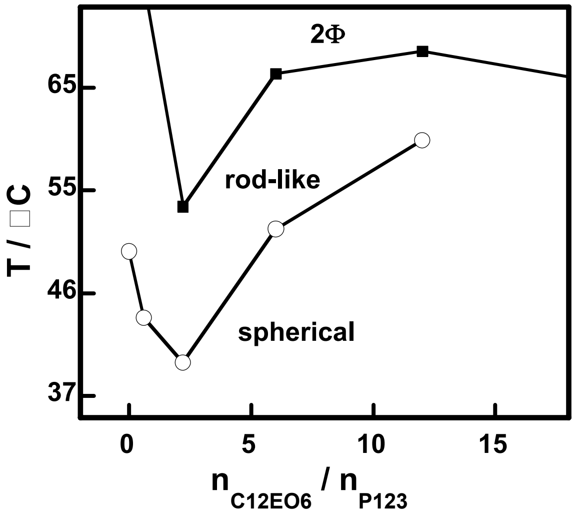

**Figure 3.** Phase map derived from visual observations (■,○) of transitions in mixtures of 1.0 wt % P123 with varying amounts of $C_{12}EO_6$ expressed as molar ratio $n_{C12EO6}$ / $n_{P123}$. The first transition line represents the onset of turbidity, whereas the second transition is at the temperature where macroscopic (liquid-liquid) phase separation was observed.

The samples started to become turbid at the temperature where the second small peak appears in the DSC curves, see Figure 2 and $T_m$(sphere-rod) in Table 1. Also, the temperatures for phase separation agree well with temperatures deduced from the DSC curves. The sphere-to-rod transition and liquid-liquid phase separation temperatures move down and then up in the same way in both observations as the molar ratio of the mixture passes the value of 2-3. For the mixture with the highest $C_{12}EO_6$ content, MR = 46, the phase separation temperature $T_{ps}$ correlated well $T_{ps}$ from the DSC study. The cloud point of a pure $C_{12}EO_6$ solution of the same concentration, 0.08 mol $L^{-1}$, is about 49 °C[43] and of 1 wt % P123 solution it is 90 °C.[2]

## ITC measurements

Figure 4 shows a calorimetric titration curve from consecutive additions of micellar solution of $C_{12}EO_6$ (1.00 wt %) to 0.30 wt % P123 solution at 15 °C.

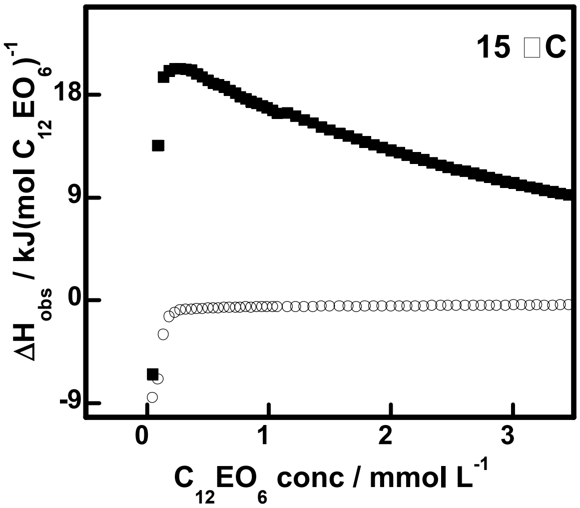

**Figure 4.** Observed enthalpy changes from addition of 1.0 wt % of $C_{12}EO_6$ to 0.3 wt % P123 solution at 15 °C.

Under these conditions P123 will be completely in the form of unimers, as shown by DSC measurements, see Figure 1. The curve for dilution of the $C_{12}EO_6$ solution in water is included. At 15 °C the cmc $C_{12}EO_6$ is estimated to $8.3 \cdot 10^{-5}$ mol $L^{-1}$ and •$H_{mic}$ to 21.4 kJ $mol^{-1}$ from results reported in ref 42. The first couple of injections in the dilution series give exothermic enthalpy values showing that the concentration in the calorimeter cell is below cmc. Further injections increased the concentration to above the cmc and the enthalpy of dilution of the $C_{12}EO_6$ solution in water became small and close to zero. The first injection into the copolymer solution was exothermic that indicates that part of added $C_{12}EO_6$ micelles break up to monomers. Further addition of $C_{12}EO_6$ to P123 solution gave large positive enthalpy changes, which are not expected from the interaction with unimers of P123. Addition of $C_{12}EO_6$ to PPO or PEO solutions does not give measurable enthalpy changes as observed in previous studies[31] and by us. However, DSC curves show that already at a $C_{12}EO_6$ concentration of 1 mmol $L^{-1}$, a significant fraction of P123 is in the form of micelles at 15 °C, see curve for MR = 0.7 in Figure 1. This means that $C_{12}EO_6$ induces aggregation of the polymer to form mixed micellar aggregates. In 0.30 wt % P123 the aggregation starts at about 0.1 mmol $L^{-1}$. In the same way, addition of $C_{12}EO_6$ to solutions of F127 $(EO_{97}PO_{69}EO_{97})$ and L64 $(EO_{13}PO_{30}EO_{13})$ at temperatures below their CMT in water was found to give large enthalpy increases (endothermic process) from induced aggregation of these copolymers.[31,32]

Addition of $C_{12}EO_6$ (10.0 wt%) to 1.00 wt % P123 solution at 40 °C gave a titration curve shown in Figure 5a.

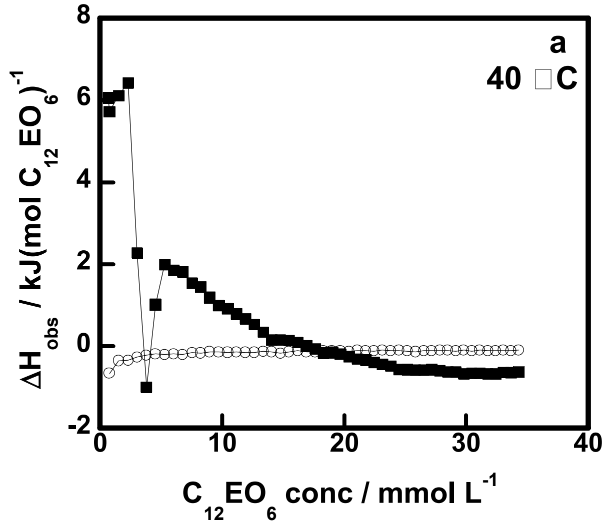

**Figure 5.** **(a)** Observed enthalpy changes from addition of 10 wt % $C_{12}EO_6$ to 1.0 wt % P123 solution at 40 °C. **(b)** Titration experiments with addition of $C_{12}EO_6$ to 0.1 (◇), 0.3 (△) and 1 (□) wt % P123 solutions at 40 °C, expressed as function of $C_{12}EO_6$/P123 molar ratio.

The first injections gave enthalpy values of about 6 kJ mol of $C_{12}EO_6{}^{-1}$, after that there was a sudden decrease to a pronounced (exothermic) minimum at a $C_{12}EO_6$/P123 molar ratio of 2.1. After the minimum, the observed enthalpies increased to about 2 kJ mol$^{-1}$. Further addition of $C_{12}EO_6$ gave a steady decrease in enthalpy changes that became zero and crossed the curve for dilution of $C_{12}EO_6$ in water at around 18 mmol L$^{-1}$ to become slightly exothermic at higher concentrations. Titration of 0.10 wt % P123 with 1.00 wt % $C_{12}EO_6$, see Figure 5b, showed that $C_{12}EO_6$ started to interact with the aggregated P123 already from the first addition, which gave a concentration of 1.5·10$^{-5}$ mol L$^{-1}$.

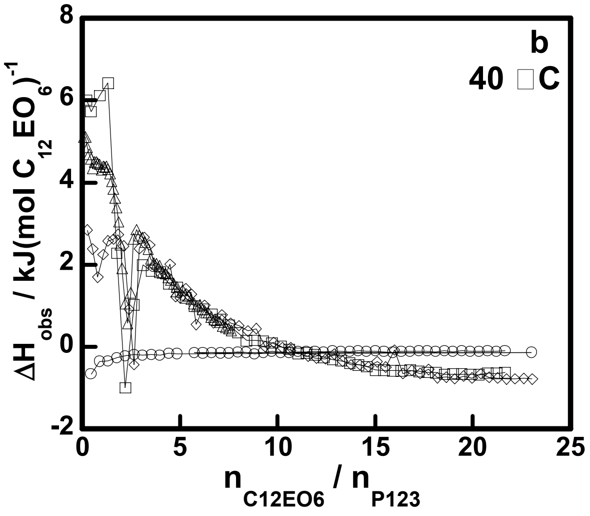

**Figure 5. (a)** Observed enthalpy changes from addition of 10 wt % $C_{12}EO_6$ to 1.0 wt % P123 solution at 40 °C. **(b)** Titration experiments with addition of $C_{12}EO_6$ to 0.1 (◇), 0.3 (△) and 1 (□) wt % P123 solutions at 40 °C, expressed as function of $C_{12}EO_6$/P123 molar ratio.

Further injections gave about the same endothermic enthalpy changes, corresponding to approximately 3 kJ mol$^{-1}$ of $C_{12}EO_6$. At a molar ratio of 3.1 (± 0.1) there was a sudden drop in the observed enthalpy values to about –1 kJ mol$^{-1}$. After the minimum the same behavior was observed as for 1.00 wt % P123 solution, see Figure 5b. The same pattern was observed for titration into 0.30 wt % P123 solutions, only that the minimum enthalpy value observed was about 0.9 kJ mol$^{-1}$, and occurred at a molar ratio of 2.4. The crossing of the surfactant dilution line was at a molar ratio of about 12, as for the other curves. Measurements with 1.50 wt % P123 (not shown) differed only in the initial values for observed enthalpies, about 6 kJ mol$^{-1}$, and with the minimum positioned at a molar ratio of 2.1.

Experiments with dilution of 1.00 wt % $C_{12}EO_6$ in water at 40 °C gave observed enthalpy changes consistent with a cmc of $5.3 \cdot 10^{-5}$ mol L$^{-1}$ and enthalpy of micelle formation of 5.5 ± 0.5 kJ mol$^{-1}$.[42,44] Dilution of both 1.00 and 10.0 wt % $C_{12}EO_6$ at concentrations above cmc gave enthalpy values close to zero.

At 40 °C P123 copolymer will be mostly in the form of micellar aggregates since this temperature is well above the CMT of P123 and micelle formation is complete, see DSC curves in Figure 1. The calorimetric titrations show that $C_{12}EO_6$ interacts with P123 already at concentrations as low as $1.5 \cdot 10^{-5}$ mol L$^{-1}$. The constant positive enthalpy values observed until the critical molar ratio region is reached indicate that $C_{12}EO_6$ monomers are solubilized in the P123 micelles, forming mixed aggregates.[34] After this initial solubilization, there is a drastic decrease in the observed enthalpy values. Furthermore, within this concentration range, the peaks measured in the titration experiment change from indicating one fast endothermic process to a composite process with one fast endothermic process occurring together with a slower exothermic one, as can be seen in Figure 6.

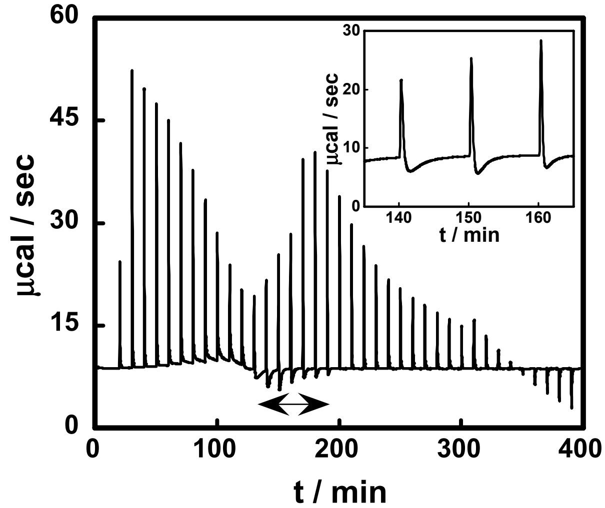

**Figure 6.** ITC raw data for addition of 10 wt % $C_{12}EO_6$ to 1.5 wt % P123 solution at 40 °C. Injections 12 to 18 (between arrow) give a composite peak with one fast endothermic process and a slower exothermic one,

see inset. (The time between each injection in this experiment, 10 min, was too short to reach equilibrium. That took 15 to 20 min.)

The design of the calorimeter employed for these measurements and its principle of operation (based on power compensation) are such that its response to instantaneous processes would be over in a few minutes. This is the common response for similar experiments with dilution of surfactant solutions, and can be observed for the initial and final peaks for a typical titration experiment, shown in Figure 6. When the $C_{12}EO_6$ concentration in the calorimeter cell approached molar ratio 2, not only a decrease in the overall heat exchanged was observed, but also the peaks showed the appearance of a much slower exothermic process, which lasted up to 15-20 min (see the inset in Figure 6). Interestingly, similar time dependence in the same concentration range was observed during the light scattering measurements (see below). For reasons stated above, this slower process differs from the dilution/interaction processes observed for smaller or larger molar ratios, and should be ascribed to another process, which occurs only in this concentration range.

Addition of $C_{12}EO_6$ to 0.05 % F127 ($EO_{97}PO_{69}EO_{97}$) at 35 °C,[31] and to 2.5 % L64 ($EO_{13}PO_{30}EO_{13}$)[32] solutions at 40 °C gave positive enthalpy changes, which shows that $C_{12}EO_6$ interacts with copolymer aggregates from the lowest concentration (about $2 \cdot 10^{-5}$ mol $L^{-1}$), in agreement with our observation. However, the enthalpy values determined in the beginning of these titration experiments are well above 30 kJ $mol^{-1}$ and much larger than the ones we observed. The enthalpy changes then decrease to zero, joining the curve for dilution of $C_{12}EO_6$ in water where the titrations ended. No exothermic break was observed in those studies. A possible reason for the large initial enthalpy values is that a significant fraction of the F127 and L64 polymers were in the form of monomers. Added $C_{12}EO_6$ would induce further polymer aggregation, giving a large enthalpy contribution, in addition to the enthalpy change from $C_{12}EO_6$ being solubilized in the aggregates. DSC curves for F127 solutions shown in Figure 1b of ref 45 show that conversion to micelles is not complete in 0.05 % at 35 °C. The same could be proposed to occur in L64 solutions at 40 °C.

## Dynamic and static light scattering

*Sphere-to-rod transition of P123-$C_{12}EO_6$ aggregates.* DLS experiments were performed on P123-$C_{12}EO_6$ solutions of molar ratios varying from 0 to 11, in order to evaluate the apparent hydrodynamic radius of the mixed P123-$C_{12}EO_6$ aggregates (or micelles) below (spheres) and at (rods) the shape transition temperature. The transition temperature for each molar ratio was chosen as the maximum of the second peak $T_m$(sphere-rod) in the DSC experiments (Figure 2 and Table 1). All of the solutions contained 1.00 wt % with respect to P123. Figure 7 presents the normalized time pseudo-cross correlation functions of the scattering intensity ($g^{(2)}(t)$-1) for $C_{12}EO_6$/P123 molar ratios MR = 2.2, 3.2 and 6.0 at two different temperatures.

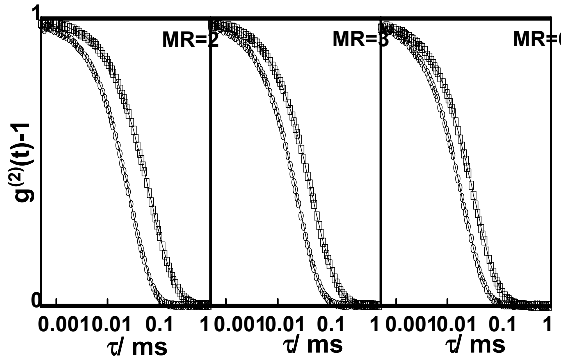

**Figure 7.** The correlation functions of the scattered light at $\theta$ = 90° at temperatures below (○) and at the sphere-to-rod transition (□) for mixed solutions containing 1.0 wt % P123 and with $C_{12}EO_6$/P123 molar ratios (MR) 2.2, 3.2 and 6.

The lower temperature was set at least 5 °C below the sphere-to-rod transition temperature, whereas the higher corresponds to the transition temperature for each molar ratio. The correlation function is shifted toward longer times at the higher temperature for all three solutions, and the difference between the two functions decreases with increasing molar ratio. The corresponding relaxation time distributions obtained by inverse Laplace transformation of the $g^{(2)}(t)$-1 functions are shown in Figure 8.

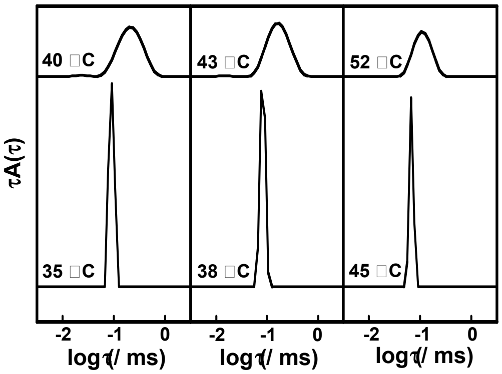

**Figure 8.** Relaxation time distributions obtained from inverse Laplace transformation of the intensity correlation functions shown in Figure 7 for $C_{12}EO_6$/P123 molar ratios: 2.2, 3.2 and 6 (from left to right). Distributions at the sphere-to-rod transition temperature (top) and below (bottom) are presented.

The narrow distributions at the bottom of the figure correspond to systems of monodisperse spherical aggregates. The upper broader relaxation curves represent the relaxation time distributions of the system at equilibrium at the sphere-to-rod transition temperature. The broadening and the shift of the relaxation modes at the shape transition temperature indicate a growth of the P123-$C_{12}EO_6$ aggregates into larger and more polydisperse particles. The single relaxation modes seen in the distributions are diffusive. This was established from the linear $q^2$ dependences of the relaxation frequencies (□) (see eq 3) obtained by performing DLS measurements at eight different scattering angles between 35-145° on each of the mixed solutions (data not shown).

For the lower molar ratios, the scattering intensity measured at a fixed angle and as a function of temperature presented a pronounced increase at a defined temperature, which corresponded well with the sphere-to-rod transition temperature obtained from the DSC results in Figure 2. For the solution of molar ratio 11, the scattering intensity showed a less distinct increase with increasing temperature than at lower molar ratios. At high molar ratios, for example at MR = 46, the mixed micelles grow both with concentration and temperature and the behavior is more like the wormlike micelles of pure $C_{12}EO_6$.[34] Therefore, they do not show a distinct shape transition temperature.

The concentration dependence of the apparent mutual diffusion coefficients (*D*) of the spherical and the rod-like mixed aggregates was also analyzed. Solutions containing between 0.3 to 1.5 wt % of P123 and of $C_{12}EO_6$ to give a molar ratio of 2.2 were prepared and *D* was determined from dynamic light scattering experiments at 36 °C and 40 °C. For each concentration, the apparent diffusion coefficients were evaluated from the slope according to eq 3. The results are summarized in Figure 9.

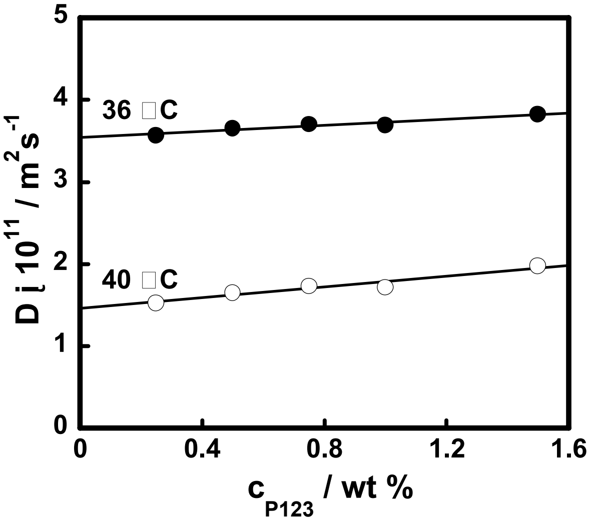

**Figure 9.** Diffusion coefficients as function of copolymer concentration for mixed P123-$C_{12}EO_6$ micelles at molar ratio 2.2 at 36 °C (●, spherical shape) and at 40 °C (○, rod-like shape). The solid lines represent linear least square fits.

The positive slopes observed in the figure indicate a repulsive interaction between the P123-$C_{12}EO_6$ aggregates in solution. The hydrodynamic radii were derived using the Stokes-Einstein relation from the values of $D$ extrapolated to zero copolymer concentration ($D_o$). At 36 °C the mixed micelles are spheres with $R_H$ = 9.1 ± 0.1 nm. At 40 °C, $R_H$ had increased to 24.1 ± 0.8 nm and the shape of the aggregates has become elongated. The hydrodynamic length ($L$) of the rod-like mixed micelles at MR = 2.2 was also estimated from $D_o$. In the model formulated by Tirado and Garcia de la Torre the relation between $D_0$ and $L$ is given by, see e. g. ref 46:

$$D_0 = \frac{kT}{3\pi\eta_0}\left(\ln(L/d) + \nu\right) \quad (5)$$

where $d$ is the diameter of the rod and

$$\nu = 0.312 + \frac{0.565}{(L/d)} - \frac{0.1}{(L/d)^2}$$

in the regime where $5 < L/d < 30$.

Assuming a rod-like particle with a cross-sectional radius equal to the radius of the sphere (= $R_H$ at infinite dilution) and using eq 5, a rod length of 104 nm was derived for the mixed micelle at molar ratio 2.2.

Static light scattering measurements were performed on the aqueous solution with $C_{12}EO_6$/P123 molar ratio 2.2 (and 1.00 wt% P123) at 40 °C to determine the apparent radius of gyration, $R_{g,app}$, of the rod-like mixed micelles using classical SLS analysis.[47] A value of $R_{g,app}$ = 46 nm was found from the angular dependence of the scattered light (data not shown). The ratio of the radius of gyration to the hydrodynamic radius ($R_g/R_H$) also provides information about the internal morphology of the scattering particle.[48] For a perfect homogenous sphere $R_g/R_H \leq 0.775$, and for an infinite rod it is > 2.[49] The apparent values obtained in our SLS and DLS experiments, $R_{g,app}$ = 46 nm and of $R_{H,app}$ = 21 nm, give a value larger than 2, which confirms the rod-like shape of the mixed micelle at MR = 2.2 and 40 °C. A rheological study performed in parallel on the same system (both at equilibrium and time-resolved measurements), presents clear evidence from the observation of shear-thinning effects that rod-like objects are formed at the transition temperature for this molar ratio.[50]

We were also interested in comparing the size of the aggregates at different molar ratios before and after the shape transition to correlate their size with the transition temperature. Values of $R_{H,app}$ of the mixed aggregates in 1.00 wt % P123 solutions with $C_{12}EO_6$/P123 molar ratios equal to 2.2, 3.2 and 6.0 are shown in Figure 10 at temperatures below and at the shape transition temperature in each case.

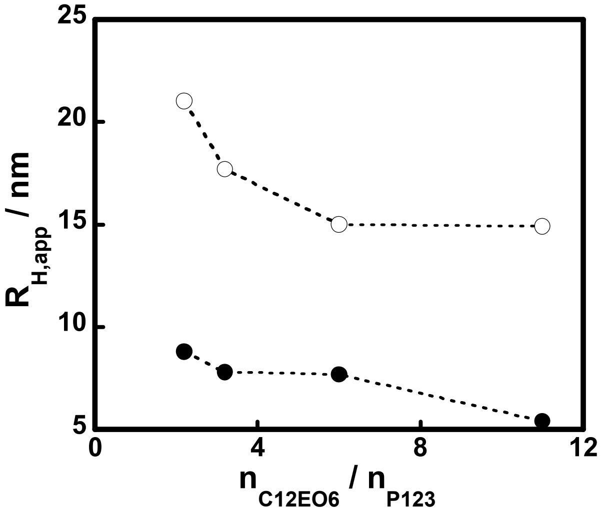

**Figure 10.** Apparent hydrodynamic radii for the mixed micelles as a function of molar ratio ($n_{C12EO6}$ / $n_{P123}$). Values obtained from DLS measurements performed below the transition temperatures (●, spherical shape) and at the sphere-to-rod transition temperatures (○, rod-like shape). The following temperatures were used: 35 and 40 °C for MR = 2.2; 38 and 43 °C for MR = 3.2; 45 and 52 °C for MR = 6 and 25 and 60 °C for MR = 11.

The data in Figure 10 reveal that the size of the mixed spherical micelles at temperatures below the transition temperature decreases with increasing

$C_{12}EO_6$ content. This was established in a previous light scattering investigation, where the values of $R_H$ of the spherical mixed micelles were analyzed at infinite dilution.[34] For example, at 40 °C, these DLS measurements gave $R_H$ = 10.1, 9.9, 7.9 and 6.4 nm for mixed micelles with MR = 0, 0.6, 5.7 and 12, respectively. Figure 10 also shows that the size of rod-like aggregates at the shape transition temperature also decreases in terms of $R_{H,app}$ with increasing content of $C_{12}EO_6$.

***Time-resolved DLS and SLS.*** Time-resolved dynamic light scattering measurements were carried out on the $C_{12}EO_6$/P123 solution of molar ratio 2.2 (containing 1.00 wt % of P123) when changing the temperature of the light-scattering cell from 36 to 40 °C. Simultaneously, the static light scattering intensity at □ = 90° was monitored over short time intervals. The results are summarized in Figure 11 where the scattered intensity *I* (normalized to the incoming laser intensity) as well as the temperature are plotted as functions of time.

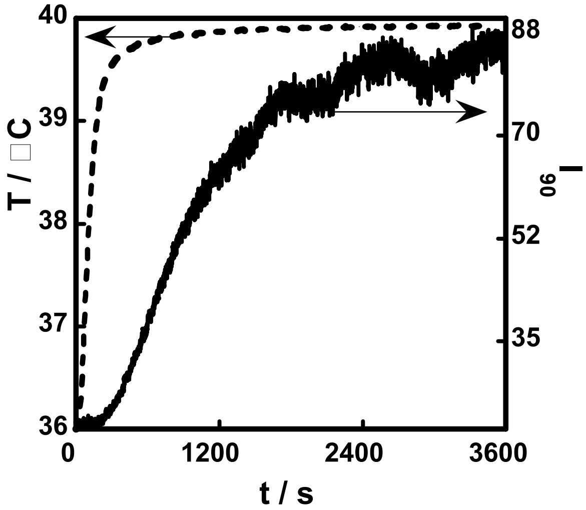

**Figure 11.** Static light scattering intensity normalized to the laser intensity (solid line) and temperature (dashed line) as functions of time for the mixed solution with $C_{12}EO_6$/P123 molar ratio 2.2 and 1.0 wt % with respect to P123. Measurements preformed at $\theta = 90°$.

After about 200 s when the temperature has reached 39.5 °C, the intensity started to increase and the change became faster as the temperature approached 40 °C. After about 1800 s the intensity started to level off but only slowly and not until after about 3600 s did it become constant. The increase in intensity is due to an increase in size of the mixed P123-$C_{12}EO_6$ micelles, since larger particles scatter more (for impermeable spheres with radius $R$, $I$ is proportional to $R^6$). The time-resolved experiments also showed that the sphere-to-rod transition is reversible. DLS and SLS measurements at 25 °C gave the same values for the scattering intensity and apparent hydrodynamic radii before and after the temperature of the sample had been raised to 40 °C. The same time-dependence of the light scattering intensity was also observed when two thermostatted stock solutions of P123 and $C_{12}EO_6$ were directly mixed to obtain a molar ratio of 2.2 in the light scattering cell at 40 °C after which the intensity recording started. The first technique with temperature increase was preferred since it was easier to control the exact amount of each component in the mixed solution.

The growth process observed in Figure 11 is surprisingly slow. As indicated by the calorimetric titration curves it is a complicated process that involves both diffusion and collision where material is rearranged to create larger elongated objects. The effect of total concentration on the rate of growth, was investigated by varying the P123 concentration between 0.25 to 1.5 wt % but keeping the $C_{12}EO_6$/P123 molar ratio constant and equal to 2.2. Figure 12 shows the normalized scattered intensity expressed as $(I-I_{min})/(I_{max}-I_{min})$ against time for mixed solutions containing 0.5, 0.75 and 1.5 wt % with respect to P123 (the temperature scan is not shown), cf. Figure 11.

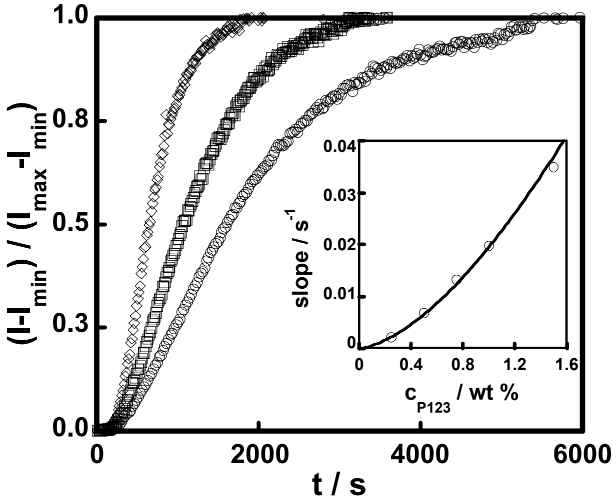

**Figure 12.** Normalized scattered intensity from SLS as a function of time for the mixed solution with $C_{12}EO_6$/P123 molar ratio 2.2 and with various amounts of P123: 0.50 wt % (○), 0.75 wt % (□) and 1.5 wt % (□). The inset presents the initial slope of the linear part of the intensity vs. time for the MR = 2.2 solution as a function of the P123 concentration (0.25, 0.50, 0.75, 1.0, 1.5 wt %).

The figure reveals the strong concentration dependence. An increase of the total concentration increases the rate of the process. It was a matter of hours to reach equilibrium in the 0.25 wt % solution while in the 1.5 wt % solution it took about 1000 s (or 16 min) to reach the equilibrated state. In order for the mixed P123-$C_{12}EO_6$ micelles to change shape and grow from spheres to elongated rods enough material is needed and that can only be achieved by encounter with neighboring aggregates. The slope of the initial, linear part of the intensity curves may represent the rate of the growth process. The insert in Figure 12 shows a plot of the initial slopes (in $s^{-1}$) against copolymer concentration (at MR = 2.2). A power law function describes the data points. The rheological investigation of the same system did not show any slow kinetic effects at P123 concentrations above 5 wt %. However, for 1.5 wt % and MR = 2.2, the rheological technique was able to detect the slow growth of the mixed aggregates.[50]

## DISCUSSION

The phase behavior of PEO-PPO-PEO copolymers in water has been investigated both experimentally and modelled theoretically.[51-55] A general phenomenon in PEO-containing polymer (or surfactant) aqueous systems is the occurrence of a lower critical solution temperature (LCST), above which there is liquid-liquid phase separation.[56] It appears because the effective solute-solute interactions become more attractive at higher temperatures. One explanation for this behavior is that the –O-C-C-O- sequence in PEO changes into a less polar form as the temperature increases and therefore PEO interacts less favourably with water.[57] A weakened PEO-water interaction at elevated temperatures favors a higher packing density at the PPO-PEO interface, which in turn favors a change in the shape of the micelles from spherical to rod-like (or cylindrical). For the same reason PEO-PPO-PEO-water systems often present a normal hexagonal liquid crystalline phase of cylindrical micelles at temperatures above that of the cubic phase, which consists of spherical micelles, see *e. g.* refs 52 and 58.

In the present study we have investigated the mixed system of the nonionic PEO-PPO-PEO copolymer $EO_{20}PO_{39}EO_{20}$ (P123) and the nonionic surfactant $C_{12}EO_6$. Even small additions of $C_{12}EO_6$ have surprisingly large effects on the liquid-liquid phase separation temperature (Figure 3). A minimum is observed at molar ratios between 2 and 3. The pure P123 micelles undergo a shape transition from spherical to rod-like at around 60 °C, see Table 1 and Figure 2. The mixed micelles formed upon addition of $C_{12}EO_6$ also show this change of shape at temperatures that vary with composition. The phase separation temperature and the sphere-to-rod transition temperature follow the same trend presenting minima at molar ratios between 2 and 3 (Figures 2 and 3).

For the pure P123 micelle at 40 °C, the aggregation number is 131 as determined by using SLS and for MR = 0.7 it is 127.[34] We propose that for low molar ratios up to 2.2, the large PPO core of the spherical aggregate is not significantly affected by the solubilization of the $C_{12}EO_6$ surfactant molecules that will be located at the PPO-PEO interface. The fact that the apparent $R_H$ values of the mixed spherical micelles are almost unchanged up to molar ratios 2.2 compared to the pure P123 micelles (see Figure 10) supports this assumption. This means that the incorporation of the $C_{12}$ alkyl chains does not affect the interior of the core and no unfavorable stretching of the PPO chains will occur. The relaxation of the PPO stretching when the PEO-PPO-PEO micelle change from spherical to rod-like is one of the factors that drives the sphere-to-rod transition in the pure PEO-PPO-PEO systems.[21] The other one is the conformation change of the PEO groups. Therefore, we may focus the discussion on the PEO conformation at the core-corona (or PPO-PEO) interface of the micelles to explain their preferred shape. At the core-corona interface of the pure block copolymer micelles, the area per $EO_{20}$ chain is such that the spherical form of the micelles is favored at ambient temperatures. This means that the area per PEO chain is large and the PEO conformation is therefore not completely stretched. It is expected that, at small additions of $C_{12}EO_6$ to the pure P123 micelles, the insertion of the surfactant molecules would lead to a separation of the $EO_{20}$ chains at the core-corona interface causing an increase in the area per $EO_{20}$ group. Thus, the $C_{12}EO_6$ molecules would act as spacers. Zheng and Davis[59] have discussed this spacer effect in the mixed $EO_{21}$-$EE_{35}$-$EO_{21}$ block copolymer–$C_{12}EO_5$ surfactant aqueous system, where EE denotes ethylethylene. In their system, the pure block copolymer micelles are cylindrical. This structure has a low curvature with stretched PEO corona chains. The addition of $C_{12}EO_5$ to the $EO_{21}$-$EE_{35}$-$EO_{21}$micelles allows the $EO_{21}$ chains to relax and adopt a more coiled conformation as the distance between the $EO_{21}$ groups increases due to the insertion of the $C_{12}EO_5$ molecules at the core-corona interface. This gives a more curved interface and the mixed micelles become spherical. However, in the P123-$C_{12}EO_6$ system we do not observe the same effect, as the curvature of the pure P123 micelles is already large. We cannot tell whether the $C_{12}EO_6$ molecules act as spacers at low additions since the spherical shape is the geometrical form that has the largest curvature of all possible geometries. As the addition of $C_{12}EO_6$ continues, still at molar ratios below 2 where the PPO core radius is unaffected, the effect is instead the opposite: the presence of the $C_{12}EO_6$ molecules with their shorter $EO_6$ chains at the PPO-PEO interface causes a decrease in the overall average PEO area. This decrease will facilitate a temperature-induced change from a spherical to a rod-like shape and, therefore, the sphere-to-rod transition temperature is lowered. In the region of molar ratios 2-3 both the shape transition and the phase separation temperatures are at the minimum, see Table 1 and Figures 2 and 3. At higher $C_{12}EO_6$ content both transition temperatures increase. At a molar ratio of 6, the aggregation number of P123 has decreased to 52 (at 40 °C).[34] The core now consists of about 50 PPO blocks and 330 $C_{12}$ chains and we expect the core radius to be slightly smaller than that at lower molar ratios. The observed change in $R_H$ from 10 to 8 nm (at 40°C) supports this assumption.[34] This means that the curvature of the mixed micelles at molar ratio 6 is larger than at molar ratio 2. In order to change the curvature into a state that fits a rod-like shape more energy needs to be put into the system. A larger curvature of the smaller micelles explains why the sphere-to-rod transition temperature for MR = 6 is higher than that at MR = 2 (Table 1).

The PEO-PPO-PEO copolymers are polydisperse both in mass and composition. This causes the micellization process to occur in a concentration range or a temperature range rather than at a specific critical concentration or temperature.[9,19,60,61] This is manifested in a broad unimer-to-micelle temperature region as seen as a broadening of the main transition peak in the DSC experiments (Figure 1a). For the mixed P123-$C_{12}EO_6$ system, a shoulder appeared on the low temperature side of the DSC peak at molar ratios 0.7 and 1.1 and the main peak became broader (Figure 1a). This shoulder was only seen for low additions of $C_{12}EO_6$. At molar ratio 2.2 the peak has moved to the position of the shoulder and also become narrower. The mixed system consists at low temperature of P123 unimers and $C_{12}EO_6$ micelles. When the temperature increases, aggregates start to form at a considerably lower temperature than in pure P123 solution. The shoulder in the DSC peaks could indicate that a new species was formed, i.e. mixed micelles with a defined stoichiometry. At molar ratio 2.2 the shoulder was replaced by a well-defined peak indicating complete conversion to micelles of about this composition. As we have not investigated the variation of the DSC peaks with composition in any more detail, we assume for the sake of simplicity that the mixed micelles contain 2 $C_{12}EO_6$ per P123 molecule. The enthalpy of aggregation •$H_{agg}$ of the mixed micelle, calculated per mol of P123, is not significantly changed but the temperature $T_m$ has decreased 5 °C compared to pure P123, see Table 1. The formation of mixed micelles with a 2:1 composition is compatible with the pronounced minima in the sphere-to-rod and liquid-liquid phase separation temperatures at $C_{12}EO_6$/P123 molar ratios in the range 2-3.

The titration of $C_{12}EO_6$ into P123 solution at 40 °C gave endothermic interaction enthalpies followed by a sharp exothermic minimum at a molar ratio between 2 and 3 depending of P123 concentration (Figure 5). After the minimum the interaction enthalpies were again endothermic but smaller than before. An inspection of the DSC curves in Figure 2 gives a possible reason for this exothermic peak. Based on results from the light scattering experiments we ascribe the small broad peak in the DSC curves to a sphere-to-rod transition of mixed micellar aggregates. According to the curves the onset temperature of this peak decreases with increasing $C_{12}EO_6$ content from 51 °C at molar ratio MR = 1.1 to 38 °C at MR = 2.2 and then increases to 41 °C at MR = 3.2 and further to 48 °C at MR = 6. This implies that at MR = 2.2 all mixed aggregates are in the form of spheres at temperatures below 38 °C and in the form of rods above 46 °C. The sphere-to-rod transition is endothermic by about 10 kJmol$^{-1}$. The isothermal calorimetric experiments at 40 °C cross the lower part of the DSC peak for MR = 2.2. If we use the Figure 2 to envisage what happens during the titration when adding $C_{12}EO_6$ to a P123 solution at 40 °C (Figure 5) we can see that in the beginning at low molar ratios, the mixed micelles are spherical and continue to be so until we reach MR about 2 where rods will start to form. Increasing the $C_{12}EO_6$ content further, more rods are formed but then at MR above 3, all the aggregates become spheres again. Thus the rods exist over only a narrow concentration range. The formation of spheres from rods will be exothermic, which gives the sharp exothermic peak in the calorimetric titration curves (Figure 5). The endothermic change we could expect to see when the rods form from spheres is probably hidden in the endothermic enthalpy changes we measure before the exothermic peak.

## ACKNOWLEDGEMENTS

We wish to acknowledge the financial support of the Swedish Research Council (VR) and the Linneus Center of Excellence “Organizing Molecular Matter” (KS); the Swedish Foundation for Strategic Research (SSF) (DL) and the

Brazilian Agencies FAPESP and CNPq (WL, AN).

## REFERENCES

(1) *Nonionic Surfactants: Polyoxyalkylene Block Copolymers*; Nace, V. M., Ed.; Marcel Dekker, Inc.: New York, 1996; Vol. 60.

(2) Brochure *Pluronic and Tetronic Surfactants*; BASF Performance Chemicals, BASF Corp.: Mount Olive, NJ, 1996.

(3) *Amphiphilic Block Copolymers: Self-Assembly and Applications*; Alexandridis, P.; Lindman, B., Eds.; Elsevier Science, BV: Amsterdam, 2000.

(4) Wu, J.; Xu, Y.; Dabros, T.; Hamza, H. *Colloids Surf. A* **2005**, *252*, 79.

(5) Fusco, S.; Borzacchiello, A.; Netti, P. A. *J. Bioact. Comp. Polym.* **2006**, *21*, 149.

(6) Kabanov, A. V.; Alakhov, V. Y. *Crit. Rev. Ther. Drug Carrier Syst.* **2002**, *19*, 1.

(7) Al-Saden, A. A.; Whately, T. L.; Florence, A. T. *J. Colloid Interface Sci.* **1982**, *90*, 303.

(8) Rassing, J.; Attwood, D. *Int. J. Pharm.* **1983**, *13*, 47.

(9) Brown, W.; Schillén, K.; Almgren, M.; Hvidt, S.; Bahadur, P. *J. Phys. Chem.* **1991**, *95*, 1851.

(10) Mortensen, K.; Brown, W. *Macromolecules* **1993**, *26*, 4128.

(11) Pedersen, J. S.; Gerstenberg, M. C. *Colloids Surf. A* **2003**, *213*, 175.

(12) Beezer, A. E.; Loh , W.; Mitchell, J. C.; Royall, P. G.; Smith, D. O.; Tute, M. S.; Armstrong, J. K.; Chowdhry, B. Z.; Leharne, S. A.; Eagland, D.; Crowther, N. J. *Langmuir* **1994**, *10*, 4001.

(13) Alexandridis, P.; Holzwarth, J. F.; Hatton, T. A. *Macromolecules* **1994**, *27*, 2414.

(14) Alexandridis, P.; Hatton, T. A. *Colloids Surf. A* **1995**, *96*, 1.

(15) Mortensen, K. *J. Phys.: Condens. Matter* **1996**, *8*, A103.

(16) Chu, B.; Zhou, Z. In *Nonionic Surfactants: Polyoxyalkylene Block Copolymers*; Nace, V. M., Ed.; Marcel

Dekker, Inc.: New York, 1996; Vol. 60; pp 67.

(17) Mortensen, K.; Pedersen, J. S. *Macromolecules* **1993**, *26*, 805.

(18) Schillén, K.; Brown, W.; Johnsen, R. M. *Macromolecules* **1994**, *27*, 4825.

(19) Batsberg, W.; Ndoni, S.; Trandum, C.; Hvidt, S. *Macromolecules* **2004**, *37*, 2965.

(20) Michels, B.; Waton, G.; Zana, R. *Colloids and Surf. A* **2001**, *183-185*, 55.

(21) Linse, P. *J. Phys. Chem.* **1993**, *97*, 13896.

(22) Jørgensen, E. B.; Hvidt, S.; Brown, W.; Schillén, K. *Macromolecules* **1997**, *30*, 2355.

(23) Wu, Y. L.; Sprik, R.; Poon, W. C.; Eiser, E. *J. Phys.: Condens. Matter* **2006**, *18*, 4461.

(24) Aswal, V. K.; Kohlbrecher, J. *Chem. Phys. Lett.* **2006**, *425*, 118.

(25) Nagarajan, R.; Barry, M.; Ruckenstein, E. *Langmuir* **1986**, *1*, 210.

(26) Nagarajan, R.; Ganesh, K. *J. Colloid Interface Sci.* **1996**, *184*, 489–499.

(27) Gadelle, F.; Koros, W. J.; Schechter, R. S. *Macromolecules* **1995**, *28*, 4883.

(28) Caragheorgheopol, A.; Caldararu, H.; Dragutan, I.; Joela, H.; Brown, W. *Langmuir* **1997**, *13*, 6912.

(29) Causse, J.; Lagerge, S.; de Ménorval, L.-C.; Faure, S.; Fournel, B. *Colloids Surf. A* **2005**, *252*, 51.

(30) Lettow, J. S.; Lanchaster, T. M.; Glinka, C. J.; Ying, J. Y. *Langmuir* **2005**, *21*, 5738.

(31) Couderc, S.; Li, Y.; Bloor, D. M.; Holzwarth, J. F.; Wyn-Jones, E. *Langmuir* **2001**, *17*, 4818.

(32) Couderc-Azouani, S.; Sidhu, J.; Thurn, T.; Xu, R.; Bloor, D. M.; Penfold, J.; Holzwarth, J. F.; Wyn-Jones, E. *Langmuir* **2005**, *21*, 10197.

(33) Hossain, K. M.; Hinata, S.; Lopez-Quintela, A.; Kunieda, H. *J. Disp. Sci. Technol.* **2003**, *24*, 411.

(34) Schillén, K.; Jansson, J.; Löf, D.; Costa, T.*, in preparation.*

(35) Glatter, O.; Fritz, G.; Lindner, H.; Brunner-Popela, J.; Mittelbach, R.; Strey, R.; Egelhaaf, S. U. *Langmuir* **2000**, *16*, 8692.

(36) Schurtenberger, P.; Cavaco, C.; Tiberg, F.; Regev, O. *Langmuir* **1996**, *12*, 2894.

(37) Jansson, J.; Schillén, K.; Olofsson, G.; da Silva, R. C.; Loh, W. *J. Phys. Chem. B* **2004**, *108*, 82.

(38) Stepanek, S. In *Dynamic Light Scattering: The Method and Some Applications*; Brown, W., Ed.; Oxford University Press: Oxford, 1993; pp 177.

(39) Vink, H. *J. Chem. Soc., Faraday Trans. 1* **1985**, *81*, 1725.

(40) Grell, E.; Lewitzki, E.; Schneider, R.; Ilgenfritz, G.; Grillo, I.; von Raumer, M. *J. Therm. Anal.* **2002**, *68*, 469.

(41) Ilgenfritz, G.; Schneider, R.; Grell, E.; Lewitzki, E.; Ruf, H. *Langmuir* **2004**, *20*, 1620.

(42) Olofsson, G. *J. Phys. Chem.* **1985**, *89*, 1473.

(43) Kaneshina, S.; Shibata, O.; Nakamura, M. *Bull. Chem. Soc. Jpn.* **1982**, *55*, 951.

(44) Comment. Values for the enthalpy of micelle formation of $C_{12}EO_6$ in water at 15 °C and 20 °C that can be derived from titration curves shown in Figures 3 and 4 of ref 31 and at 25 °C from Figure 13 of ref 32 are 4.3 to 5.0 kJ/mol lower than results reported in ref 42. We have no explanation for this discrepancy.

(45) da Silva, R. C.; Olofsson, G.; Schillén, K.; Loh, W. *J. Phys. Chem. B* **2002**, *106*, 1239.

(46) Borsali, R.; Nguyen, H.; Pecora, R. *Macromolecules* **1988**, *31*, 1548.

(47) Kratochvil, P. *Classical Light Scattering from Polymer Solutions*; Elsevier Science Publishers B. V.: Amsterdam, 1987.

(48) Burchard, W.; Schmidt, M.; Stockmayer, W. H. *Macromolecules* **1980**, *13*, 1265.

(49) Burchard, W. *Adv. Polymer Sci.* **1999**, *143*, 113.

(50) Löf, D.; Schillén, K.; Torres, M. F.; Muller, A.*, in preparation.*

(51) Wanka, G.; Hoffmann, H.; Ulbricht, W. *Macromolecules* **1994**, *27*, 4145.

(52) Zhang, K.; Khan, A. *Macromolecules* **1995**, *28*, 3807.

(53) Hecht, E.; Mortensen, K.; Hoffnann, H. *Macromolecules* **1995**, *28*, 5465.

(54) Alexandridis, P.; Olsson, U.; Lindman, B. *Langmuir* **1998**, *14*, 2627.

(55) Svensson, M.; Alexandridis, P.; Linse, P. *Macromolecules* **1999**, *32*, 637.

(56) Holmberg, K.; Jönsson, B.; Kronberg, B.; Lindman, B. *Surfactants and Polymers in Aqueous Solution*; John Wiley & Sons, Ltd.: Chichester, 2003.

(57) Karlström, G. *J. Chem. Phys.* **1985**, *89*, 4962.

(58) Glatter, O.; Scherf, G.; Schillén, K.; Brown, W. *Macromolecules* **1994**, *27*, 6046.

(59) Zheng, Y.; Davis, H. T. *Langmuir* **2000**, *16*, 6453.

(60) Linse, P. *Macromolecules* **1994**, *27*, 6404.

(61) Hvidt, S.; Trandum, C.; Batsberg, W. *J. Colloid Interface Sci.* **2002**, *250*, 243.

# CAPÍTULO V – ARTIGO

**II**

*J. Phys. Chem. B,* **2008**, 112, 727

# Interaction of ethylene oxide-propylene oxide copolymers with ionic surfactants studied by calorimetry: random *versus* block copolymers.

Anna Niemiec and Watson Loh*

*Institute of Chemistry, Universidade Estadual de Campinas (UNICAMP),*
*Caixa Postal 6154, 13083-970, Campinas, SP, Brazil*

*corresponding author : wloh@iqm.unicamp.br, Phone : + 55 19 3521 3148,
Fax: + 55 19 3521 3023.

# ABSTRACT

The present study used these techniques to follow the interaction of random and block ethylene oxide (EO) – propylene oxide (PO) copolymers with ionic surfactants. Features such as the intensity of the interaction (evaluated through their critical aggregation concentrations) and the profile of the isothermal titration calorimetry (ITC) curves were comparatively analyzed for random and block copolymers with similar composition (number of EO and PO units). Random copolymers displayed an interaction similar to that observed with other hydrophilic homopolymers, with the additional characteristic that the intensity of the interaction increased with the increase in the copolymer hydrophobicity (as determined by its PO content), revealing that these copolymers display an intermediate behavior between PEO and PPO. For non-aggregated block copolymers (unimers) with large enough EO blocks (M above 2000 g $mol^{-1}$), ITC curves revealed that the anionic surfactant SDS interacts with the PO and EO blocks almost independently, being more favorable with the PO block, which controls the c.a.c. value. Effects of temperature and of the nature of the ionic surfactants on their interaction with these copolymers were found to agree with the previously reported trends.

## INTRODUCTION

Aqueous solutions containing polymers and surfactants are found in a large number of industrial and pharmaceutical/cosmetic formulations. In general, their properties differ from the ones of the pure components, due to an interaction resulting in the formation of different kinds of mixed aggregates. Most of the physical-chemical aspects of these mixtures have been summarized in recent books and review articles such as references 1 to 4. These mixtures are currently investigated by using a variety of techniques, among them the calorimetric techniques isothermal titration and high sensitivity differential scanning calorimetry, respectively known by the acronyms ITC and HSDSC. References 3 and 4 present a summary of recent investigations employing these techniques and review the main information they are capable of providing on such mixtures. A search in the literature (as shown in reference 3) indicates a great recent increase in the use of both ITC and HSDSC in studies on surfactant and/or polymer association due to their high sensitivity and to the possibility of following the evolution of the aggregation process as either composition or temperature is varied. These techniques allow direct evaluation of the intensity of this interaction (typically assessed by their critical aggregation concentration, c.a.c.), but also, especially in combination with other techniques, of information such as changes in polymer hydration, determination of the number or surfactant molecules bound per polymer chain, on the packing of surfactant molecules among others.

Investigations on surfactant-copolymer mixtures are more scarce, and mostly devoted to the widely used family of ethylene oxide – propylene oxide triblock copolymers (EO-PO-EO), which display surfactant behavior and a rich self-assembling in aqueous solutions.[5-7] It has been shown that this aggregation may be prompted by changes both in temperature (associated with a critical micelle temperature, cmt) and in concentration (above a well-defined critical micelle concentration, cmc.[8] This aggregation is an endothermic process whose driving force is the entropy gain associated with the release of water molecules solvating the hydrophobic PO units upon micellization, which are mostly hidden from water inside the aggregates.[5,7-9] Formation of other types of aggregates with different geometries by these copolymers has been also reported, including all of the classical types of mesophases[10] or vesicles.[11] Addition of surfactants provokes significant changes in these copolymers aggregation. With the addition of ionic surfactants such as sodium dodecylsulfate, SDS, both their mesophases and micelles are disrupted[12-15] resulting in the formation of more water soluble mixed aggregates that, in some cases, may co-exits with another population of aggregates, as detected by light scattering measurements.[13,14] Nonionic surfactants also interact with these copolymer aggregates, but with less intensity,[15,16] though leading to interesting phenomena such as the one recently reported on the changes in shape of these mixed aggregates with surfactant/polymer ratio and temperature.[17]

Studies on surfactant interaction with polymers of star architecture (star PEO),[18] revealed that polymer geometry is also an important parameter in controlling their association. The same group has investigated the interaction of surfactants with copolymers of different architectures: telechelic (or hydrophobically end-capped PEO) [19] and reverse (PO-EO-PO) block copolymers.[20]

These earlier studies prompted the present work, which aims at comparing the surfactant association with EO/PO copolymers with random structure with that of their similar block copolymers in order to assess the effect of copolymer architecture on this interaction.

Random EO/PO copolymers have been already investigated as alternative to the use of EO-PO-EO block copolymers in the formation of aqueous two-phase systems, with the aim of use in bioseparation processes.[21] Random copolymers are also water soluble, of low toxicity and, when compared to their similar block copolymers, display lower cloud points (critical solution temperatures),[22] allowing the formation of aqueous two-phase systems at lower temperatures. Light scattering studies revealed no sign of aggregation in aqueous solutions of these random copolymers below their cloud points,[23] indicating that the monomer sequence along the polymer chain does not allow significant interaction among the more hydrophobic PO units, as has been observed for the block copolymers.

For the present study, a series of random and block EO/PO copolymers with similar composition (number of EO and PO units) was selected, and their interaction with ionic surfactants was followed mostly by using isothermal titration calorimetry. These results are then analyzed as a function of copolymer architecture and composition, as well as of other parameters such as temperature and surfactant type.

## Experimental

**Materials.** Random and triblock copolymers containing ethylene oxide (EO) and propylene oxide (PO) units with different compositions were used. Their chemical composition and other main features are described in Table 1.

**Table 1**:Physical-chemical characteristics of the block and random copolymers used in this study.

| **Triblock copolymers (commercial names)** | **% EO (wt.)*** | **M [g/mol]**$^a$ | $\left(\frac{\mathbf{Mw}}{\mathbf{Mn}}\right)^b$ | **Random copolymers** | **% EO (wt.)** $^c$ | **M [g/mol]**$^a$ | $\left(\frac{\mathbf{Mw}}{\mathbf{Mn}}\right)^b$ |
|---|---|---|---|---|---|---|---|
| $EO_{11}$-$PO_{16}$-$EO_{11}$ (L35) | 50 (65) | 1900 | 1.14 | $EO_{19}$-$PO_{15}$ | 50 (53) | 1900 | 1.19 |
| $EO_{13}$-$PO_{31}$-$EO_{13}$ (L64) | 50 (59) | 2900 | 1.24 | $EO_{34}$-$PO_{25}$ | 50 (56) | 2900 | 1.22 |
| $EO_{114}$-$PO_{31}$-$EO_{114}$ (F88) | 85 (86) | 11800 | 1.32 | $EO_{116}$-$PO_{48}$ | 65 (66) | 8000 | 1.27 |
| - | - | - | - | $EO_{43}$-$PO_{11}$ | 75 (78) | 2500 | 1.19 |
| $EO_{52}$-$PO_{35}$-$EO_{52}$(F77) | 75 (79) | 6600 | 1.29 | $EO_{106}$-$PO_{27}$ | 75 (75) | 6600 | 1.29 |
| $EO_{95}$-$PO_{62}$-$EO_{95}$(F127) | 75 (80) | 12000 | 1.53 | $EO_{204}$-$PO_{52}$ | 75 (79) | 12000 | 1.44 |

a ) nominal molar masses, as provided by the manufacturers.

b) Mw and Mn refer to weight and number average molar masses, respectively.

The ratio (Mw/Mn) refers to the polydispersity of the sample molar mass distribution.

c) in parentheses values determined by NMR spectroscopy (see text for details) .

Block copolymers were a gift from ICI, England, and BASF, USA (F127), and were used as received. GPC analyses of these samples (see details in the methods section) showed only one elution peak in most of the cases and two elution peaks only in the case of the block copolymer F127. Polydispersity indices, represented as the ratio $M_w/M_n$, are listed in the Table 1. Random copolymers were a gift from Laporte Performance Chemicals, England, and were also used without further treatment. GPC analyses revealed polydispersity values for these samples within 1.2 and 1.4 as shown in Table 1. The EO/PO ratio for these copolymer samples was determined by NMR spectroscopy (see details in the methods section) and the obtained values, shown in Table 1, agree very well with their nominal ones. No attempt was made to determine their actual molar masses, and nominal values are used throughout.

Samples of PEO 600 and 2000, PPO 2000 and dimethyl PEO 2000 were purchased from Aldrich, and used as received. Sodium dodecylsulfate (SDS) and dodecyltrimethylammonium bromide (DTAB) were obtained from Aldrich. Hexadecyltrimethylammonium bromide (CTAB) was purchased from BDH Chemicals Ltd. Poole, England. These surfactants were all of the highest purity available, and were used as received. Dodecylammonium chloride (DAC) was prepared as reported in a previous investigation.[22] Water used throughout was of Milli-Q grade. All solutions were prepared by weight and the polymer solutions were prepared at least 24 h prior to use.

## METHODS

**Isothermal Titration Calorimetry.** A VP-ITC (MicroCal, Northampton, MA) isothermal titration calorimeter was used. This sample cell has a volume of 1.43 mL. Consecutive injections of surfactant solution were made, with a gastight syringe that also acts as a stirrer (working at 550 rpm). The interval between injections was set as 600 s. Injection volumes varied between 3 and 15 μL. The cell volume was kept constant by an overflow of solution, which was taken into account during calculations of the actual surfactant concentrations in the cell.

These experiments allow controlled addition of surfactant to a polymer solution recording the enthalpy changes during both surfactant dilution (polymer dilution heat effects are negligible) and surfactant-polymer interaction. These values are reported as observed enthalpy changes ($\Delta H_{obs}$) as a function of final surfactant concentration, ascribing the interaction heat exchanged to the total amount of surfactant added, and, more importantly, they differ from the actual interaction enthalpies because the fraction of the added surfactant molecules that interacts with the polymer is not known. A comprehensive thermodynamic description can be obtained by using complementary techniques such as the use of surfactant selective electrodes to determine the surfactant binding isotherms, as reported, for instance, in references 3, 15 and 16.

**Differential Scanning Calorimetry.** A VP-DSC (MicroCal, Northampton, MA), differential scanning calorimeter was used. This equipment contains 0.542 mL twin cells for the reference (filled with water) and sample solutions, whose temperature is varied under control rate (both in heating and cooling mode) allowing the detection of phase transitions and the determination of enthalpy changes associated with them. Transition temperatures are determined as $T_{onset}$, for the beginning of transition, and $T_m$ for the maximum of the peak, and enthalpy changes were calculated by integration of the peaks. Measurements were performed using a scan rate of 30 degrees $h^{-1}$ in the temperature range of 5 - 100°C.

**Nuclear Magnetic Resonance.** These measurements were performed on a Varian Unity Inova 500 spectrometer, at 25°C. All of the random copolymers and block copolymers listed in Table 1 have been studied. 1mL of 100 mg/L solutions, with $D_2O$ ($\delta = 4.62$ ppm) as solvent, were placed in 5 mm diameter tubes. NMR spectra allowed the calculation of the actual ratio between EO and PO units by analyzing the integrated height of the signal for $CH_3$ hydrogens (positioned ca. $\delta = 1$ ppm) and CH hydrogens (positioned ca. $\delta = 3\text{-}4$ ppm) belonging to the PO groups of the polymer versus the $CH_2$ hydrogens (positioned ca. $\delta = 3\text{-}4$ ppm) from PO and EO polymer groups. As can be seen in Table 1, these calculated values agree well with those provided by the manufacturer.

**Gel Permeation Chromatography.** Instrumentation Waters 510 GPC was used, along with a PEDV column (7,8x300mm, $\Phi_p$ =10μm, V=0,7ml/min) purchased from Polymer Laboratories, Inc. and a refractive index detector, IR 410.

Measurements were performed with 2% solutions in THF, at 30 $^{o}$C, using standards of poly(styrene) in the molar mass range of 450 – 1,030,000 Da. Elution curves were analyzed using the Millennium Acquisition Report program, version 2.15, provided by Waters Co.

**Cloud point measurements.** Cloud points were determined for solutions of some block and random copolymers following the same procedure as described elsewhere.[24] Typically, these samples were investigated upon controlled heating (ca. 1 degree min$^{-1}$) and the cloud point was considered as the temperature in which we observed the appearance of the first persistent turbidity. Replicates produced results that agree within 1 $^{0}$C.

## RESULTS

### Interaction between SDS and random copolymers.

Use of isothermal titration calorimetry for the investigation of the interaction between surfactants and polymers can be exemplified by the results shown in Figure 1, which describes the interaction between an anionic surfactant, SDS, and a random copolymer, $EO_{19}$-$PO_{15}$, at 25 $^{o}$C. This experiment is arranged so that a concentrated surfactant solution (well above its cmc) is consecutively added to a dilute polymer solution, which is placed into the calorimeter cell.

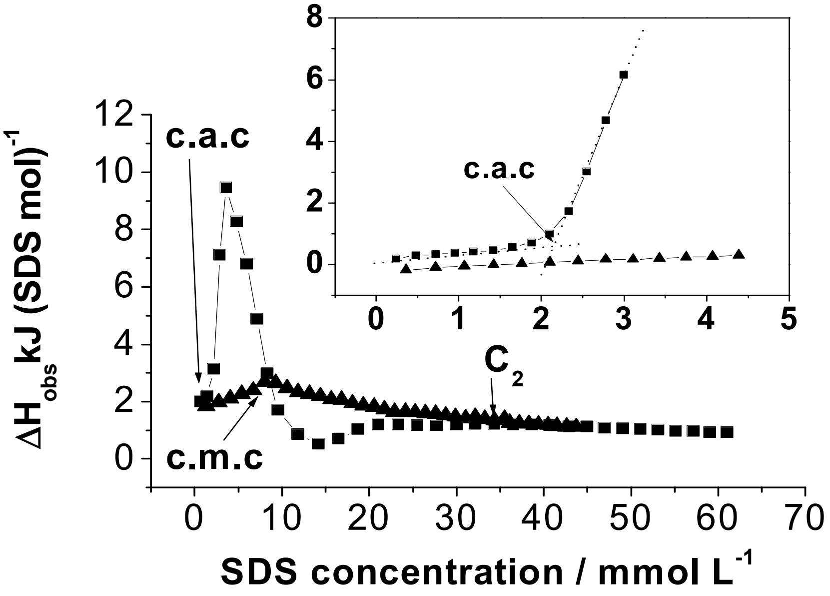

**Figure 1:** ITC curves for titration of 10 wt % SDS into Δ water and ■ 0.1 wt % solution of EO$_{19}$-PO$_{15}$, at 25°C.

On the right, titration of 1.0 wt % SDS into Δ water and in ■ 0.1 wt % solution of EO$_{19}$-PO$_{15}$, at 25°C, which allows a more precise determination of c.a.c. values (notice that enthalpy values are different from the ones in the complete curve due to different SDS concentrations being used in the syringe for each experiment).

At low surfactant concentration, the addition of SDS to polymer solution produces slightly more positive enthalpy values, indicating some sort of endothermic interaction between them. As surfactant concentration passes a critical value, the so called critical aggregation concentration, c.a.c., a much greater enthalpy change accompanies each addition, in a process that is highly cooperative and which is ascribed to the formation of small surfactant aggregates around the polymer chain. This aggregation is assumed to occur facilitated by the presence of polymer (c.a.c. values are always smaller than c.m.c. ones), and the extent to which it is affected by the polymer can be estimated by the ratio of c.a.c. to c.m.c. values: the smaller, the more intense the interaction (see, for instance, reference 25). The large and positive enthalpy values are generally ascribed to the dehydration of polymer chains upon their interaction with these aggregates[26,27] and, as other possibilities, to dehydration of surfactant counter-ions [16] or to changes in the strain of unfavorable conformations of the polymer chain.[28] As the surfactant binding progresses, the difference between the two dilution curves reaches a maximum and then decreases as surfactant concentration increases. This decrease in the enthalpy difference suggests a smaller extent of polymer dehydration upon surfactant binding, which continues until passing through a minimum, under the surfactant dilution curve, indicating an exothermic process probably due to polymer rehydration, followed by a new increase in enthalpy until the two dilution curves merge at the point called $C_2$ (or saturation concentration). Above this concentration, micelles of SDS added are only diluted with no further polymer-surfactant interaction.

Among the different random copolymers studied, there was only one exception for this general behavior, which were the results obtained for the interaction of SDS with the random copolymer containing 75 % of EO units and with molar mass of 2500 g mol$^{-1}$ ($EO_{43}PO_{11}$), shown in Figure 2.

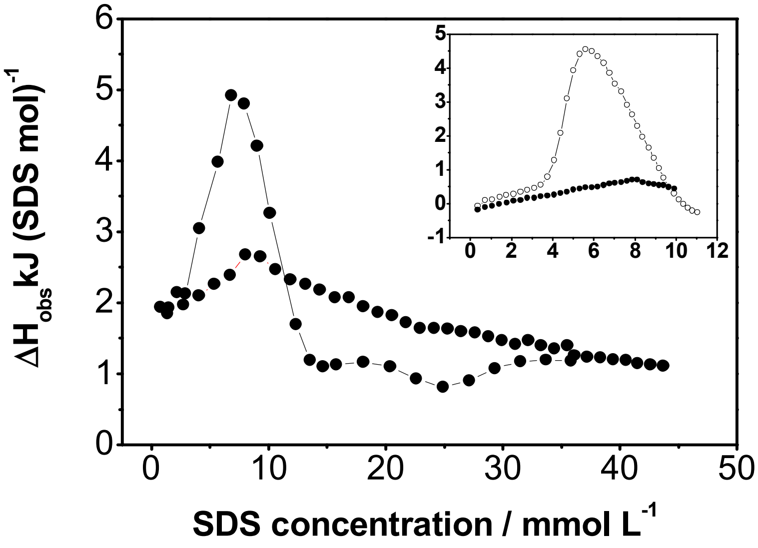

Figure 2: ITC curves for titration of 10 wt % SDS into ● water and ○ 0.1 wt % solution of $EO_{43}$-$PO_{11}$, at 25°C. On the right, titration of 1 wt % SDS into ● water and ○ 0.1 wt % solution of $EO_{43}$-$PO_{11}$, at 25°C.

For this copolymer, the ITC curve goes under the one for dilution of SDS in water, but displays two minima, at ca. 15 and 25 mmol L$^{-1}$. ITC curves with deviations such as shoulders or double minima have been reported for the interaction of SDS with PEO of molar mass in the range of 7,000 to 11,000 g mol$^{-1}$,[18, 27, 29] and have been explained as consequence of the formation of more than one surfactant aggregate per polymer chain. In the region where the interaction curves lie below the dilution ones, the approximation of two SDS aggregates interacting with the same polymer chain should lead to an increase in enthalpy due to mutual electrostatic repulsion, which, summed with the regular interaction curve leads to appearance of shoulders or double minima. It is somewhat surprising that the same behavior is observed with a rather small polymer (M = 2500 g mol$^{-1}$), and, moreover, that other copolymers with the same EO content (75 %), but with larger molar masses (6200 and 12000 g mol$^{-1}$) do not show the same behavior. If the occurrence of these two minima reflects the formation of a second SDS aggregate by interaction with this polymer chain, it would imply that these aggregates are significantly smaller than the ones formed around PEO chains.

C.a.c. values obtained at 15 and 25 $^{o}$C for the interaction of SDS with different random copolymers are shown in Figure 3. These values change with the copolymer composition and lie between the limit c.a.c values obtained with PEO and PPO, taken from the literature.[18, 27, 29] SDS interaction with PPO is assumed to be more favorable than with PEO due to the more hydrophobic nature of the former, which would lead to a less intense interaction with water and, consequently, smaller competition with SDS.

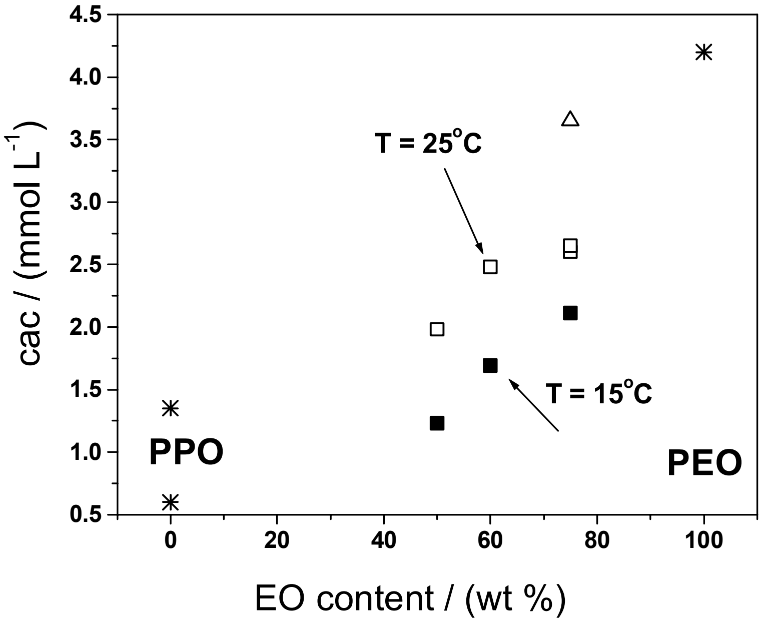

Figure 3: Effect of the copolymer EO content on the interaction between random copolymers and homopolymers with SDS, ■ random copolymers of 50 wt %, 65 wt %, 75 wt % of EO at 15°C, □ random copolymers of 50 wt %, 65 wt %, 75 wt % of EO at 25°C, * 0.1 wt % PEO 3350 at 25°C (data from references 26 and 27) , ○ 0.1 wt % PPO 1000 and 2000 at 25°C (data from reference 30), Δ random copolymer of MW 2500 and 75 % of EO groups in the polymer chain.

Literature c.a.c. values do not display changes with PEO molar mass above ca. 2000 g mol$^{-1}$ [27, 29], but they vary for PPO 1 000 and 2 000 g mol$^{-1}$ 30. Despite this variation, it is clear from the analysis of data in Figure 3 that SDS interaction becomes more intense as the PO content of the random copolymers increases, at the two studied temperatures. Hence, these random copolymers behave like polymers with an intermediate hydrophobicity between PEO and PPO. The only point that seems slightly out of this trend is the one for the copolymer whose ITC curve shows two minima ($EO_{43}PO_{11}$), which has been discussed above. In this case, it is likely that the same cause for the two minima also turns its interaction with SDS slightly less favorable, producing larger c.a.c. values.

In a similar way, the comparison of the ITC curves for the interaction of SDS with random copolymers of different EO contents, as shown in Figure 4, indicates that their profiles are also intermediate to the ones for the interaction with PEO (a more pronounced minimum) and with PPO (not shown, but based on literature data,[26,30] displaying a rather shallow minimum).

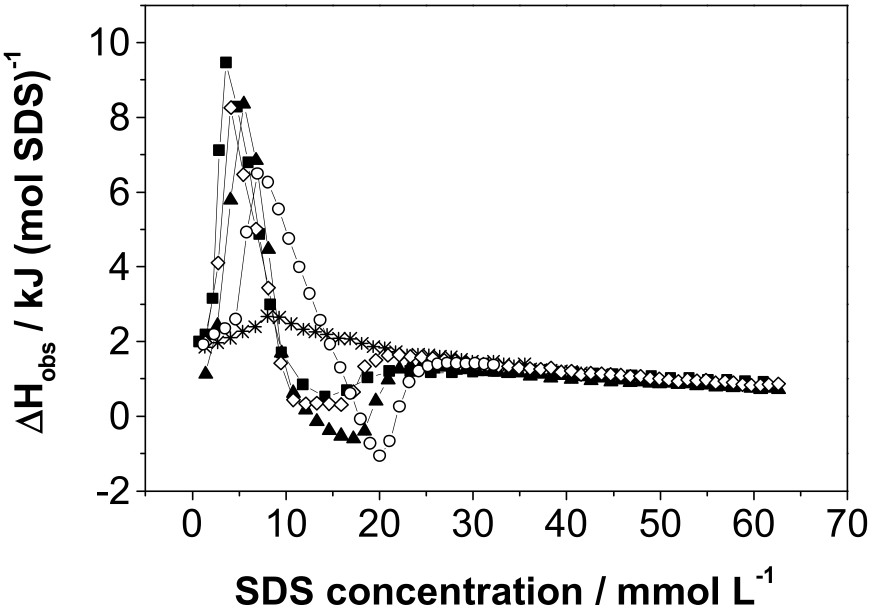

Figure 4: ITC curves for titration of 10 wt % SDS into:(*) water and 0.1 wt % solution of (■) EO$_{19}$-PO$_{11}$, (▲) EO$_{116}$-PO$_{48}$, (◇) EO$_{204}$PO$_{52}$, (o) PEO 3350 (data from reference 27) at 25°C.

### Random copolymers versus block copolymers.

The comparison of the interaction of SDS with random versus block copolymers requires that studies with block copolymers be conducted at temperatures below their critical micelle temperatures (c.m.t.), at which they should be present in non-aggregated state, also referred to as unimers.[5-7] We have performed DSC measurements for L64, EO$_{13}$-PO$_{31}$-EO$_{13}$ (data not shown), which reveals a critical micellization temperature of 28 °C for a 0.1 % solution, in agreement with the results reported in reference 16. We have not determined this value for F77 solutions, but based on literature data [9] and for its greater EO content, it is expected to be significantly higher, as is the case for F 127, whose c.m.t. for 0.1% solution was determined as ca. 30 °C (results not shown, but in agreement with the ones reported earlier in reference 13). Therefore, for all of these copolymers, the ITC measurements were conducted at 15 °C, safely below their aggregation temperatures.

The ITC investigation on the interaction of SDS with L64 unimers, $EO_{13}$-$PO_{31}$-$EO_{13}$, revealed a curve, shown in Figure 5, with general features that are very similar to those obtained for other hydrophilic polymers, such as with PEO of molar masses above ca. 1500-2000 g mol$^{-1}$ 27, 29 and PVP 4. ITC experiments were also conducted on the interaction of SDS with PEO 600 and PPO 2000, which have the same molar mass as the blocks of L64, at the same temperature. These results confirm that PEO 600 does not display the same interaction with SDS as PEO above 1500 (results not shown here, but agreeing with those previously reported [27, 29]). Moreover, the results shown in Figure 5 reveal that the interaction of L64 resembles that of PPO 2000 with SDS, both in the shape of the curves and in the c.a.c. values determined, 0.80 and 0.90 mmol L$^{-1}$ for L64 and PPO 2000, respectively. Figure 6 also shows that SDS interacts with a mixture of PEO 600 and PPO 2000 essentially in the same way as with L64 or pure PPO 2000, confirming that the more hydrophobic block controls this interaction.

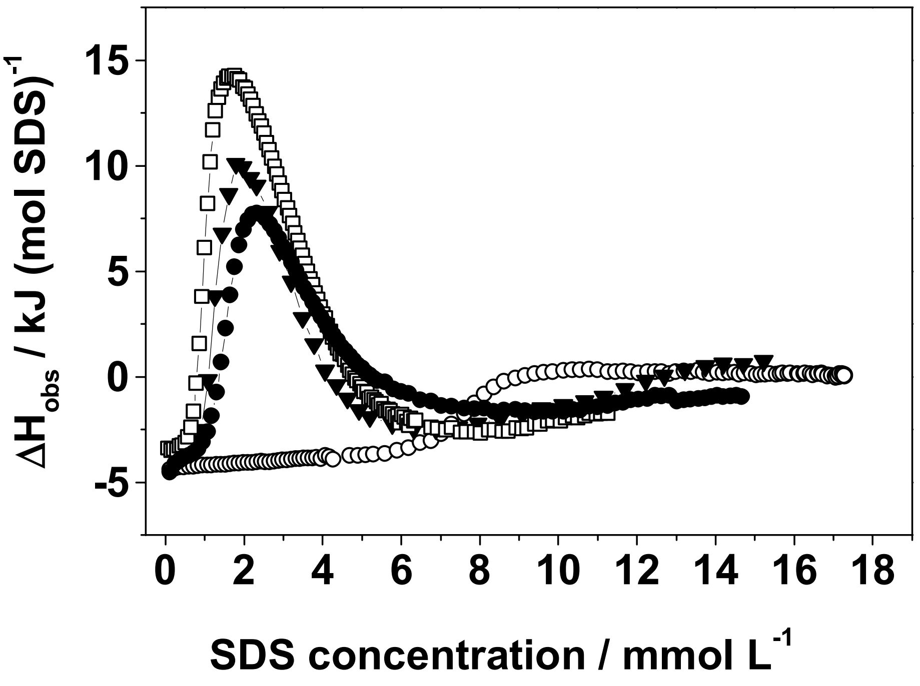

**Figure 5:** ITC curves for titration of 10 wt % SDS into ○ water and ■ 0.1 wt % PPO 2000 and ▼solution with 0.1 wt % PEO 600 and 0.1 wt % PPO 2000, ● 0.1 wt % solution of $EO_{13}$-$PO_{31}$-$EO_{13}$, at 15°C.

The ITC results for the interaction of SDS with unimers of another block copolymer, F77, however, reveal a different picture. The interaction curve, shown in Figure 6, displays two endothermic peaks between the beginning and the end of SDS-copolymer interaction. F77, $EO_{52}PO_{35}EO_{52}$, contains larger PEO blocks, each one with ca. 2000 g mol$^{-1}$, that are now capable of inducing the formation of SDS aggregates as described previously. This hypothesis is confirmed by investigation of SDS interaction with a mixture of PEO 2000 and PPO 2000, also shown in

Figure 6, which bears strong resemblance with the results obtained with F77.

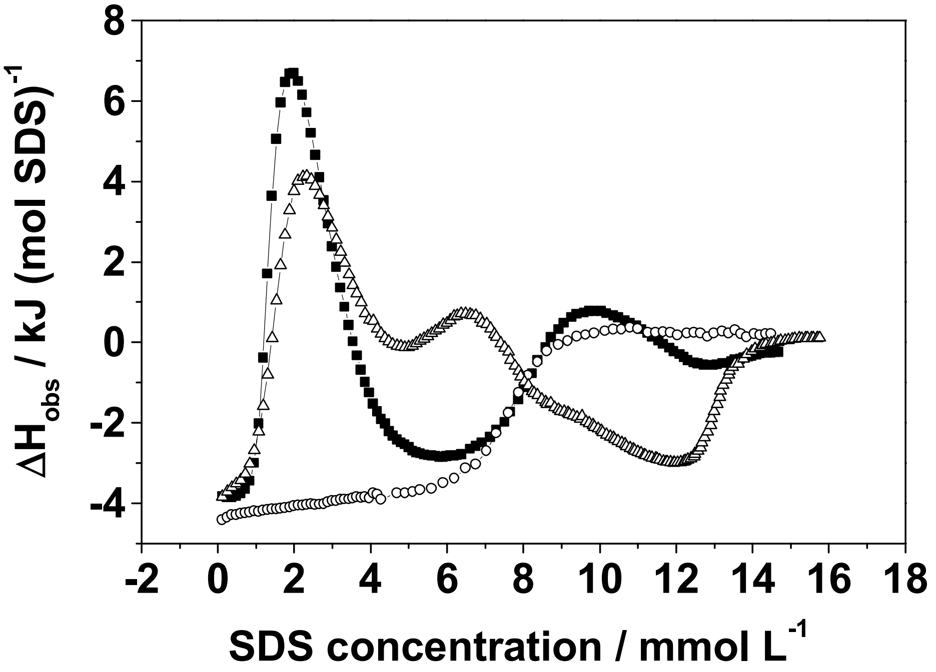

**Figure 6:** ITC curves for titration of 10 wt % SDS in ○ water and ■ 0.1 wt % $EO_{52}$-$PO_{35}$-$EO_{52}$, Δ solution with 0.1 wt % PEO 2000 and 0.1 wt% PPO 2000, at 15 °C.

C.a.c values obtained in both curves are around 0.8 mmol L$^{-1}$. The minimum that appears between the two endothermic peaks, is located in both curves around 5-6 mmol L$^{-1}$, close to the c.a.c. values reported for the interaction of SDS with PEO.[27, 29] All of these evidences suggest that SDS interacts almost independently with the PEO and PPO blocks of F77. A similar picture is observed for the interaction of SDS with F127, $EO_{95}PO_{62}EO_{95}$, which also possesses a large PEO block and whose ITC interaction curves (not shown), also display two endothermic peaks and the same features described for F77. The smaller enthalpy values observed with the PEO + PPO mixture may be a consequence of a smaller fraction of SDS molecules binding to PPO due to some interaction with PEO, the latter not being expected to produce such an intense enthalpy increase.

A comparison between the c.a.c. values obtained for the interaction of SDS with unimers of block copolymers and with

similar random copolymers, as listed in Table 2, indicates that these values are always smaller for the block copolymers, although with variable differences among the three pairs studied, indicating a more intense effect of these block copolymers on SDS aggregation.

**Table 2**:Comparison of c.a.c values for the interaction of SDS with 0.1 % solutions of block vs. random copolymers, at 15°C.

| Block copolymers | c.a.c [mmol/L] | Random copolymers | c.a.c [mmol/L] |
|---|---|---|---|
| $EO_{95}$-$PO_{62}$-$EO_{95}$ (F127) | 0.34±0.02 | $EO_{204}$-$PO_{52}$ | 2.60±0.01 |
| $EO_{13}$-$PO_{31}$-$EO_{13}$ (L64) | 0.80±0.04 | $EO_{34}$-$PO_{25}$ | 1.98±0.03 |
| $EO_{52}$-$PO_{35}$-$EO_{52}$ (F77) | 1.07±0.03 | $EO_{106}$-$PO_{27}$ | 2.48±0.02 |

* average values and standard deviations calculated from, at least, three replicates.

### Effects of temperature and surfactant structure on the interaction

Temperature effect on this interaction was assessed by following the interaction of SDS with a random copolymer, $EO_{34}PO_{25}$, at three different temperatures, as summarized in Figure 7a.

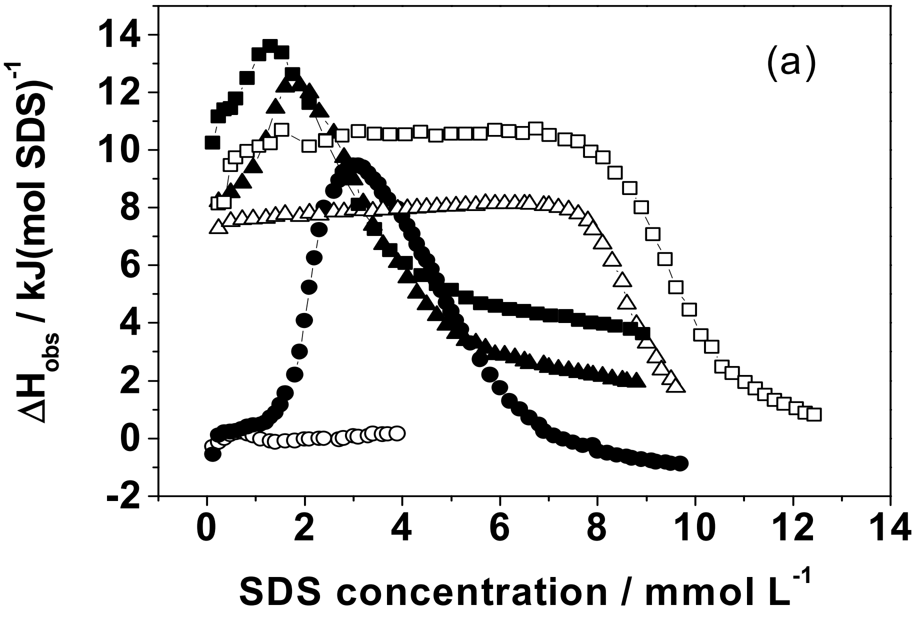

Figure 7: (a) ITC curves for titration of SDS 1.0 wt % into 0.1 wt % solution of $EO_{34}$-$PO_{25}$, ● at 25°C, ▲ at 45°C, ■ at 55. Open symbols represent dilution of SDS into water at each temperature.

These results show that c.a.c. values decrease from 1.98 mmol L$^{-1}$ at 25 $^{o}$C to 0.89 and 0.60 mmol L$^{-1}$, respectively at 45 and 55 $^{o}$C. Moreover, the endothermic peak associated with aggregate formation around the polymer chain becomes less pronounced (decreasing to roughly 1/3 of its area) as temperature increases, as already observed for the interaction between SDS and PEO.[27]

The cloud point for 0.1wt. % solutions of this copolymer was determined as slightly above 58 °C and ITC results obtained at 60 °C, above the clouding temperature, shown in Figure 7b, now display an initial part where the interaction curve lies below the results for SDS dilution in water, indicating the occurrence of an exothermic process.

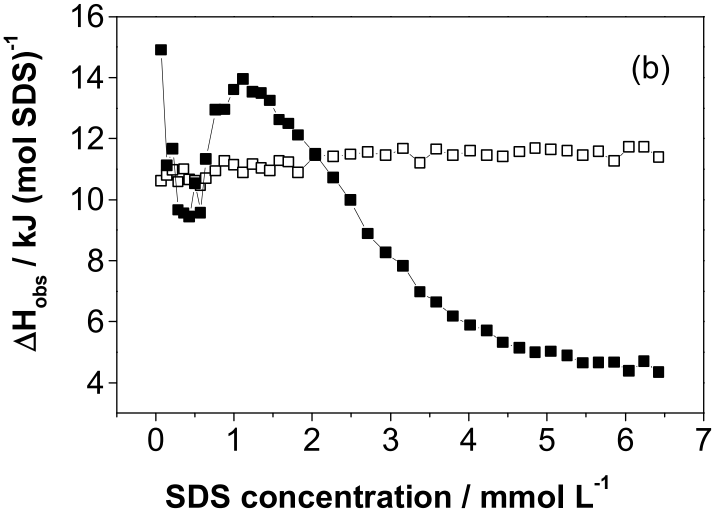

Figure 7: (b) titration of SDS 1.0 wt % into 0.1 wt % solution of $EO_{34}$-$PO_{25}$, 2.95 kg/mol (●) in water (□) at 60°C.

This process is most likely the rehydration of aggregated copolymer chains as a consequence of their interaction with SDS. Similar behavior was reported for the disruption of block copolymer micelles upon surfactant addition[13] or redissolution of PNIPAM above its cloud point in the presence of SDS.[31]

For comparison, ITC experiments were run with dodecyl and hexadecyltrimethylammonium bromides, respectively DTAB and CTAB, and dodecylammonium chloride, DAC, interacting with $EO_{34}PO_{25}$ at 58 $^{o}C$, as shown in Figure 8 a,b.

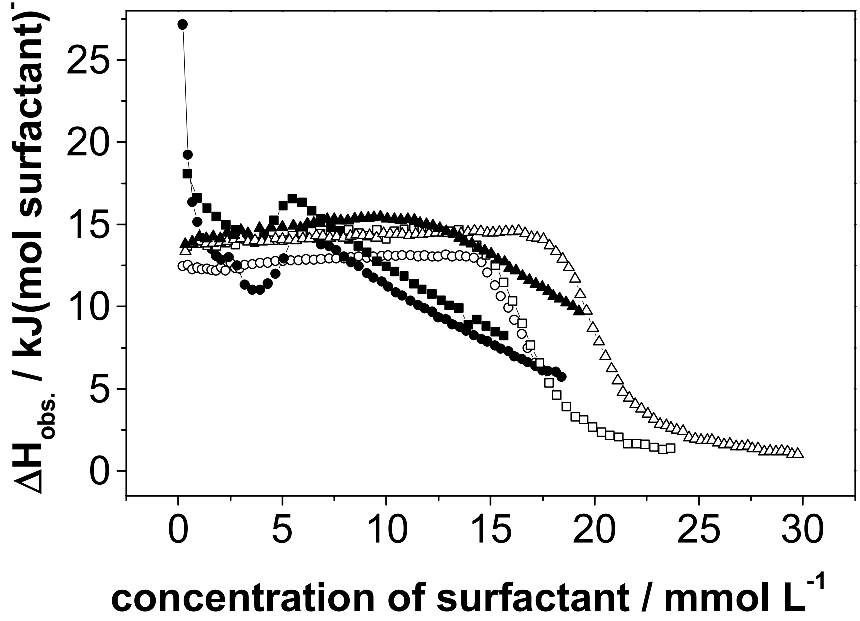

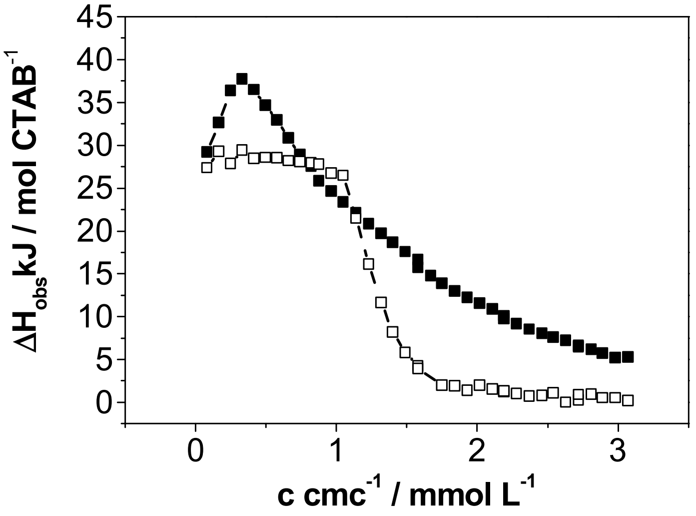

Figure 8: (a) ITC curves for titration of 1.0 wt % DAC into 0.1 wt % solution of $EO_{34}$-$PO_{25}$ ■ at 58°C ● at 60°C and ITC curve for titration of 1.0 wt % DTAB into 0.1 wt % solution of $EO_{34}$-$PO_{25}$ ▲ at 58° C. Dilution of surfactants in water at: □ 58 °C, Δ 58°C, ○ 60°C. (b) titration of ■ CTAB 1.0 wt % into 0.1 wt % solution of $EO_{34}$-$PO_{25}$ at 58°C. □ dilution of CTAB in water at 58 °C.

In all of these experiments, copolymer solutions were clear (confirming to be below their cloud points, in agreement with the lack of an exothermic interaction at low surfactant concentration, as the one shown in Figure 7a). Using the ratio between c.a.c. and c.m.c. values to estimate the extent of interaction, one can see that the interaction of cationic surfactants with EO/PO random copolymers is much less pronounced than that with SDS, as will be discussed later.

## Discussion.

The ITC curves obtained for the interaction of ionic surfactants, especially SDS, with random copolymers are similar to the ones reported for the interaction with other hydrophilic polymers such as PEO [18, 26, 27, 29] or PVP,[4] and slightly different form the ones reported for interaction of SDS with more hydrophobic polymer such as PPO[26, 30] or PNIPAM,[25] in the sense that with random copolymers a pronounced minimum is observed, where enthalpy values in the presence of polymer are lower than the ones obtained for dilution of SDS. This minimum has been most commonly associated with the rehydration of polymer chains proposed to occur as the surfactant aggregates grow, becoming more compact and not needing the incorporation of polymer molecules to shield the surfactant alkyl chains from water contact.[26, 27] This observation may indicate that, despite the presence of up to 50 wt. % in PO units, SDS molecules or aggregates sense them as mostly hydrophilic polymers. It is interesting to notice, as shown in Figure 4, that there is a decrease in the intensity of this minimum as the PO content increases, supporting the idea that it is closely related to the polymer hydrophilicity. Interestingly, similar changes in ITC profiles were reported for the interaction of SDS with two hydrophobically modified celluloses,[31] with the more hydrophilic one displaying the most pronounced minimum.

One point that remains unclear is the reason for the appearance of double minima in the ITC curves for the interaction of SDS with $EO_{43}PO_{11}$, as shown in Figure 2. As mentioned before, similar changes in the shape of ITC curves have been ascribed to the transition of a regime where only one aggregate is formed around each polymer chain to another where many aggregates are present. At this interval, which for SDS + PEO was observed for polymers larger molar masses, between 8,000 and 11,000 g mol$^{-1}$,[18, 28] formation of a second aggregate would lead to an increase in enthalpy due to mutual electrostatic repulsion, causing the appearance of shoulders or double minima. The molar mass of this copolymer, 2500 g mol$^{-1}$, is much smaller than that of PEO which display these characteristics, what would imply that aggregates around random EO/PO chains be much smaller than the ones formed around PEO chains. Calorimetric techniques have no capability of assessing the size of these aggregates; hence, these findings will have to be verified by use of other techniques.

This gradual change in random copolymer hydrophilicity with EO content also shows in the observed changes in c.a.c. values as a function of copolymer composition, as can be seen in Figure 3, indicating that the intercalation of EO and PO unit in the random copolymer structure leads to global polymer properties in between those of PEO and PPO. This finding may be of importance for other situations where polymers with general properties between the extreme ones of PEO and PPO are needed as, for instance, in the formation of aqueous two-phase systems.[21] It also rules out the formation of domains with predominance of the same monomer, especially the more hydrophobic PO, along these random copolymer chains. Moreover, these ITC results obtained at temperatures below the cloud points of these dilute random copolymer solutions do not show any sign of

exothermic interaction at low surfactant concentration, which would be expected if they display some sort of polymer aggregation, agreeing with previous light scattering studies that rule out aggregation on similar copolymer solutions.[23] This is only verified for temperatures above their cloud points, as shown in Figure 8a, and supports the suggestion of ITC measurements of the interaction with ionic surfactants as a very sensitive means of detecting the occurrence of polymer aggregation.

Significant differences, however, are observed when these calorimetric results are compared with those for block copolymers of similar composition. For a block copolymer displaying a small PEO chain, $EO_{13}PO_{31}EO_{13}$, the ITC curves (see Figure 5) are similar to those observed for other hydrophilic polymers (including the random EO/PO copolymers). However, for copolymers with larger PEO blocks (see, for instance, results for $EO_{52}PO_{35}EO_{52}$, shown in Figure 6), a second endothermic peak appears. Comparison of the position of these peaks with those of a mixture of PEO and PPO of the same molar mass as in the block copolymer confirms that SDS interacts almost independently with the different blocks. Interaction starts with the more hydrophobic block, PPO, displaying c.a.c. values for the block copolymers that are close to the ones observed for PPO homopolymers. As the concentration of surfactant increases and approaches the c.a.c. values observed for the interaction of SDS with PEO, the PEO blocks start to interact with added surfactant, producing an increase in the overall enthalpy values that appears as the second peak. For block copolymers, this second peak begins at concentration around 5-6 mmol $L^{-1}$, slightly above the reported c.a.c. values for SDS interaction with PEO (4-5 mmol $L^{-1}$)[27,29] and of those observed for the PEO + PPO mixture. Because part of the added SDS is already interacting with the PPO blocks, the actual concentration of SDS molecules available to interact with the PEO blocks is smaller and, hence, a larger total concentration is needed. It is interesting, however, that this second increase in enthalpy (ascribed to the interaction with PEO blocks) occurs at higher concentrations for the block copolymer in comparison with the physical mixture of PPO + PEO. This may indicate that SDS interaction with the PEO blocks of these copolymers is slightly more unfavorable than with PEO homopolymer, with respect to SDS interaction with the PPO block or homopolymer.

One point that may be raised is the effect of the hydroxyl end-groups of PEO and PPO, which are not present in the block copolymer, but that are known to affect the solution behavior of these polymers.[32, 33] For this reason, we have studied the interaction of SDS with dimethylated PEO 2000 (results not shown here) and the ITC curves were essentially the same as obtained with PEO 2000, suggesting that for polymers with this molar mass, the hydroxyl end-groups have no significant contribution to their interaction with SDS.

It is worth noticing that many of the previously discussed features of this interaction were detected by ITC measurements because this technique allows following the evolution of this process as surfactant concentration is increased. This applies to the minimum observed in some ITC curves, but especially to the observation that SDS molecules see the PEO and PPO blocks of these copolymers as almost independent, similarly to the interaction that occurs when they are only mixed, as shown in Figures 5 and 6. A similar process of stepwise association was previously proposed by Dai *et al.*[19] for the interaction of SDS with a reverse (PPO-PEO-PPO) block copolymer also displaying ITC curves with similar features.

Comparing the interaction of SDS with random versus that with block copolymers of similar compositions, one notices also that c.a.c. values are always smaller with

block copolymers, as revealed by data listed in Table 2. This is an interesting outcome of the present investigation and may be rationalized considering the evidences from ITC studies with block copolymers that SDS interacts first and preferentially with the more hydrophobic PPO block and, at higher concentrations, starts to interact with the PEO blocks. Because c.a.c values reflect the beginning of the interaction, for block copolymers they are essentially the same as observed for interaction with the equivalent PPO homopolymer. For random copolymers, on the other hand, ITC results indicate that SDS senses the interaction with a polymer displaying mixed properties in between those of PEO and PPO, depending on the copolymer composition. Therefore, the presence of EO units mixed with PO along the random copolymer chain makes this interaction less favorable than the one with PPO homopolymer, by increasing the observed c.a.c. values.

By employing different ionic surfactants contributions from their headgroup features : electrical charge (anionic, SDS versus cationic DTAB or DAC) or size (trimethylammonium, DTAB, versus ammonium, DAC) as well as from their hydrocarbon chains (dodecyl, DTAB, versus hexadecyl, CTAB), may be evaluated. From the c.a.c and c.m.c. values derived from the ITC measurements summarized in Figures 8a and 8b, the intensity of interaction between these surfactants and a random copolymer, $EO_{34}PO_{25}$, at 58 $^{o}$C, was calculated by using

$$\Delta G_{ps}=\Delta G_{agg} - \Delta G_{mic} = RT\ \ln(\frac{c.a.c}{c.m.c.}) \qquad (1)$$

This equation produces values for the Gibbs energy difference, $\Delta G_{ps}$, between a surfactant monomer present in a free micelle and a monomer in the aggregate that is formed around the polymer chain. Therefore, the more negative its value, the more favorable its transfer to the polymer-induced aggregate suggesting a more intense polymer-surfactant interaction.[25,34] The values obtained through equation (1) for $\Delta G_{ps}$ are -5,0; -3,9;-2,7; -1,2 kJ/mol, respectively for SDS, CTAB, DAC and DTAB. This sequence is exactly the same obtained in a previous investigation using another nonionic polymer, poly(N-isopropylacrylamide), PNIPAM,[25] and indicates that anionic surfactants display a more intense interaction with these polymers than cationic ones. Moreover, among the cationic surfactants, the interaction is more intense for the more hydrophobic surfactant, indicating that the transfer of methylene units from the free micelle to the polymer-induced aggregate is favorable, what suggests a more hydrophobic environment at the latter. Additionally, when comparing the two dodecyl cationic surfactants, DAC and DTAB, the former displays a more intense interaction probably due to its smaller headgroup. Because these surfactants do not contain the same counter-ions (dodecylammonium bromide could not be used due for its high Kraft point), additional contribution of different effects from chloride and bromide to this interaction cannot be ruled out.

Temperature effect on this interaction can be estimated from the results shown in Figure 7a and, once more, they agree with the previous observations with PNIPAM,[25] that the higher the temperature, the more intense the interaction. This difference could be related to the LCST (lower critical solution temperature) behavior displayed by these polymers aqueous solutions, indicating a less intense hydration at increased temperatures, which would then cause less competition with the surfactant by the polymer. At temperatures slightly above their cloud points, however, the ITC curves change, as shown in Figures 7b and 8a, displaying an exothermic interaction at low surfactant concentrations (below their c.a.c.'s) which can be ascribed to the rehydration of polymer chains due to surfactant induced redissolution of polymer aggregates (in agreement with the observed increase in the cloud points at these surfactant concentrations). A similar behavior, also from ITC measurements, was reported for the redissolution of block copolymer micelles upon addition of ionic surfactants.[13]

## Conclusions

In summary, the present investigation has revealed some new features of the interaction of ethylene oxide-propylene oxide copolymers with ionic surfactants. Random EO/PO copolymers display an interaction resembling that observed for other hydrophilic polymers, with the additional feature that its characteristics lay between those of the homopolymers PEO and PPO. ITC results have also shown that, below their cloud points, random copolymer solutions show no sign of aggregation. The interaction of non-aggregated block copolymers, on the other hand, provided that the PEO block is large enough, display ITC results that are consistent with a process as if the surfactant interacts almost independently with the EO and PO copolymer blocks. For this reason, the interaction of surfactant with block copolymers is more intense (as measured by a smaller c.a.c. value) than that with a random copolymer of similar composition. Information obtained on other features such as the dependence of this interaction on temperature and on the surfactant chemical nature confirms previously reported findings. In addition to these insights, the present investigation is also a fine example of the kind of information that calorimetric techniques such as ITC and DSC are capable of providing for studies of polymer-surfactant interaction.

## Acknowledgements

The authors acknowledge the support from the Brazilian Agencies FAPESP (financial support to this research project) and CNPq (PhD scholarship to A.N. and a research productivity grant to W.L.). Fruitful discussions with Gerd Olofsson on the present results are also gratefully acknowledged.

## References

1. Ananthapadmanabhan, K. P. In *Interactions of Surfactants with Polymers and Proteins*; Goddard, E. D.; Ananthapadmanabhan, K. P., Eds.; CRC Press, Boca Raton, 1993; p 5.
2. Jonsson, B; Lindman, B.; Holmbert, K.; Kronberg, B.; *Surfactants and Polymers in Aqueous Solution*, Wiley, Chichester, **1998**
3. Tam, K.C.; Wyn-Jones, E. *Chem. Soc. Rev.* **2006**, 35, 693
4. Olofsson, G.; Wang, G.; *Pure Appl. Chem.* **1994**, 66, 527
5. Loh, W.; *Block copolymer micelles.* In: Arthur Hubbard. (Ed.). Encyclopedia

of Colloid and Surface Science. New York: Marcel Dekker, 2002, p 802

6. Mortensen, K. *J. Phys. Cond. Matt.* **1996**, 8, 103

7. Alexandridis, P.; Hatton, T. A.; *Colloids Surf. A,* **1995,** 96, 1 .

8. Lopes, JR; Loh, W. *Langmuir* 1998, 14, 750

9. Beezer, A.E.; Loh, W.; Mitchell, J.C.; Royall, P.G.; Smith, D.O.; Tute, M.S.; Armstrong, J.K.; Chowdhry, B.Z.; Leharne, S.A.; Eagland, D; Crowther, N.J.; *Langmuir* **1994**, 10, 4001

10. Alexandridis P, Hatton T.A . *Colloids Surf. A* **1995**, 96, 1

11. Bryskhe, K.; Jansson, J.; Topgaard, D.; Schillen, K.; Olsson, U. *J. Phys. Chem. B* **2004**, 108, 9710

12. Hecht, E.; Hoffmann, H. *Langmuir,* **1994**, 10, 86

13. da Silva, RC.; Olofsson, G.; Schillén, K.; Loh, W. *J. Phys. Chem. B* **2002**, 106, 1239

14. Jansson, J; Schillen, K; Olofsson, G; da Silva, RC; Loh, W. *J. Phys. Chem. B* **2004**, 108, 82

15. Li, Y.; Xu, R.; Couderc, S.; Bloor, D.; M, Wyn-Jones E.; Holzwarth, J.F. *Langumir* **2001**, 17, 183

16. Couderc, A.S.; Sidhu, J.; Thurn, T.; Xu, R.; Bloor, D. M.; Penfold, J.; Holzwarth, J. F.; Wyn-Jones, E. *Langmuir* **2005**, 21, 10197

17. Löf, D.; Niemiec, A.; Schillen, K.; Loh, W.; Olofsson, G. *J. Phys. Chem. B* **2007**, 111, 5911

18. Dai, S.; Tam, K.C. *Colloids Surf. A* **2006**, 289, 200

19. Dai, S.; Tam, K.C.; Li, L. *Macromolecules* **2001**, 34, 4673

20. Dai, S.; Tam, K.C.; Li, L. *Macromolecules* **2001**, 34, 7049

21. Cunha M.T., Tjerneld F.,Cabral J.M.S., Aires-Barros M.R.; *J. Chromat. B,* **1998**, 53, 60

22. Niemiec, A.; Loh, W.; unpublished results

23. Nilsson, A.; Neves-Petersen, M.T.; Johansson, HO.; Jansson, J.; Schillen, K.;
Tjerneld, F.; Petersen, S.B. *Biochim. Biophys. Acta- Proteins and Proteomics,* **2003**, 1646, 57

24. da Silva, RC; Loh, W. *J. Colloid Interface Sci.* **1998**, 202, 385

25. Loh, W.; Teixeira, L.A.C.; Lee, L.T. *J. Phys. Chem. B,* **2004**,108,3196

26. Wang G., Olofsson G., *J. Phys. Chem. B*, **1998**, 102, 9276

27. da Silva, RC; Loh, W; Olofsson, G *Thermochim. Acta* **2004,** 417, 295

28. Bernazzani, L.; Borsacchi, S.; Catalano, D.; Gianni, P.; Mollica, V.; Vitelli,
M.; Asaro, F.; Feruglio, L. *J. Phys. Chem. B,* **2004**, 108, 8960
29. Dai, S.; Tam, K.C. *J. Phys. Chem. B,* **200**1, 105, 10763
30. Dai, S.; Tam, K.C. *Langmuir* **2004**, 20, 2177
31. Brasil, D.A.; Loh, W. unpublished results
32. Spitzer, M; Sabadini, E; Loh, W. *J. Phys. Chem. B* **2002**, 106, 12448 and Spitzer, M; Sabadini, E; Loh, W. *J. Braz. Chem. Soc.* **2002** ,13, 7
33. Anselmo, A.G.; Sassonia, R. C.; Loh, W.; *J. Phys. Org. Chem.* **2006,** 19, 780
34. Chu, D.; Thomas, J.K. *J. Am. Chem. Soc.* **1986**, 108,

# CAPÍTULO VI – MANUSCRITO

*manuscript*

# A comparison of binary phase diagrams of block and random copolymers in water and organic solvents

Anna Niemiec, Juliana da Silva Bernardes and Watson Loh*

*Institute of Chemistry, Universidade Estadual de Campinas (UNICAMP),*

*Caixa Postal 6154, 13083-970, Campinas, SP, Brazil*

*corresponding author : wloh@iqm.unicamp.br, Phone : + 55 19 3521 3148,
Fax: + 55 19 3521 3023.

## Abstract

Determination of binary phase diagrams is an important tool in investigating the phase behavior of copolymers solutions. The present study used visual inspection to detect phase changes in these systems of random and block ethylene oxide (EO) – propylene oxide (PO) copolymers in aqueous and organic solvents as a function of temperature. Contributions from effects such as: the architecture of the polymer, and nature of the solvent, and the profile of the binary phase diagrams curves were comparatively analyzed for random and block copolymers with similar composition (number of EO and PO units). In general, EO/PO copolymers showed different solubility versus temperature dependences with the solvent; an LCST (lower critical solution temperature) in water and a UCST (upper critical solution temperature) in organic solvents were observed. Moreover, random copolymers due to their lack of aggregation displayed slightly different phase behaviour than block copolymers and homopolymers. Random copolymers presented lower cloud point temperatures in water and a wider miscibility region in organic solvents.

# Introduction

The phase diagram of a mixture shows the system phase behavior under certain conditions of temperature and composition. Phase diagrams are very important for the study of polymer/water systems which are widely used for the extraction, separation and purification of amino acids, peptides, proteins, steroids, organelles and live cells[1]. They have been studied by many groups around the world and for several types of polymers, such as polyethylene oxide (EO), polypropylene oxide (PO), copolymers EO/PO (random or block), N-isopropylacrilamide polymers, EHEC polymers, etc[2,3,4].

A good understanding of the phase behavior of copolymers is of relevance in many industrial applications such as paints, foodstuffs, enhanced oil recovery, pharmaceuticals and detergents as well as in our understanding of biological systems. Apart from these important fields of application, the phase behavior of copolymers is of fundamental importance in basic surface and colloid chemistry[5].

Comprehensive understanding of biphasic liquid-liquid systems is nowadays of scientific and technologic importance. Systems can produce phases with distinct physical-chemical proprieties (polarity, density, composition etc.) and because of this facility, they have wide application in alternative processes of separation and purification. Aqueous systems are widely applied in the biomedical area such as, in cell and proteins partitions or in the environmental area for metal extraction from one phase to another. Further more, systems formed with organic solvent have applications in applicability to the development process of catalysts, which often requires the absence of water. Rosa et.al[6], studied two organic biphaic systems containing poly(ethylene oxide), heptane and either $CH_2Cl_2$ or methanol for the catalytic hydrogenation of hex-1-ene. To improve the selectivity of catalyst partitioning, they cooled the reaction system below the UCST (upper critical solution temperature) where a polymer phase separate occurs and it was possible to selectively separate the catalyst and reaction product. Further, the catalyst could be recycled and recovery of the reaction product, n-hexane, was performed by extraction with heptane.

However, it is even more common to find in the literature reports for applications of aqueous two- phase systems for metal separations or biological material purification. The recent consumption of metal in industries has promoted the research on inexpensive methods of removal and recovering of metals as for example, Cr(III) and Cu(II) or Cd (II) from industrial effluents as well as from lake water, mineral water and tobacco samples. Removal and recovering usually involves an initial metal complex formation. In case of cadmium (Cd) complexed with ammonium, *O*,*O*-diethyldithiophosphate (DDTP) is formed followed by a cloud point extraction using the surfactant phase with Triton X-114 (a nonionic octylphenol ethoxylate surfactant) for extraction of the metal[7,8].

Tjerneld et al[9,10]. very extensively studied the thermoseparation polymer systems in aqueous two–phase extractions of biomolecules. Various ATPS (aqueous two-phase systems) have been reported, where partition of hydrophobic and hydrophilic peptides occurred. The most well-known aqueous systems employed in these investigations are the two polymer systems of poly (ethylene oxide) / dextran and the systems[11] with PEO and a salt as for example PEO / phosphate. One can also find in the literature the description of the phase equilibrium of triblock copolymers / dextran aqueous phase systems. In all these cases, the copolymer usually can be recovered for reuse after thermal separation and protein is recovered from the aqueous phase. Due to varying cloud point temperatures of copolymers, a suitable system can be chosen for proteins purification to avoid protein denaturation.

Random EO/PO copolymers have been also investigated as alternative to the use of EO-PO-EO block copolymers in the formation of aqueous two-phase systems, for use in bioseparation processes[12]. They are water soluble, of low toxicity and, when compared to their similar block copolymers, display lower cloud points (critical solution temperatures), which allows the formation of aqueous two-phase systems at lower temperatures. Previous studies[13,14] by light scattering and calorimetry revealed no sign of aggregation in aqueous solutions of these random copolymers below their cloud points, indicating that the monomer sequence along the polymer chain does not allow significant interaction among the more hydrophobic PO units, as has been observed for the block copolymers. Also, when analyzing the interaction of these random copolymers with ionic surfactants[15], it was observed that the interaction is different from that in the case of block copolymers and similar to that observed for other hydrophilic homopolymers with the additional characteristic that the interaction intensity increases with the increase of polymer hydrophobicity. This interaction between random copolymers and ionic surfactants is significantly affected by temperature, which influences the hydration of the polymer.

The occurrence of biphasic liquid-liquid systems is very extensive and depends on the correct choice of two partially miscible liquids. In one of their papers, Silva and Loh[15] investigated the forces responsible for phase separation in the system PEO/dextran/ electrolytes. The results obtained confirmed that enthalpic contributions are relevant to biphase formation in the presence of electrolytes such as lithium and sodium sulfates, but not in the case of sodium chloride. Phase separation for all cases was accompanied by an enthalpy increase, indicating that entropy increase is the driving force for aqueous two-phase formation.

Depending on the system, phase separation can occur with an increase or a decrease of temperature. This phenomenon is called LCST (lower critical solution temperature) or UCST (upper critical solution temperature). UCST is typical for systems such as water-phenol and LCST is observed for water-triethylamine and for chloroform and poly (ethylene oxide)[16]. There are also systems for which both UCST and LCST behavior is present in one phase diagram such as in the case of polystyrene and acetone studied by Siow et al[17]. As presented in studies by Kuwahara et al[18]., appearance of both the UCST and LCST is common in polymer solutions and usually UCST is raised and the LCST is lowered with increase of the molar mass of the polymer. If a poor solvent is chosen, the temperature region where polymer/solvent complete miscibility occurs merges, leading to coalescence of two regions (UCST and LCST).

When phase separation leads to formation of two phases, each rich in one of the components (for example in a mixture of polymer/solvent/non-solvent) this behavior is called segregative and can be also observed for systems of two polymers and one solvent as well[19]. In other cases, phase separation in the associative regime is observed which means that one phase contains high volume fractions of both polymers and the second phase is mainly solvent. Associative phase separation usually takes place in case of polymers presenting effective attraction between each other as for example in the case of aqueous solution of polymers with acidic or basic character such as the system of poly(ethylene oxide) and poly (acrylic acid). In these cases, a simple change the pH of these systems may change the regime of phase separation from segregative to associative or vice-verse[20].

A phase separation in binary mixtures is usually identified by cloud point measurements. This technique consists in a visual determination of the turbidity, which occurs during a temperature variation. This technique can be used to construct phase diagrams of these mixtures.

The importance of these biphasic systems and of the relative lack of data for aqueous or organic solvent systems of block and homopolymers which would allow a direct comparison of these phase diagrams motivated this investigation. Data on the phase equilibria in these binary systems have been collected in order to determine the conditions for the formation of two-phase systems.

In the present study, a series of random and block EO/PO copolymers with similar composition (number of EO and PO units) was selected and their phase behavior in aqueous and organic solutions was studied. The results were analyzed as a function of copolymer architecture and composition, as well as other parameters such as the nature of the solvent.

# Experimental

## Materials.

Random and triblock copolymers containing ethylene oxide (EO) and propylene oxide (PO) units with different compositions were used. Their chemical composition and other main features are described in Table 1.

**Table 1**:Physical - chemical characteristics of the block and random copolymers used in this study.

| **Triblock copolymers (commercial names)** | **EO content (wt.%)*** | **M [g/mol]**** | **Random copolymers** | **EO content (wt.%)*** | **M [g/mol]**** |
|---|---|---|---|---|---|
| $EO_2$-$PO_{20}$-$EO_2$<br>(L31) | 10 | 1100 | ----------- | ----- | ------ |
| $EO_5$-$PO_{83}$-$EO_5$<br>(L121) | 10 | 4400 | ----------- | ----- | ------ |
| $EO_{11}$-$PO_{16}$-$EO_{11}$<br>(L35) | 50 | 1900 | $EO_{19}$-$PO_{15}$ | 50 | 1700 |
| $EO_{13}$-$PO_{31}$-$EO_{13}$<br>(L64) | 40 | 2900 | $EO_{34}$-$PO_{25}$ | 50 | 2900 |
| ------------------------ | ------ | ----------- | $EO_{116}$-$PO_{48}$ | 65 | 8000 |
| ------------------------ | ------ | ----------- | $EO_{43}$-$PO_{11}$ | 75 | 2500 |
| $EO_{52}$-$PO_{35}$-$EO_{52}$<br>(F77) | 75 | 6600 | $EO_{106}$-$PO_{27}$ | 75 | 6600 |
| $EO_{95}$-$PO_{62}$-$EO_{95}$<br>(F127) | 75 | 12000 | $EO_{204}$-$PO_{52}$ | 75 | 12000 |
| $EO_{127}$-$PO_{58}$-$EO_{127}$<br>(F108) | 80 | 14000 | ------------ | ------- | ----------- |
| $EO_{17}$-$PO_{72}$-$EO_{17}$<br>(P103) | 30 | 4950 | ----------- | ------- | ----------- |
| $EO_{44}$-$PO_{20}$ –$EO_{44}$<br>(F38) | 80 | 4800 | ----------- | ------- | ----------- |

* EO quantities as provided by the manufacturer

** Nominal molar masses, as provided by the manufacturers

Block copolymers were a gift from ICI, England and BASF, USA (F127), and were used as received. GPC and NMR analyses of these samples were performed and were recently described elsewhere[14]. With GPC, most of the copolymers showed only one elution peak and two elution peaks were observed only in the case of the block copolymer F127. GPC analyses revealed polydispersity values for these samples from 1.2 to 1.4. The EO/PO ratio for these copolymers samples determined by NMR spectroscopy[14] agrees very well with their nominal values. No attempt was made to determine their actual molar masses and nominal values are used throughout. Random copolymers, as described elsewhere[14], were a gift from Laporte Performance Chemicals, England and were also used without further treatment.

Water used throughout was of Milli-Q grade and chloroform or methanol were purchased from Merck (purity: 99.0-99.4 wt %). All polymers solutions were prepared by weight at least 24 h prior to use.

## Methods

### Phase Binary Diagrams Determination by Visual Analysis Method

The cloud point experiments were carried out in a concentration range of 0.1 – 20 wt% of copolymer in aqueous solutions and 0.1 – 40 wt % of copolymer in organic solvent solutions. All of the solutions were prepared 24 hours in advance and stored in a refrigerator.

In the case of aqueous solutions, a water bath was used and for the organic solvent solutions, an acetone bath with dry ice was used to achieve lower temperatures. The temperature variation was controlled at 1.0°C per minute and measured by a thermocouple. Two different methods were applied; for the aqueous solutions, the samples were heated until the first cloudy sign and the organic solvents solution were cooled down until the phase separation. Some experiments were carried out with cooling for aqueous solutions and with heating for organic solvent solutions to determinate the homogenization temperature. After repeating the same experiments several times it was possible to achieve reproducibility better than 0.7°C for measurements carried out with temperatures above 0°C for aqueous solutions and reproducibility better than 4.0°C for transition temperatures below –5.0°C.

## Results

### 1. Binary phase diagrams of random vs. block copolymers in water.

For the systems presented in Figure 1, phase separation was found to occur with an increase of temperature and present a Lower Critical Solution Temperature (LCST). This behavior was previously reported by Spitzer et al [21] and Saeki et al [25] for PEO and PPO aqueous solutions.

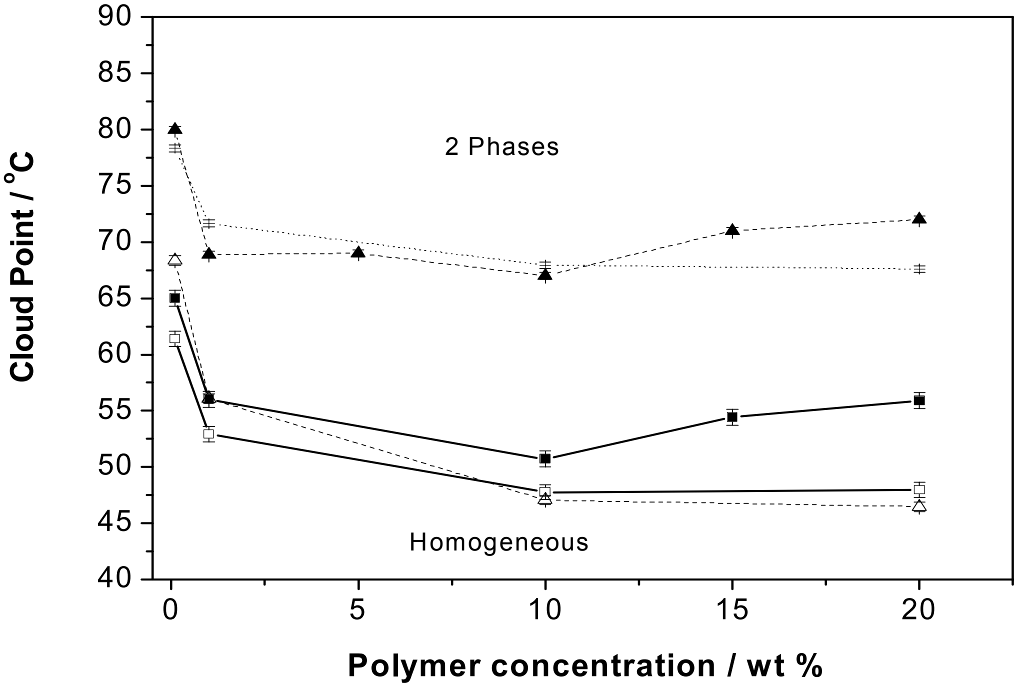

**Figure 1**: Cloud points of aqueous binary solutions of random (open symbols) and block copolymers (full symbols) with different composition, molar mass and copolymer architecture:

—□— $EO_{34}$-$PO_{25}$ (2900 g $mol^{-1}$); —■— $EO_{13}$-$PO_{31}$-$EO_{13}$ (2900 g $mol^{-1}$);
—△— $EO_{19}$-$PO_{15}$ (1700 g $mol^{-1}$); —▲— $EO_{11}$-$PO_{16}$-$EO_{11}$ (1900 g $mol^{-1}$);
—+— $EO_{116}$-$PO_{48}$ (8000 g $mol^{-1}$);

In Figure 1, copolymers with smaller molar mass (2900 g/mol) and lower quantity of EO groups in the polymer chain (50 wt %) can be compared with a polymer with a higher molar mass (7900 g/mol) and higher EO quantity (65 wt %) in the polymer chain. For the block copolymer $EO_{61}$-$PO_{48}$-$EO_{61}$, a cloud point temperature above 100ºC was observed[22,23]. In the case of the two different combinations (random vs. block copolymers of similar molar mass and EO/PO quantity), the random copolymers present a lower cloud temperature in water than the block copolymers. The random copolymers, with different molar mass (1700 g/mol vs. 2900 g/mol) but with 50 wt % of EO groups in the polymer chain present similar cloud points.

The behaviour of these copolymers in binary aqueous system shown in Figure 1 is then probably affected more prominently by the copolymer architecture, than by the ratio of EO/PO groups or the molar mass. Due to the regular distribution of EO/PO groups in the polymer chain, block copolymers display a wide distribution of cloud point temperatures. The block copolymer with lower molar mass of 1900 g/mol, and equivalent amount of EO groups in the polymer chain shows phase separation at much higher temperatures then the block copolymer with higher molar mass 2900 g/mol and 50 wt % EO groups in the chain. The same behaviour has been observed for the block copolymers L31 (1100 g/mol, 10 wt % of EO) and L121 (4400 g/mol, 10 wt % of EO), where the cloud point temperatures for the first copolymer was maintained in the range of temperatures equal to 30 - 40ºC for concentrations of 1.0 – 10.0 wt % solution and in the case of the second copolymer, the cloud points occur in the range of 5 - 10ºC .Silva et al[Error! Bookmark not defined.]. also compared two other pairs of block copolymers with similar molar mass as L121 (4400 g/mol, 10 wt % of EO) with P103 (4950 g/mol, 30 wt % of EO). In this case, P103 presented cloud points about 40 ºC higher due to the higher amount of EO groups in the polymer chain. This once again confirms that hydrophobic - hydrophilic balance between EO/PO groups in each polymer has a predominant influence on phase separation of the system. For the random copolymer of molar mass 8000 g/mol this effect is even more pronounced, due to the 65wt % amount of EO groups in the polymer chain, which is four times more hydrophilic (analyzing in terms of quantity of EO groups) than the previously described polymers.

## 2. Binary phase diagrams of random vs. block copolymers in organic solvent.

The behavior of organic solutions of block and random copolymers of ethylene oxide (EO) and propylene oxide (PO) with similar compositions is shown in Figures 2-7. These results indicate that the EO/PO copolymers in organic solvents show an inverse dependence of the solubility with temperature and have a UCST. This behavior was also reported for solutions with PEO of different molecular masses studied by Saeki et al[25]. in various organic solvents such as methyl, ethyl, n-propyl and isobutyl acetates.

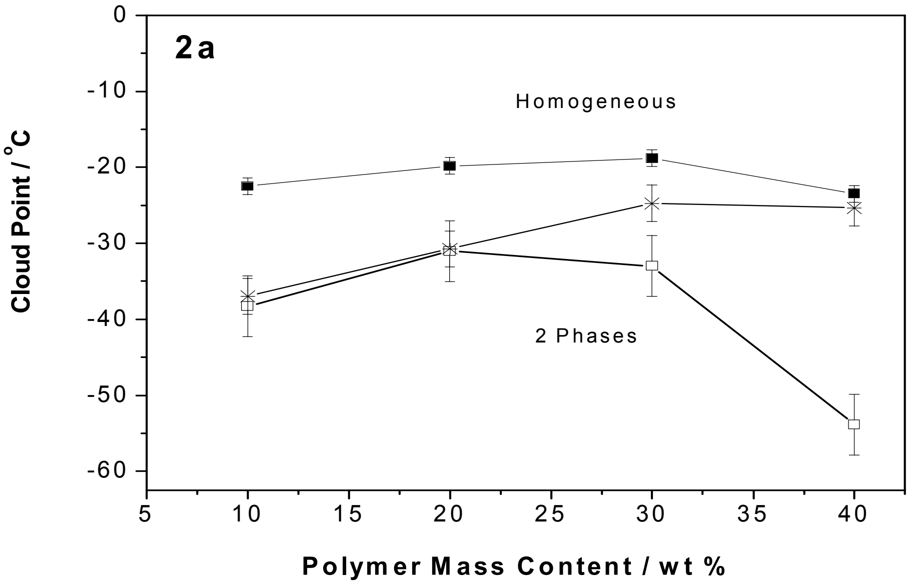

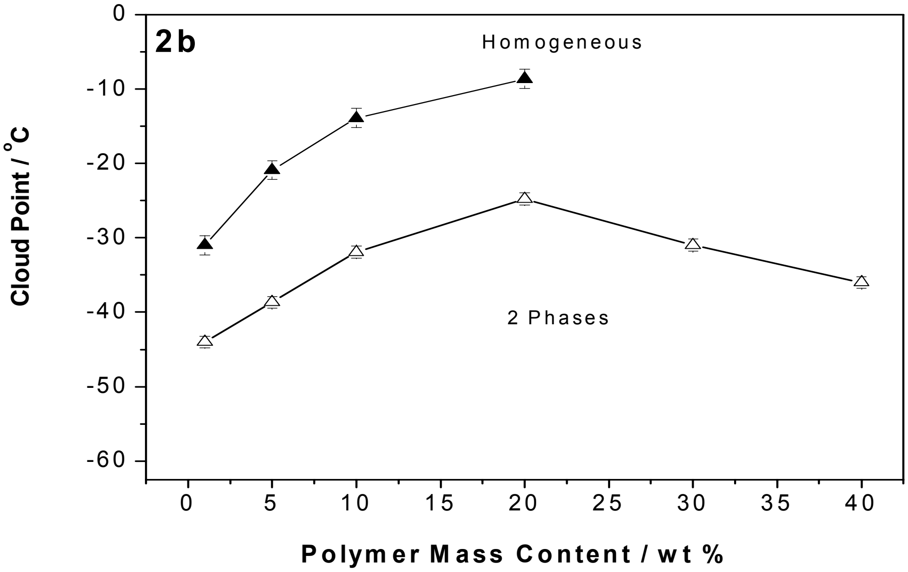

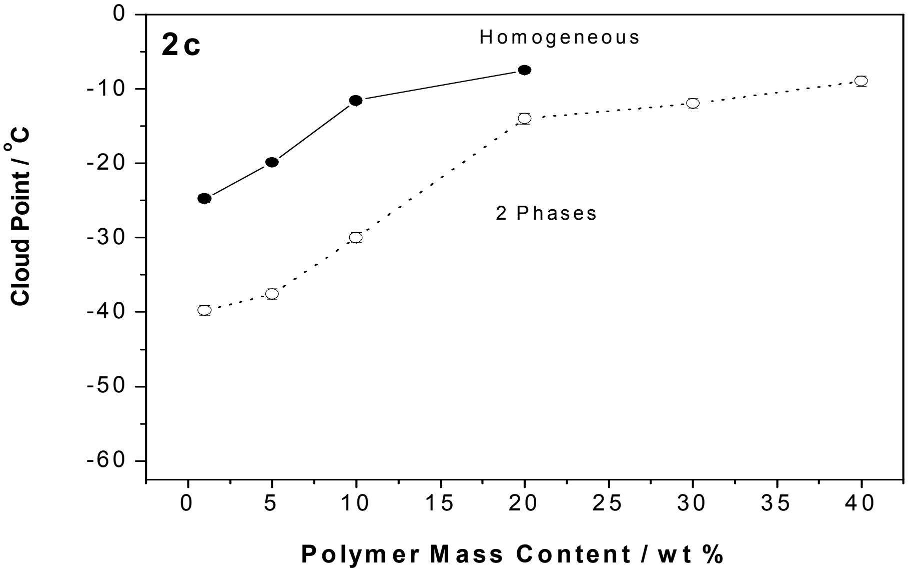

**Figure 2a, b, c:** Cloud points for binary aqueous solutions of random (open symbols) and block copolymers (full symbols) with different composition, molar mass and copolymer architecture in chloroform binary systems:

a) —■— $EO_{44}$-$PO_{20}$-$EO_{44}$ (4800 g mol$^{-1}$); —□—$EO_{43}$-$PO_{11}$ (2500 g mol$^{-1}$);
—*— $EO_{11}$-$PO_{16}$-$EO_{11}$(1900 g mol$^{-1}$);

b) —▲— $EO_{52}$-$PO_{35}$-$EO_{52}$(6600 g mol$^{-1}$); —△—$EO_{106}$-$PO_{27}$ (6600 g mol$^{-1}$);

c) —●— $EO_{95}$-$PO_{64}$-$EO_{95}$(12000g mol$^{-1}$); —○—$EO_{204}$-$PO_{32}$(12000g mol$^{1}$);

In Figure (2b, 2c) comparison of the phase diagrams for random vs. block copolymers is possible. For block copolymers, the phase separation occurs at higher temperatures than that for the corresponding (in terms of EO wt % and molar mass) random copolymers. This behavior is observed for a wide range of molar masses of copolymers, from 2500 - 12000 g/mol with around 75 wt % EO groups in the polymer chain.

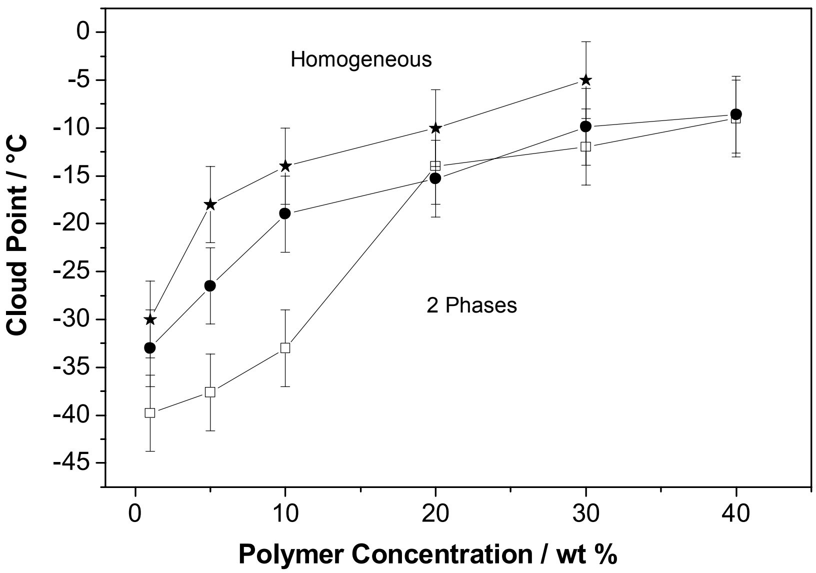

s

**Figure 3**: Effect of polymer composition on the binary phase diagrams of block copolymer (full symbol), and random copolymer (open symbol) and homopolymer (full star symbol):

—□— $EO_{204}$-$PO_{32}$ (12000 g mol$^{-1}$);

—●— $EO_{127}$-$PO_{58}$ –$EO_{127}$ (14000g mol$^{-1}$); (F108)

—★— PEO 10000 g mol$^{-1}$. [21]

Figure 3 presents a direct comparison between one chosen random copolymer, a block copolymer and a homopolymer in chloroform.

As expected for all these polymers, the phase behavior is very similar since all the polymers have approximately the same molecular weight and the two copolymers are predominantly composed of EO groups (75 and 80% EO). These results reveal that all of these binary systems present UCST behavior, in contrast to those observed for aqueous solutions, where the separation occurs with temperature increase (LCST behavior). Since the experimental uncertainty is around ±4ºC for the dry ice solvent bath temperature, these curves are almost equivalent. Thus, one could conclude that both random and block copolymers present almost the same behaviour as PEO homopolymer, especially in the case of more concentrated block copolymer solutions (20 wt % - 40 wt %) where the curves are superposed. For random copolymers, the cloud points for a wide range of concentrations is around 5ºC lower than those of similar block copolymers. This indicates that the amount of EO groups in the polymer chain plays an important role as well as the architecture of the polymer.

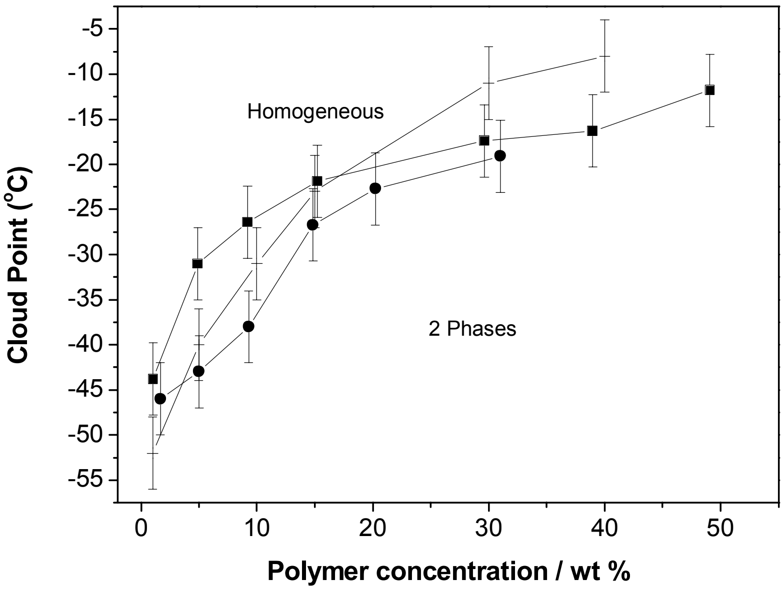

**Figure 4**: Effect of the composition on the binary phase diagrams of block copolymers (full symbol) and homopolymer (cross symbol) in chloroform :

—■— $EO_{44}$-$PO_{20}$ –$EO_{44}$ (4800 g $mol^{-1}$); (F38)

—●— $EO_{17}$-$PO_{72}$ –$EO_{17}$ (4950 g $mol^{-1}$); (P103)

—+— PEO 3350 g $mol^{-1}$ .[21]

Figure 4 presents another comparison of a pair of block copolymers compared with a homopolymer. In this case these copolymers have similar molar masses and different amount of EO groups in the chain: 87 vs. 33 and 76. Previous studies[26] with PPO 425 and PPO 2000 in $CHCl_3$, have shown that PPO is very soluble in organic solvents, because no phase separation was observed with PPO solutions up to 30 wt % when temperature was reduced to – 60°C. Therefore, it was expected that in the case of P103 block copolymer, which has a high PO content in the polymer chain, the one phase region could be much larger than for the case of the block copolymer F38, which has a high EO content, or for the case of the homopolymer PEO 3350 g/mol.

In addition to the composition effect, the polymer molecular mass, also plays a very important role on phase equilibria. Figures 5 and 6 present this effect for random and block copolymers separately. The studies were performed in chloroform and one can see from these curves that increasing the polymer molar mass increases the region of two phases. In both cases, the amount of EO groups in the polymer chain is within 75-80 wt %.

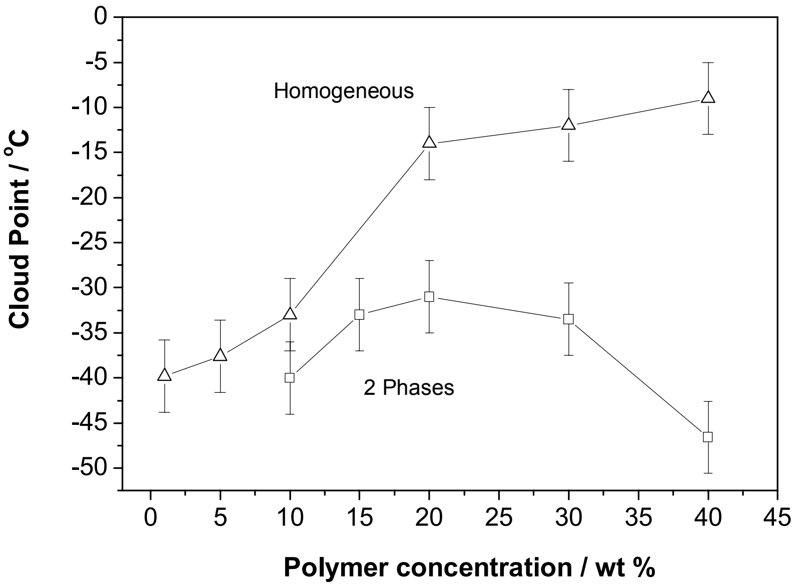

**Figure 5:** Molar mass effect on binary phase diagrams in chloroform of:

—□— $EO_{43}$-$PO_{11}$ (2500 g mol$^{-1}$) and

—△— $EO_{204}$-$PO_{52}$ (12000 g mol$^{-1}$)

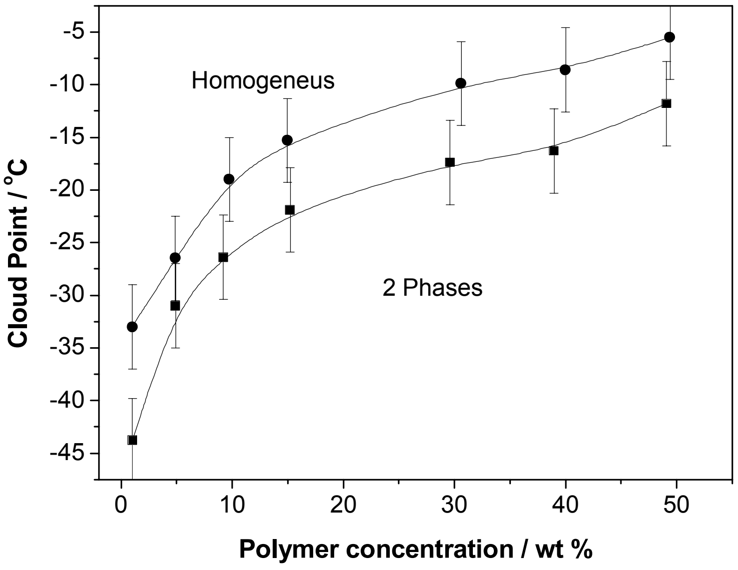

**Figure 6:** Molar mass effect on binary phase diagrams in chloroform of:

—■— $EO_{44}$-$PO_{20}$ –$EO_{44}$ (4800 g $mol^{-1}$); (F38) and

—●— $EO_{127}$-$PO_{58}$ –$EO_{127}$ (14000 g $mol^{-1}$) (F108)

The phase behavior of PEO homopolymer of various molar masses in various polar solvents has been reported[21]. All phase diagrams are of the UCST type and showed that phase separation occurs first at higher temperatures in methanol followed by chloroform and dichloromethane. In the case of block copolymers, the same behavior was observed as shown in Figure 7 and the same behavior is expected to be observed for random copolymers, although we have not studied their miscibility with methanol or dichloromethane. This indicates means that solvation of block/random copolymers in organic solvents is less favorable for methanol, which in this case is considered as the worst solvent for the studied systems and presents the largest region of two phases in comparison with the two other solvents.

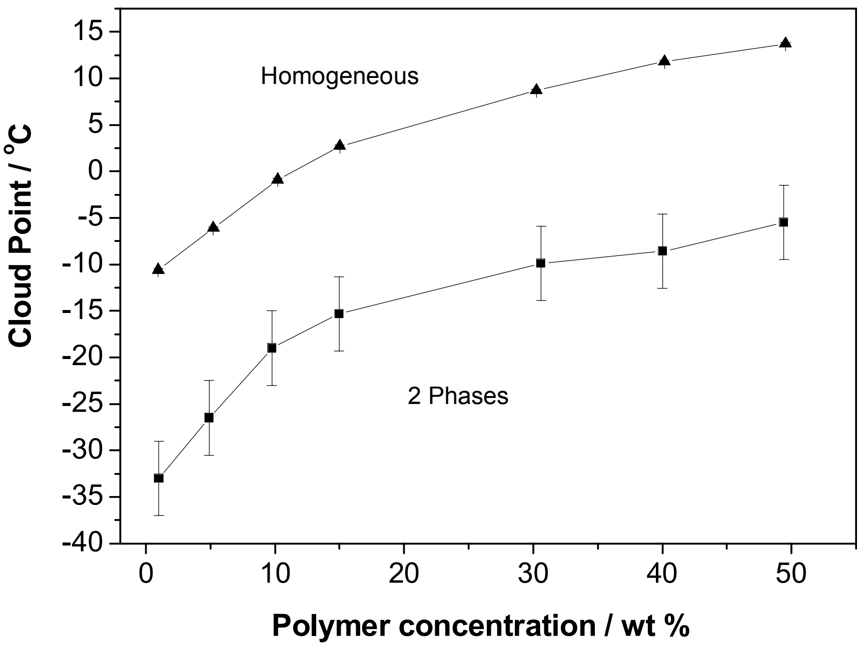

**Figure 7**: The effect of the solvent on binary phase diagrams of:

—▲— $EO_{127}$-$PO_{58}$ –$EO_{127}$ (14000g $mol^{-1}$) in methanol; (F108)

—■— $EO_{127}$-$PO_{58}$ –$EO_{127}$ (14000g $mol^{-1}$) in chloroform; (F108)

## Discussion

The fact that random copolymers show lower (or in some cases similar value) cloud points in water, when compared with similar block copolymers can be explained by the lack of aggregation in the case of random copolymers due to the irregular distribution of EO and PO groups in the polymer chain. Lack of aggregation inhibits the possibility of the copolymer to hide the hydrophobic parts of the polymeric chain (PO groups) from water, what leads to a larger region of two phases for this kind of system. On the other hand, the block copolymers of similar molar mass and EO content in relation to random copolymers, presented higher cloud temperatures (smaller region of two phases), due to their self-association in water. These copolymers manage to hide their less hydrophilic parts (PO units) and expose the more hydrophilic one (EO units), by forming micellar structures and some other mesophases. For example, for a 0.1 wt % aqueous solution of $EO_{13}$-$PO_{31}$-$EO_{13}$ (L64) (as shown in Figure 1), at temperatures higher than 28°C the dehydration of the polymeric chain starts, due to the breaking of the hydrogen bonds between water and the EO units and the formation of aggregates occurs, promoting the growth of the copolymer aggregates until phase separation (at 65°C). It is also worth noticing that the shape of the curve is very similar to the one previously reported for PEO homopolymers of different molar masses[25] in aqueous solutions. These results show that EO/PO copolymers also have an inverse dependence of the solubility with temperature with a LCST behavior in water. In the literature, a few models have been proposed to explain the high solubility of PEO in water and its phase separation of LCST type. Some of these models are based on Flory - Huggins theory, as for example the theory proposed by Goldstein[27], which proposes that PEO is very soluble in water, because it has the capacity of hydrogen bond formation. Some others models also exist, as for example the one introduced by Karlström[28], which proposes that phase separation is caused by the balance between polymer-polymer and polymer-water interactions, as well as by conformational changes of EO groups in the polymer chain at higher temperatures. Less polar polymer conformations occur at higher temperature which decreases the solvation of the polymer leading to the predominance of polymer-polymer interaction and, as a consequence, to phase separation.

When taking into consideration copolymers with the same EO quantity in the polymer chain, as for example 50 wt %, it is possible to analyze the effect of molar mass on the phase separation in water. In case of random copolymers, it is not possible to note any difference, but for block copolymers, this difference is quite pronounced which can be due to formation of different aggregation states of these copolymers. Lopes and Loh[29] have carefully studied this subject and concluded that larger polymers associate at lower concentrations even if the increase of the size is due to the EO chain. That paper also reports an empirical equation correlating the polymer cmc to the polymer molar mass and to the overall number of monomer units, which supports this view.

On the other hand, random copolymers present greater miscibility in organic solvents (smaller region of the two phases) than similar block copolymers and their solutions phase separate at lower temperatures. For better understanding of this behavior some other techniques as for instance, rheology should be employed for further studies.

In the case of block copolymers in organic solvent, the region of two phases is larger than that for similar random copolymers. There are two possibilities for aggregate formation under these conditions: as spherical micelle formation in selective solvent for the block in the middle of the polymeric chain or micellar network formation in selective solvent for the block in the middle of the polymeric chain[30]. The first would be aggregates, where the EO groups (end blocks) associate (or are aggregated) inside the micelle. In this conformation, the polymer middle blocks (PO groups, in this case) need to form a necklace around the micelle to compensate the loss of entropy in the system. In the second type of aggregate, the PO block force the two EO terminal blocks to move into the solvent which is easier when the EO blocks are small enough or when the polymer concentration increases. In this case, hydrophilic end groups simply arrange themselves in a micellar network with separation distances, determined by the length of the PO groups. In practice, for both types of copolymers block and random in the concentration range from 5- 40 wt % an increase in viscosity occurs with a decrease of temperature and formation of a gell-like viscous homogenous phase occurs at low temperatures. Similar networks were observed previously for urethane end group of ethylene oxide[31].

Figure 2 shows the effect of the molar mass on the phase diagram of random versus block copolymers in chloroform. A phase separation was observed for molar masses in the range of 2500-12000 g/mol, at higher temperatures for systems where the copolymer presents smaller molar mass. This effect was reported previously by Spitzer et al[32]. for PEO in methanol, chloroform, dichloromethane and the same behavior was also observed for the other block copolymers in chloroform (F38, 4800 g/mol and F108, 14000 g/mol), as shown in Figure 6. The variation of miscibility as a function of the polymer molar mass is explained satisfactorily by the Flory-Huggins theory, which proposes that the mixing entropy for a system is directly proportional to the number of all possible configuration with the polymer and solvent molecules can achieve. The interaction parameters of Flory-Huggins reported in the literature[33,34,] for systems such as PEO 150 000 g /mol or PEO 6000 g/mol in $CHCl_3$, $CH_3OH$, $CH_2Cl_2$ can help to identify which polymer/solvent interaction would be more favorable. In case of the systems cited above, the interaction between PEO/$CH_3OH$ is less favorable (interaction parameter 1.9) than interactions of PEO/ $CHCl_3$ or PEO/$CH_2Cl_2$ (respectively Flory parameters of -0.52, -1.25), and also more favorable then the interaction for EO/PO copolymers.

## Conclusions

In summary, this investigation showed that random and block copolymers present different behavior in aqueous solutions and in solutions with organic solvents. In aqueous solutions, block copolymers present higher cloud point values, due to their ability to self- aggregation, which separates PO units from contact with the solvent.

In the case of organic solvents, the behavior is opposite. It is not clear at this stage, which kind of copolymer association causes the observed viscosity increase at lower temperature. In general, for all of the cases reported here, the solution behavior depends mainly on the copolymer composition (EO or PO contents) and in the case of solutions in organic solvents, also on its molar mass and on the chemical nature of the solvent. This indicates that solvent quality/affinity for the copolymer units/blocks plays a very important role.

## Acknowledgements

The authors acknowledge the support from FAPESP and CNPq (PhD scholarship to A.N. and for a research grant to W.L.).

## References

[1] Johansson, H.O.; Karlsröm, G.; Tjerneld, F; *Macromolecules,* **1993**, 26, 4478

[2] Ananthapadmanabhan, K.P.; Goddard, E.D; *Colloids Surf.,* **1987**, 25, 393

[3] Heskins, M.;Guillet, J.E; *J Macromol Sci Pure Appl Chem*, **1969**,2,1441

[4] Wang, G.; Ethyl(hydroxylethyl) cellulose and Some Model Uncharged

Polymers: A Calorimetric Study of Their Interaction with Surfactants in Aqueous Solution, Universidade Lund 1997, PhD thesis

[5] Zhang K.; Karlström G.; Lindman B; *J. Phys. Chem.*, **1994**, 98, 4411

[6] Da Rosa, R.G.; Martinelli, L; Silva, L.H.M.; *Chem. Commun*, **2000**, 33.

[7] G.M.Campese[I]; E.M.G.Rodrigues[II]; E.B.Tambourgi[I] ; *Braz. J. Chem. Eng*, **2003**, 20, 3

[8] Coelho, M . L; Arruda, Z.M.A; *Spectrochimica Acta Part B: Atomic Spectroscopy*, **2005**, 60, 743

[9] Johansson, HO.; Person J.; Tjerneld F; *Ind. Eng. Chem. Res.,* **2000**, 39, 2788

[10] Nilsson, A.; Mannesse, M; Egmond, M.R.; Tjerneld, F; *J.Chromat. B,* **2002**, 946, 141

[11] Tada, E.S.; Loh, W.; Pessoa – Filho, P.A; *Fluid Phase Equilibria* , **2004**. 218, 221.

[12] Cunha M.T.; Tjerneld F.;Cabral J.M.S.; Aires-Barros M.R; *J. Chromat. B,* **1998**, 53, 60

[13] Nilsson, A.; Neves-Petersen, M.T.; Johansson, HO.; Jansson, J.; Schillen, K.; Tjerneld, F.; Petersen, S.B; *Biochim. Biophys. Acta- Proteins and Proteomics,* **2003**, 1646, 57

[14] Niemiec A.; Loh W; *J. Phys. Chem. B,* 2008, **112**, 727

[15] Da Silva, L.H.M.; Loh, *J.Phys*. Chem. B, **2000**; 104; 10069.

[16] Flory, P.J.; Principles of Polymer Chemistry, Cornell University Press, Ithaca, NY, 1953

[17] Siow, K.S.; Delms, G.; Petterson, D; *Macromolecules,* **1972**, 5, 29.

[18] Kuwahara, N.; Saeki, S.; Chiba T.; Kaneko, M; *Polymer*, **1974**, 15, 777

[19] Dobry, A.; Boyer-Kawenoki, F; *J. Polym. Sci,* **1947**, 2, 90

[20] Smith, K.L.; Wislow, A. E.; Petersen, D.E; *Ind. Eng. Chem.,* **1959**, 51, 1361

[21] Spitzer, M.; Silva, L.H.M.; Loh,W; *Journal of Brazilian Chemical Society*, **2000**, 11, 375

[22] Kjellander, R.; Florin, E; *J.Chem.Soc. Faraday Trans. 1*, **1981**, 77, 2053

[23] Bailey, F.E., Koleske, J.V; Poly(ethylene oxide), Academic Press, New York, 1976, 29

[24] da Silva, R. C.; Loh, W; *J. Colloid Interface Sci.*, **1998**, 202, 385

[25] Saeki, S.; Kuwahara, N.; Nakata, M.; Kaneko, M; Polymer, **1976**,17, 685

[26] Bernardes, J.S; unpublished results

[27] Goldstein, R. E; *J. Chem. Phys,* **1984**, 80, 5340

[28] Karlström, G; *J. Phys. Chem.*, **1985**, 89, 4962

[29] Lopes, R. J.; Loh, W; *Langmuir*., **1998**, 14,750

[30] Loh,W. Encyclopedia of Colloid and Surface Science, A. Hubbard, (ed.), Marcel Dekker, New York 2002, 802

[31] Maechling-Strasser, C.; Clouet, F.; Francois, J. *Polymer,* **1992**, 33, 1021

[32] Spitzer, M.; Termodinâmica de soluções de poli(óxido de etileno): equlíbrio líquido líquido em sistemas ternários e partição em sistemas bifásicos de água e solventes orgânicos, Unicamp 2002, Master thesis.

[33] Kim, H.H.; Won, Y. S.; Choi, J. S; *Fluid Phase Equilib.* , **1998**, 146, 223

[34] Galin, M; *Polymer*, **1995**, 36, 3533

# CAPÍTULO VII - CONCLUSÃO GERAIS

Este trabalho compreendeu o estudo de interação entre surfatantes iônicos/ não iônicos com copolímeros bloco vs. estatísticos e também estudo de sistemas binários destes copolímeros em solução aquosa e em solventes orgânicos.

Com a investigação calorimétrica foi possível estabelecer contribuições distintas das estruturas de diferentes surfatantes iônicos na interação com copolímeros. Desta forma observou- se que SDS devido a sua carga elétrica interage bem mais fortemente do que DAC, DTAB, CTAB. Devido o menor volume do grupo polar o DAC interage melhor do que DTAB e quando o volume do grupo polar seria comparado hidrofobicidade da cadeia polimérica prevalecerá nesta interação (CTAB vs. DTAB). Os valores de ΔG (-5,0; -3,9;-2,7; -1,2 kJ/mol) para interação surfatante-copolímero estatístico determinaram a seqüência de intensidade de interação entre surfatante e copolímero: **SDS>CTAB>DAC>DTAB.**

Para os surfatantes não – iônicos foi encontrado o novo fenômeno, isto é a interação entre copolímero bloco P123 e surfatante $C_{12}EO_6$ formando complexos mistos que apresentaram alteração na sua forma (esférica para bastonetes), dependendo da temperatura e razão molar entre o polímero e surfatante. Esta mesma situação não foi confirmada para copolímeros estatísticos, mesmo fazendo os experimentos em temperatura de turvação de polímero o que confirma que este tipo de interação é especial para o sistema de P123 e $C_{12}EO_{6.}$

Com o estudo calorimétrico também foi possível encontrar evidencias de que a interação entre copolímero bloco e surfatante iônico é mais intensa do que para copolímero estatístico e semelhante com a interação entre mistura de homopolímero e surfatante. Além disso, a interação entre copolímeros estatísticos com surfatantes iônicos é significativamente afetada pela temperatura, causando alterações na hidratação do polímero. Foi observado também, que a interação entre copolímeros e surfatantes torna se mais intensa com o aumento da porcentagem de unidade de PO na cadeia polimérica. As curvas calorimétricas dos copolímeros estatísticos na interação com SDS são comparáveis com as curvas dos copolímeros bloco na interação com este mesmo surfatante a temperatura 15°C, quando os copolímeros bloco existem na forma de unímeros e confirma o que era previsto que não existe agregação em soluções aquosas de copolímeros estatísticos.

Por último, através do estudo de sistemas binários foi concluído que os copolímeros EO/PO apresentaram uma dependência oposta em função de temperatura: LCST (Lower Critical Solution Temperature) em água e UCST (Upper Critical Solution Temperature) em solventes orgânicos. Devido a falta de auto- agregação dos copolímeros estatísticos observou-se menores temperaturas de turvação para estes copolímeros em comparação com copolímeros em bloco. A influencia da composição do polímero, massa molar e tipo de solvente aplicado neste estudo foram apontados como importantes fatores que influenciam nestes sistemas bifásicos.